7. BASE YEAR MODEL APPLICATION

CAMx was run for the two historical episodes of July 31 – August 2 2000 and July 11 – 12 1999, and the performance of the model was evaluated against available air quality data. The purpose of the evaluation is to build confidence in the model's reliability as an ozone prediction tool. The proposed evaluation plan followed the procedures recommended in the EPA and CARB guidance documents for 1-hour ozone (EPA, 1991; CARB, 1992), and new draft guidance for 8-hour ozone (EPA, 1999). The philosophical approach to the model performance evaluation for this project was provided in the project Modeling Protocol (ENVIRON et al., 2002).

SUMMARY OF CAMx SIMULATIONS PERFORMED

Since the fall of 2002, when the initial CCOS emission inventory and preliminary RAMS simulations for the July/August 2000 episode first became available, ENVIRON and the BAAQMD have conducted on the order of 50+ CAMx simulations. Considered to be "developmental" model applications, most of these runs were made for the July/August 2000 episode each time the emission and/or meteorological inputs were incrementally updated; later, developmental CAMx runs were also made for the July 1999 episode as inputs became available. A portion of these runs were made with the interim versions of the emission and meteorological inputs to test photochemical model sensitivity to various options, treatments, and ancillary inputs. All developmental simulations were run using CAMx v3.10 with the CB-IV chemistry mechanism. A mixture of RAMS and MM5 meteorology were used to drive the photochemical model.

Developmental CAMx simulations were discussed at the Model Advisory Committee meetings, which were held every one or two months since project inception. The results have also been documented on the project web site (www.environ.org/basip2004/results.html, user=basip2004, password=goldengate) through early spring of 2004, when the CAMx modeling effort shifted primarily from ENVIRON to the District. Throughout the course of these CAMx applications, two key performance issues constantly emerged in both modeling episodes: (1) the emissions inventory (using CB-IV speciation of VOC) did not appear to be sufficiently reactive in producing ozone, suggesting that major proportions of emissions were either lacking or incorrectly speciated; and (2) flow fields in the Bay Area meteorology were either too fast and/or insufficiently convergent in the east bay, leading to over-ventilation of both precursors and ozone. Initially, these problems led to under predictions of peak observed ozone in the Bay Area by ~40 ppb, yet this deficit was incrementally improved to a shortfall of ~15-20 ppb after the numerous updates to the emission and meteorological inputs. Furthermore, significant under predictions were seen throughout central California, particularly in the central and southern San Joaquin Valley (SJV), where even larger ozone shortfalls were simulated.

It should be noted that the CB-IV chemistry mechanism was used in the developmental simulations because of it's speed and the preponderance of evidence (by many groups involved in CCOS) that the common signal from SAPRC99 is a <10 ppb increase in peak simulated ozone levels formed from NOx-rich urban environments. That is, the SAPRC99 chemical mechanism was not seen as the key solution for the various California-wide under prediction problems, but was rather reserved as a final "polish" once an acceptable BAAQMD simulation was achieved and all major inventory and meteorological improvements were stabilized.

The specific sensitivity tests conducted as part of the developmental process (excluding the numerous major meteorological and emission updates) included the following:

- Impacts from reducing area + mobile NOx by 30%
- Impacts from increasing area + mobile VOC emissions by 50%
- Impacts from increasing biogenic VOC emissions by 50%
- Impacts from NOx+VOC mobile emission scaling to reflect Harley (2003) emission estimates based on basin-specific fuel consumption
- Impacts from using EPA CB-IV speciation profiles in place of CARB profiles
- Impacts from reducing winds speeds 50%
- Impacts from reducing PBL depths by 50%
- MM5 vs. RAMS meteorology
- Use of high-resolution meteorological fields (~1 km grid spacing)
- Influences from initial and boundary conditions
- Role of fire emissions
- Role of temperature on biogenic emission rates and ozone predictions
- Role of temperature on motor vehicle emission rates and ozone predictions
- Impacts from invoking the Plume-in-Grid option
- Impacts from invoking drought stress (affects deposition rates)
- Impacts from reducing horizontal diffusion by a factor of 3

The findings from these tests are summarized below, arranged generally in order of their impacts on peak simulated ozone in the Bay Area, although impacts in other areas are noted. Additional information for each run is provided on the project web site at the "CAMx Results" link (www.environ.org/basip2004) and in the MAC presentation documents provided at the "Documents" link.

Emission Sensitivity

Model sensitivity was consistently largest for cases in which portions of the emission inventory were modified. This result was also found by Tesche et al. (2004) in their CCOS modeling of the San Joaquin Valley for the CARB. As stated above, CAMx/CB-IV results consistently indicated either a lack of emissions and/or improper speciation of VOC. This was later verified by Process Analysis evaluations undertaken by Vizuete et al. (2004) for this project (described later in this chapter), whereby a lack of VOC mass and reactivity was evidenced in the marginally active photochemical plume exiting the Bay Area through the Sacramento River Delta and through the Livermore Valley.

The early emission sensitivity tests were undertaken to maximize reactivity in the Bay Area by reducing NOx and increasing VOC. Separate scaling tests were conducted for biogenic and anthropogenic (area + motor vehicles) sources. An additional test was undertaken that scaled mobile emissions to better match the results of Harley (2003), who suggested that the CCOS NOx and VOC inventory was under estimated, particularly in the San Joaquin Valley, based on his regional fuel-based estimates.

The 30% reduction of NOx verified that the central Bay Area is NOx-rich and VOC-lean, and it led to higher levels of ozone both in the core Bay Area (~5 ppb, as expected) and in the downwind plume over eastern Alameda, eastern Contra Costa, and into northwestern SJV counties (up to nearly 20 ppb, not expected). This signal clearly indicated that Bay Area NOx remains sufficiently high (or VOC:NOx ratio remains low) as it rapidly transports out of the region and continues to suppresses ozone formation well downwind of the key source areas. On the other hand, ozone reductions generally resulted from this test in the VOC-rich central valley. Comparisons of modeled and observed NOx concentrations at sites throughout the CCOS region indicated that NOx was well replicated using the unmodified NOx emissions, suggesting a lack of VOC rather than an abundance of NOx.

Tests with increased biogenic and anthropogenic VOC emissions by 50% each led to 10-15 ppb increases in ozone in the downwind Bay Area ozone plume (eastern Alameda, eastern Santa Clara, and western SJV), consistent with biogenic source areas. Little to zero impact was seen in the central Bay Area due to ozone suppression within the NOx-rich conditions. In this case, the high NOx exiting the Bay Area mixed with higher VOC along its path, increasing the VOC:NOx ratio to regimes that are more conducive to rapid ozone formation.

The effects of basin-specific mobile emission scaling (to match Harley [2003], see Table 7-1) were moderate in the Bay Area (~5 ppb ozone increase in central Alameda and Contra Costa Counties) where the scaling factors were relatively small. Note that the Bay Area upward scaling of VOC and downward scaling of NOx are both in directions that maximize ozone production for the Bay Area environment. However, larger ozone increases approaching 10 ppb were seen in central/southern SJV, primarily due to higher NOx emissions, and downwind of Sacramento in the Sierra foothills due to higher VOC.

Table 7-1. Emission scaling factors applied by air basin to the July/August 2000 CCOS emissions inventory to match totals given by Harley (2003).

	Scaling Factor		
Air Basin	**CO**	**NMOC**	**NOx**
Sacramento	0.92	1.47	1.00
Bay Area	0.79	1.29	0.94
SJV	0.88	1.52	1.52
Other	0.84	1.39	1.15

As part of the their quality assurance of the CCOS emission inventory processing, Alpine Geophysics raised their concern regarding the CB-IV speciation profiles used in EMS-95. Several deficiencies were noted, including improper assignment of CB-IV VOC profiles to various source categories, and questionable profiles that allocated huge proportions of TOG to un-reactive species, among several other problems. Alpine evaluated the CARB CB-IV profiles against default profiles provided by EPA, which are currently used in a major photochemical and PM modeling project in the southeastern U.S. Significant differences were found for certain source categories, and to test the impact of these, Alpine regenerated the July/August 2000 emission inputs using the EPA CB-IV profiles. Impacts to daily maximum ozone in the Bay Area were minimal with the largest differences reaching only a few ppb.

Meteorological Sensitivity

Besides emissions, CAMx predictions of ozone were rather sensitive to changes in meteorological inputs. In two simple tests, changes were made to RAMS-derived input winds and PBL depths in directions that were assumed to increase ozone levels. In the test in which 3-dimensional winds were uniformly reduced by half, dramatic increases in ozone levels resulted in the central valley (>30 ppb). However, only marginal (~5 ppb) increases were seen in the eastern Bay Area. Evidence at the time suggested that RAMS was over-ventilating the Bay Area, but verifications against wind observations consistently showed that RAMS was performing rather well in replicating wind speeds in the Bay Area and generally throughout the CCOS domain. The latest evidence suggests that while RAMS performed well in simulating afternoon sea breeze development, the inland extent was too great and the model missed an essential convergence zone in the east bay that could be a major cause for the buildup of ozone in the Livermore area. Therefore, the reduction of wind speeds by 50% everywhere was considered too extreme as it would deviate significantly from observed conditions.

Reductions in PBL depth by 50% made much less impact, with the largest signals centered over all of the urban areas in the CCOS domain. In these locations (eastern Bay Area included), ozone was reduced by 2-7 ppb due to the concentrating effect of urban NOx, which squelched the production of ozone. Ozone increases were seen downwind of Sacramento in the Sierras and along an ozone front exiting the Bay Area through Solano, Yolo, and Sacramento Counties. In both areas, concentrated VOC emissions increased the VOC:NOx ratio and increased ozone formation. In a run with both reduced winds and PBL depth, the opposing effects combined to lead to practically zero impact in the eastern Bay Area.

As RAMS meteorology was developing, several groups including NOAA and CARB were undertaking MM5 modeling of the same July/August 2000 episode and reporting higher (better) CAMx ozone performance throughout the CCOS domain with those meteorological fields. A CAMx test was run using the best NOAA MM5 simulation at the time. Whereas RAMS-based meteorology was leading to under predictions of ozone at Livermore by ~40 ppb, the MM5-based meteorology halved the difference. In-depth evaluations of the differences revealed that the MM5 winds were indeed much lighter than RAMS, and more surface-based convergence was evident in extreme eastern Alameda County. As described in Section 4 of this report, and by ATMET (2004), the lighter MM5 winds were a direct result of nudging toward CCOS observations, many of which were taken at 2 m probe height (i.e., they measure weaker winds). Further, CARB has adopted MM5/CALMET hybrid meteorological fields (which are defined by the same observational dataset) to drive their July/August 2000 CAMx applications, and have achieved much higher ozone levels than even the MM5-based runs. We believe that it is inappropriate to use such data for nudging, blending, or evaluating meteorological model performance, and have thus developed an alternative CCOS meteorological dataset for these uses that remove all known 2 m sources of wind measurements (see Section 4 and Emery and Tai, 2004a).

During the developmental CAMx simulations, both ATMET RAMS and BAAQMD MM5 applications were configured with special high resolution grids placed over the Bay Area in an attempt to improve upon the definition of topography and land-water shorelines. RAMS employed a 1-km resolution while MM5 used a 1.33-km grid spacing. Meteorological modeling results from both RAMS and MM5 did not show the level of valley channeling and terrain blocking/trapping that was expected and needed for improved precursor transport pathways and

ozone buildup. In fact, the RAMS results indicated an actual speeding up of sea-breeze winds through the Bay Area (ATMET, 2004) due to heightened temperature gradients and terrain slopes. Tests with the resulting high-resolution meteorological fields on special 1/1.33-km CAMx nests also did not show significant impacts on predicted ozone.

Ultimately, the use of MM5 was adopted for all Bay Area CAMx applications as a way to maximize the consistency between CARB and BAAQMD modeling efforts.

Initial/Boundary Condition Sensitivity

Early developmental CAMx simulations conducted by ENVIRON used rather clean and uniform boundary conditions that were based on Ozone Transport Assessment Group (OTAG) modeling[1]. At the same time, the group at the University of California at Riverside (UCR) undertook CAMx modeling for the July/August 2000 episode using boundary conditions adopted from the SARMAP modeling. The UCR/SARMAP boundary conditions defined much higher ozone aloft (up to 70 ppb in the mid troposphere) as well as higher NOx and VOC concentrations. Furthermore, the UCR/SARMAP boundary conditions defined separate regimes for the western (over ocean) boundary and the inland (east, north, south) boundaries.

UCR was achieving rather good performance in the Bay Area using CAMx in conjunction with the NOAA MM5 meteorological inputs. Using RAMS meteorology and OTAG-based boundary conditions, ENVIRON was achieving very good results for all sites in the Bay Area that measured moderately low ozone (north bay and the urban core area), but was drastically under predicting all ozone levels measured above 100 ppb. It was found that the ozone differences between the UCR and ENVIRON results were less than half due to the different meteorology (as described above), but mostly due to the different boundary conditions. We conducted a simple test in which ozone boundary conditions were increased from 35 ppb (OTAG) to 60 ppb everywhere (no changes were made to precursor levels). Results showed promise in increasing the highest ozone levels, but the performance for all other sites in the Bay Area was degraded because of a consistent over prediction bias.

At the same time, it was becoming clear that the July/August 2000 episode was particularly influenced by regional wildfires, especially in the San Joaquin Valley where a large fire in the southern Sierras had led to aloft ozone measurements of 90-100 ppb (from ozone-sondes at Parlier and Granite Bay), and up to 160 ppb (from aircraft flights above Kern County). Other fires were raging throughout the western U.S. for several days before and during the modeling episode, so a regional buildup of NOx, hydrocarbons, and ozone was clearly obvious in aloft measurements. A procedure was devised to reflect these conditions within the CAMx initial and boundary conditions (described in Section 6). Ozone and precursors were increased substantially based on the UCR/SARMAP values, and special boosts in NOx, VOC, and CO were applied along certain boundary segments through known fire areas in Nevada and southern California. Although little sensitivity (1-2 ppb) was seen in the Bay Area from this change, it had much larger influence in the Central Valley, southernmost Kern County, the Sierras, and Nevada (5-20

[1] OTAG modeling was conducted in the mid-1990's to evaluate regional precursor and ozone transport in the mid- and eastern U.S. The OTAG boundary conditions were set to very clean conditions to reflect the remote location of the domain boundaries.

ppb) where fire influences were observed. The "fire-influenced" boundary conditions were maintained for all remaining developmental runs.

Fire Emissions Sensitivity

Given the clear evidence for high concentrations of forest fire emissions in the aloft measurements, there was an obvious potential for significant fire impacts on surface ozone levels during the July/August 2000 episode, particularly in the central valley. In fact, this potential was seen to be so large for Kern County that the MAC deliberated the utility of this episode for SIP development in the San Joaquin Valley. Besides the enormous uncertainty associated with fire emission estimates and its impact on simulated ozone for this episode, concerns about an approach to treat such fire influences in future year emission inventories continue to be raised at this time.

A separate CAMx simulation (using MM5 meteorology and original OTAG boundary conditions) was conducted to isolate the role of estimated "natural" emissions (fires and biogenics) during the July/August 2000 episode. With the general lack of natural NOx emissions, ozone remained near background levels (35-40 ppb) over the entire domain. However, in the immediate fire vicinity in the southern Sierras, fire emissions resulted in a 120 ppb ozone peak, with 50-60 ppb ozone spreading into the southern San Joaquin Valley. This indicated that 15-85 ppb of ozone was generated by the fire above background levels. However, practically zero impact was seen in the Bay Area, Sacramento Valley, and northern SJV in this simulation as the MM5 winds transported the fire plume to the northeast into Nevada.

Two additional cases were run with the full emissions inventory, one with RAMS meteorology and one with the NOAA MM5 meteorology, to investigate the differences in transport of fire emissions aloft (~3 km AGL). These were compared to satellite imagery to gauge which model was more accurately representing the dispersion of the plume, and to determine if CAMx was generating ozone near the levels observed by aircraft. The MM5 meteorology consistently sent the fire plume to the northeast into Nevada through July 31 – August 2. Little ozone carryover was seen day-to-day over California. The RAMS meteorology produced more day-to-day variation, with a tight plume transported northward along the spine of the Sierras on the afternoon of July 30 (exactly agreeing with satellite imagery), and later a more stagnant upper-level flow that slowly moved the diffuse plume of 50-60 ppb ozone all over central California from the evening of July 31 through August 2. This also agreed well with visible satellite imagery of the smoke plume on these days, as well as aircraft and ozone-sonde observations. For this reason, the RAMS simulated meteorology was considered to give a better representation of flow aloft. We were also comfortable that the forest fire emission estimates could produce ozone concentrations aloft near measured levels.

Emission Temperature Sensitivity

The CARB developed CCOS emission estimates for temperature-sensitive sources (biogenics and on-road mobile) using temperature fields derived from their own in-house MM5 applications from very early in the project. Evaluation of MM5 performance indicated that the model under predicted surface temperatures. This could lead to under estimates of emissions, which as described above, are consistently the largest source of sensitivity in CAMx. Therefore, we

undertook two tests in which the biogenic and on-road mobile emission estimates were re-processed through EMS-95 using temperature fields that more faithfully replicated observed conditions through the episode. However, it was not enough to simply use observational data due to lack of coverage in rural areas of the domain where biogenic sources were most important. Since RAMS had shown much better performance for temperature, a hybrid field combining temperatures from RAMS and observations was constructed specifically for these tests.

Separate CAMx tests were conducted for revised biogenics and on-road mobile emissions. In both cases, the emission estimates did increase slightly over the standard CCOS inventory. Bay Area impacts from the biogenics test indicated peak changes within ±5 ppb, with the largest increases in the north bay, and largest decreases in the south bay. Very little change was seen in ozone for the revised mobile emissions test. It was clear from these tests that temperature influences were not the cause of insufficient emissions in the model, and therefore not the primary cause of the overall under prediction magnitude.

However, we cannot ignore the possibility that temperature errors used in EMS-95, in combination with various other emission uncertainties (speciation, VOC and NOx estimates for major source categories, etc.), could additively build toward a significant change in the emission inventory if taken together. A final all-encompassing emissions sensitivity test was conducted that included the following changes:

- Biogenics based on the RAMS-hybrid temperature fields
- On-road mobile based on the RAMS-hybrid temperature fields
- On-road mobile scaled according to the Harley (2003) factors described above for each basin in the domain
- An additional 30% increase in SJV area sources for all species

This run did not include any change in CB-IV speciation using the EPA default profiles. Impacts to daily peak ozone in the Bay Area remained modest (~5-8 ppb), but increases of up to 15 ppb were predicted by CAMx in the San Joaquin Valley, with the largest increases in Kern County. While the emission modifications listed above certainly fall within the emission uncertainty bounds and may reflect an appropriate level of adjustment, their impacts continue to fall well short of the necessary ozone increases needed in all basins to reach adequate model performance.

CAMx Algorithm Sensitivity

Several sensitivity tests were run in the early developmental simulations to test the impacts of various CAMx options and input processing techniques. The first invoked the CAMx PiG sub-model. This treatment is designed to handle the chemical aging of large NOx point source plumes to alleviate the immediate dilution of fresh NOx emissions to the grid and to age the NOx via several important inorganic pathways until the plumes can be better spatially resolved and treated on the grid. All anthropogenic point sources emitting more than 1 ton/day NOx were flagged for this treatment; fire sources were not flagged. Impacts to simulated ozone throughout the CCOS domain were very minimal. The fact that California does not posses large NOx point sources equivalent to the major coal-fired power plants of the Midwest (the design focus for PiG) was a major reason for the lack of sensitivity. Other reasons for the lack of sensitivity may

include: (1) the tendency for many point sources to be located in generally NOx-rich environments where ozone is already suppressed; and (2) the relatively high resolution grid leads to early release of PiG emissions to the grid and minimizes the chemical impacts of the PiG model. Thus, the PiG was not invoked for the remainder of the developmental simulations.

The second test invoked drought stress in the dry deposition routine. The CAMx deposition model was developed by Wesley (1989) and includes a default seasonal dependence on vegetation activity to control surface uptake of gaseous pollutants into biota and other surfaces. However, the defaults are based on conditions in the mid- and eastern U.S., which for the summer season is in stark contrast to the much drier conditions in the western U.S. Except for irrigated croplands, much of California could be considered to be drought stressed during the summer season relative to the rest of the country. CAMx includes adjustments to vegetative uptake rates to emulate reduced exposure to stressed biota. With reduced dry deposition rates, ozone and precursor concentrations should increase. As expected, however, little impact on ozone was seen in this test. Drought stress was not carried through the remainder of the developmental simulations.

The third test investigated model sensitivity to the rates of horizontal diffusion diagnosed within CAMx. Unlike vertical diffusion rates, CAMx internally calculates horizontal diffusion rates based on grid resolution and deformation of horizontal winds (shearing, etc.). If these rates are too large, then ozone gradients and peaks may be smeared and under prediction bias results. In this test, the horizontal diffusion was shut off completely to bound the problem. Indeed the results clearly showed much tighter plumes, stronger gradients, and higher peaks in the Bay Area ozone patterns. Peak ozone on July 31 increased on the order of 5-10 ppb in eastern Alameda and Contra Costa Counties. Certainly the horizontal diffusion treatments in all air quality models are a concern and need to be reviewed (and possibly improved). This may lead to a reduction in diffusion rates in the future, but they can never be zero; any reduction less than 100% as demonstrated in this test will lead to minimal impacts to the ozone pattern.

A more important and always contentious issue is the estimation of vertical diffusion rates. In CAMx, these rates are supplied via external file as a way to maximize model flexibility and testing of alternative approaches. All past modeling using various photochemical platforms have shown a great range of sensitivity to this parameter, and as such, it has been identified as a convenient way to tune model results toward desirable performance. Although the "tuning" process is to be avoided (and is explicitly inadvisable in model guidance), it is nevertheless important to understand model sensitivity to vertical diffusion rates and mixing depths in each application. We believe that a significant reason for the CARB's good CAMx ozone performance in the central valley with the MM5/CALMET hybrid meteorological fields is due to their direct artificial reduction in the PBL depths (and thus vertical diffusion rates) in that region to ~500-700 m.

We conducted one test in which we did not allow vertical diffusion rates to decrease below certain minimum values for all layers within 100 m of the ground. These minimum values were based on land use characterization in each grid cell, in which no impact occurs over water, and maximum impact occurs over the roughest surfaces such as urban and forest. The reason for this "patch" on the diffusion is to ensure that some level of moderate mixing occurs near the surface, particularly at night, to alleviate an artificial buildup of NOx (especially) and the resulting slow ozone buildup after sunrise. Very often the output from models such as RAMS and MM5, from which diffusion rates are derived, result in zero vertical diffusion at night, thereby "over-

stabilizing" the atmosphere near the surface. The patching technique is a standard procedure that ENVIRON has applied in nearly every CAMx application around the country to date. Impacts from the use of the revised vertical diffusion rates for the July/August 2000 episode were well within +/- 5 ppb on the afternoon ozone peaks. Additional tests on the input diffusion fields should be conducted to fully understand model response and the role of vertical mixing in both episodes under consideration.

EVALUATION OF VOC PERFORMANCE

A large body of evidence was compiled from the developmental simulations conducted in this project, as well as from modeling undertaken by the CARB and Alpine Geophysics for the San Joaquin Valley (Tesche et al., 2004), which strongly suggested that CAMx ozone under predictions were chiefly a result of insufficient VOC emissions and/or incorrectly speciated CB-IV compounds. An analysis was undertaken by ENVIRON that compared VOC measurements and CAMx predictions for the July/August 2000 episode in the Bay Area, Sacramento Valley, and San Joaquin Valley. This analysis is summarized below; see Emery and Tai (2004b) for additional details.

Approach

The hydrocarbon measurements were taken from the CCOS air quality database, and the CARB provided "species keys" that provided a mapping of the several hundred individual hydrocarbon species listed in the database to equivalent CB-IV and SAPRC99 compounds. Two sets of measurement data were provided: a set of 3-hour lab-analyzed canister data from several sites in the CCOS study area, and a set of 1-hour field-calibrated GC-MS Saturn instrument data from three sites. Both sets of data were prepared and evaluated for this analysis. At the time, the CCOS air quality database did not include any data from PAMS sites, which utilize auto-GC instruments.

The 1-hour GC-MS data provided many more samples, with many more species reported per sample, relative to the 3-hour dataset, which exhibited a paucity of canister samples and species. We therefore believe that the 1-hour data provided a much more robust source of VOC measurements, with the caveat that the precision of the GC-MS data may not have been as accurate as lab-analyzed canisters. Many samples (primarily from 3-hour canisters) were disregarded due to lack of data.

CB-IV VOC predictions were derived using CAMx v4.03; meteorological data came from a BAAQMD MM5 run, while emissions data came from an interim CARB inventory from the fall of 2003. Some relatively minor updates to area and on-road mobile source emissions, and to the CB-IV speciation profiles used in EMS-95, have since been incorporated. The initial/boundary conditions were ENVIRON's "fire-influenced" set (as described in Section 6). All other inputs remained consistent with previous CAMx runs performed for the District.

Plots were developed comparing measured and simulated VOC concentrations for sites and periods at which sufficient data were available. Total VOC and CB-IV compounds (ppbC) are shown for the 6-9 AM period. The hours of 6-9 AM were chosen because this period should best represent primary VOC emissions in the data and in the model, as it coincides with peak

commute hours, low mixing rates, and zero to low reactive decay. Data from 1-hour GC-MS sites were averaged over the 6-9 AM period. The 3-hour canister samples directly coincided with the 6-9 AM period.

Results from three areas are shown: the San Francisco Bay Area (SFBA), the Sacramento Valley (SAC), and the San Joaquin Valley (SJV). For sites in the SFBA, the comparisons between observations and predictions focus on the morning of July 31; however, 6-9 AM averages of 1-hour GC-MS data from the Sunol site were calculated over July 30 – August 1 for comparison. Multi-day averages were not calculated from SFBA 3-hour canister data due to insufficient data to develop reliable numbers. For sites in the Sacramento (SAC) and San Joaquin (SJV) valleys, the comparisons between observations and predictions focus on the morning of August 1. Averages over multiple days were not calculated for any SAC and SJV sites due to insufficient data.

Evaluation of Total VOC

Figure 7-1 shows comparisons of measured and simulated 6-9 AM total VOC among the three sites that provided 1-hour VOC data: Sunol (SUNO, SFBA), Granite Bay (GNBY, SAC), and Parlier (PLR, SJV). Total VOC at Sunol is provided for July 31 and for the average over July 30 – August 1. It is interesting to note that on the day of highest ozone in the SFBA (July 31) the total VOC at Sunol is actually slightly lower than the 3-day average. Model performance is acceptable at Sunol and Granite Bay, but indicates a significant under prediction at Parlier by a factor of 2.5.

Figure 7-2 shows measured and simulated total VOC at 6-9 AM July 31 among the five SFBA 3-hour canister sites: Sunol (SUNO), Bodega Bay (BODB), San Leandro (LEAN), Bethel Island (BTI), and Patterson Pass (PATP). Insufficient data were available in the 3-hour dataset to construct 3-day averages or to show total VOC at Patterson Pass on July 31. All sites show under predictions, with model values at Bodega Bay and Bethel Island being low by about a factor of three. Note that canister data at Bodega Bay (a "background" site) indicate higher total VOC than Sunol. A comparison of 1-hour and 3-hour total VOC at Sunol on July 31 shows that the 3-hour VOC is higher by 35 ppbC, even though the 1-hour data contained significantly more hydrocarbon species than the 3-hour data (140 vs. 49). The reason for this is unclear.

Figure 7-3 presents total VOC at 6-9 AM August 1 at San Andreas (SGS, SAC) and Turlock (TSM, SJV), the only sites with sufficient 3-hour canister data in these regions. Both measurements are on par with 1-hour GC-MS data from Parlier. Both show under predictions, with San Andreas indicating that the model is low by more than a factor of 3.5.

Evaluation of CB-IV Speciated VOC

Figures 7-4 and 7-5 show the CB-IV species performance against 1-hour data at Sunol on July 31 and for the 3-day average, respectively. On July 31, the model performance is rather good and this agrees with performance for total VOC. For the 3-day average, performance for PAR is good but other species exhibit more of an under prediction bias by typically 50%. This is mainly due to higher measured values in the average while model values remain consistent with those on

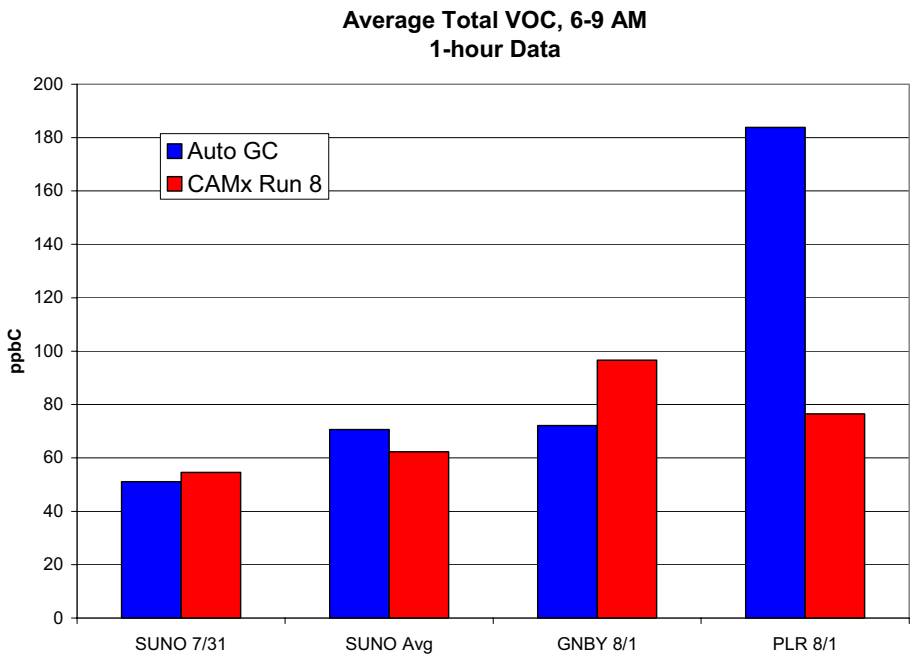

Figure 7-1. Total VOC measurements and predictions at three 1-hour GC-MS sites in the CCOS domain.

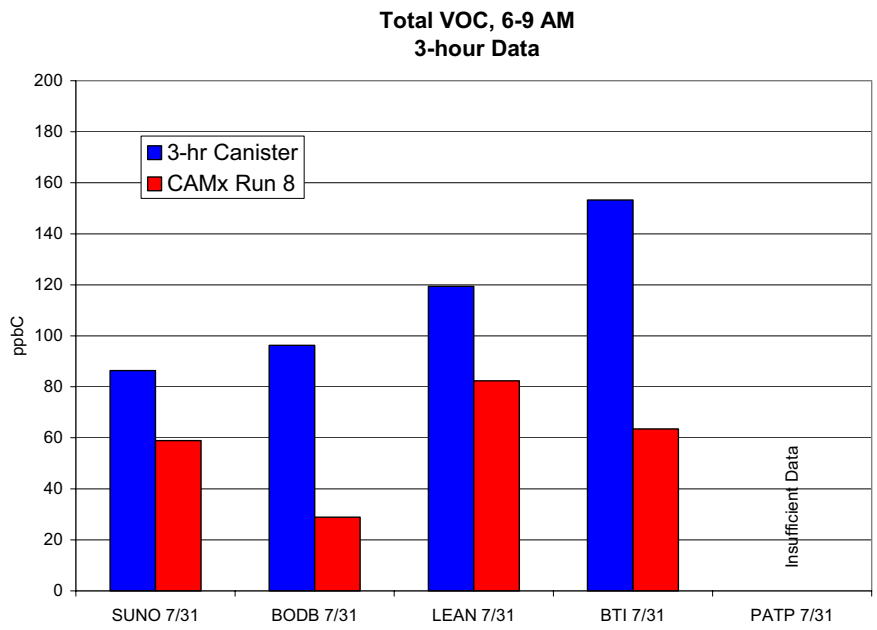

Figure 7-2. Total VOC measurements and predictions at five 3-hour canister sites in the SFBA region.

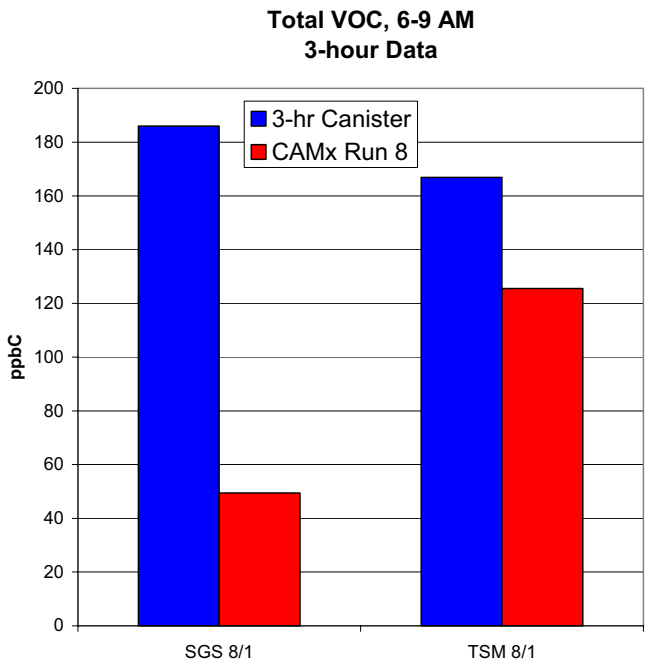

Figure 7-3. Total VOC measurements and predictions at two 3-hour canister sites in the SAC (SGS) and SJV (TSM) regions.

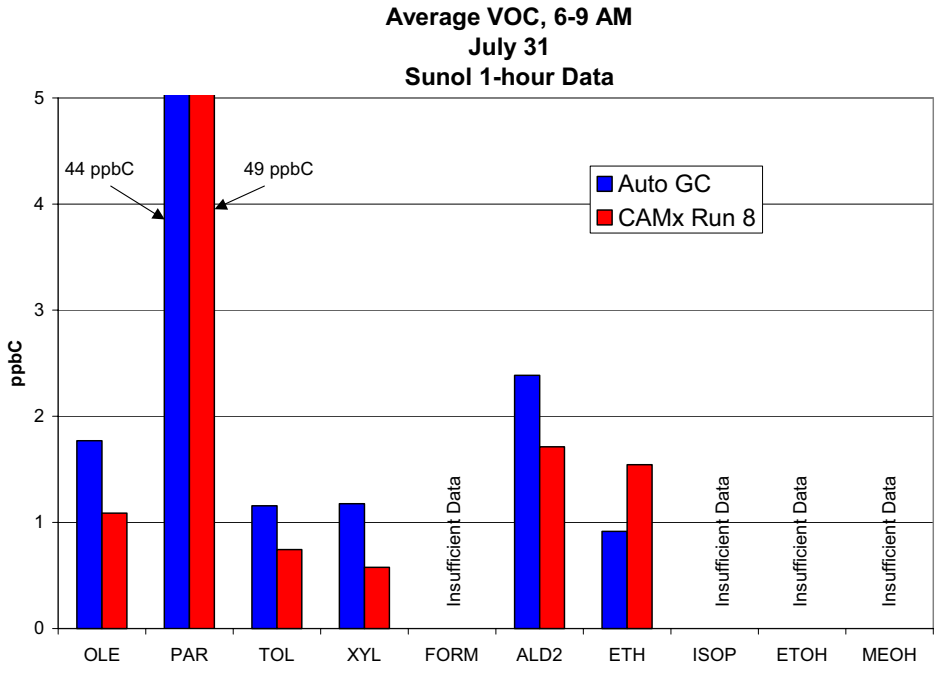

Figure 7-4. CB-IV speciated measurements and predictions at the Sunol 1-hour GC-MS site on July 31.

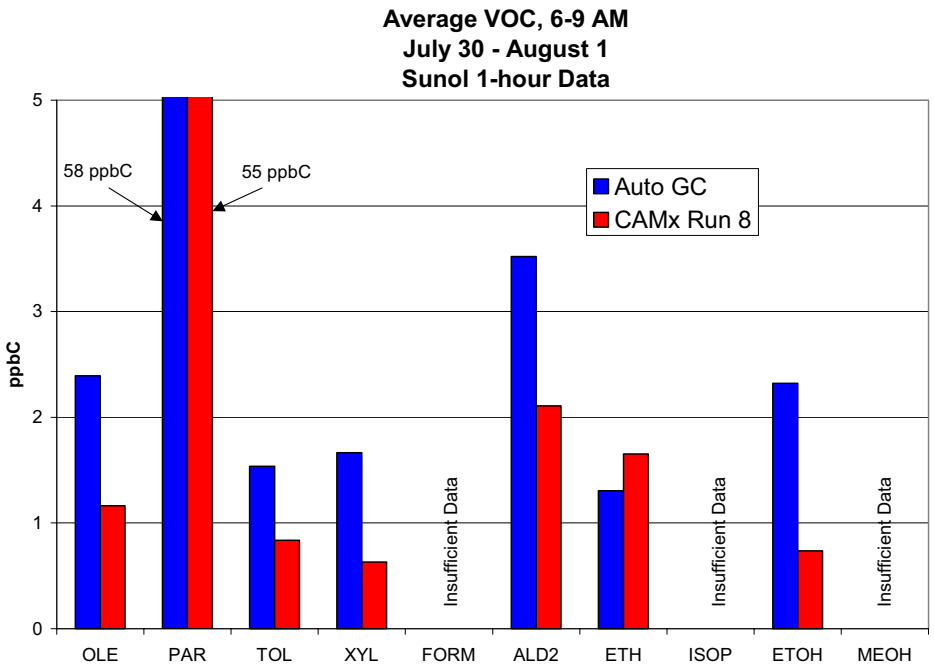

Figure 7-5. CB-IV speciated measurements and predictions at the Sunol 1-hour GC-MS site averaged over July 30 – August 1.

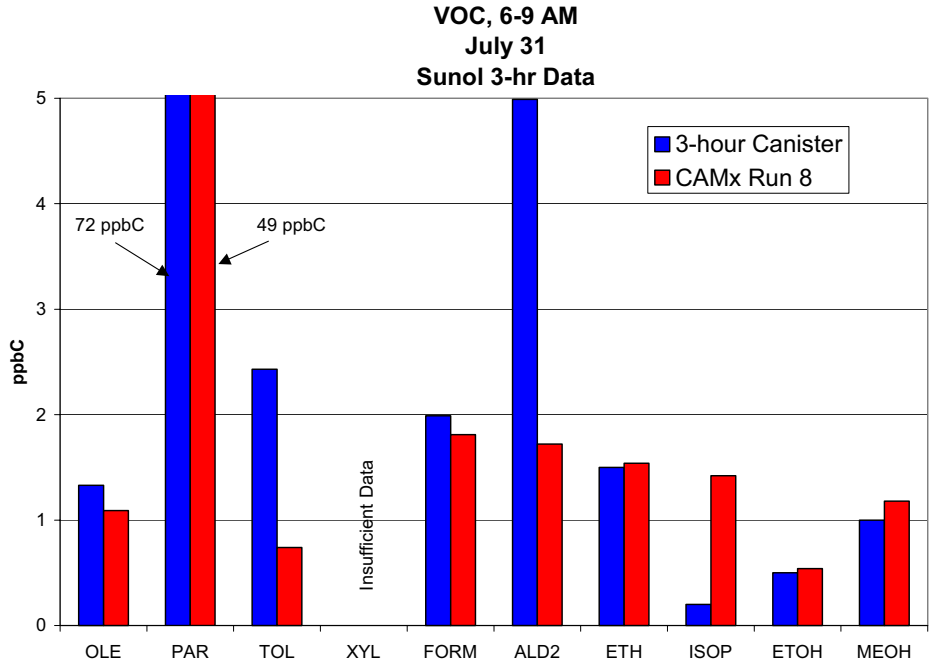

Figure 7-6. CB-IV speciated measurements and predictions at the Sunol 3-hour canister site on July 31.

July 31. The missing contributions from FORM, ISOP, ETOH, and MEOH would generally contribute a few more ppbC to total VOC.

Figure 7-6 presents CB-IV species performance relative to 3-hour data at Sunol on July 31. This plot reveals the cause of the higher 3-hour measured total VOC at this site: PAR is nearly double the 1-hour value. Furthermore, TOL is more than doubled, and ALD2 shows a 5 ppbC contribution, both of which are severely under predicted.

Figures 7-7 through 7-10 display the CB-IV species at Bodega Bay, San Leandro, Bethel Island, and Patterson Pass. The severe under prediction of total VOC at Bodega Bay is due to PAR (93 ppbC measured vs. only 26 ppbC simulated), where the PAR prediction is primarily comprised of the 20 ppb boundary conditions. Model performance for other species is acceptable. If the PAR sample data are correct, then further investigation into its source is necessary (possibly fire activity well to the north) and this may need to be modeled through higher boundary and/or initial conditions. Similar performance is seen for San Leandro (Figure 7-8), where PAR is under predicted by ~30% and ALD2 is under predicted by a factor of 3. Performance for other species is acceptable. At Bethel Island (Figure 7-9), PAR is under predicted along with OLE and ALD2 (although not as severely as San Leandro). Bethel Island also exhibits a strange spike for MEOH. Much data are missing at Patterson Pass on July 31 (Figure 7-10), but for those CB-IV samples that are provided, model performance is generally acceptable. Note the much higher ALD2 in the data that is a consistent feature at most sites.

Moving to the Sacramento region, Figure 7-11 presents the model performance against 1-hour CB-IV measurements at Granite Bay on August 1. In this case, the slight over prediction of total VOC is caused by too much PAR; performance for other species appears to be acceptable. However, note the strange spike in ethanol (ETOH) in the measurement data. The only other site in this region with sufficient data to make a comparison is San Andreas. Figure 7-12 shows the 3-hour canister data for this site on August 1. Here there are under predictions in most species that exhibit concentrations of more than 1 ppbC, including PAR (the biggest contributor), OLE, FORM, and ALD2. Concentrations of TOL and XYL are appropriately low.

Finally, in the San Joaquin area, Figure 7-13 shows model performance against 1-hour CB-IV measurements at Parlier on August 1. The large under prediction of total VOC at this site (Figure 7-1) is seen to be caused by under predictions of CB-IV species virtually across the board, but especially for PAR and ALD2. Other reactive VOCs (OLE, TOL, XYL, ETH) are all low by factors of 3 to 6. Given that we consider the GC-MS data to be more robust than the canister dataset (based on consistently more samples and more chemical compounds per sample), this could be a significant finding. Note, however, that GC-MS data quality is highly dependent on field calibration and the general consensus among the chemists is that canister data is usually more reliable (when available) than the GC-MS data. At Turlock (Figure 7-14), model performance against the 3-hour canister data is much better and agrees rather well with most CB-IV species. While OLE is under predicted by a factor of 3, TOL and XYL are over predicted. The consistent under prediction of ALD2 appears at this site as well.

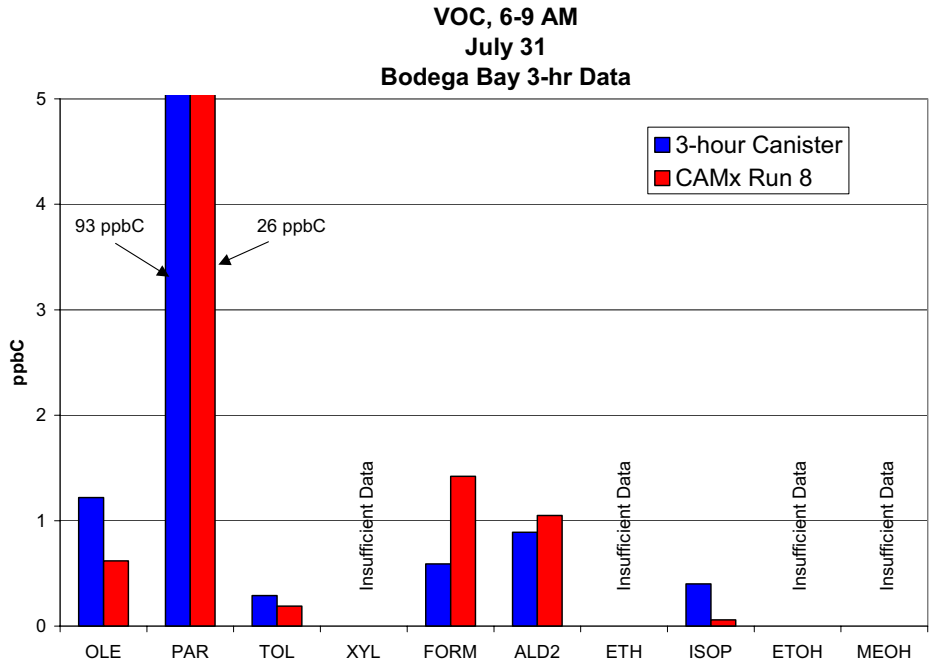

Figure 7-7. CB-IV speciated measurements and predictions at the Bodega Bay 3-hour canister site on July 31.

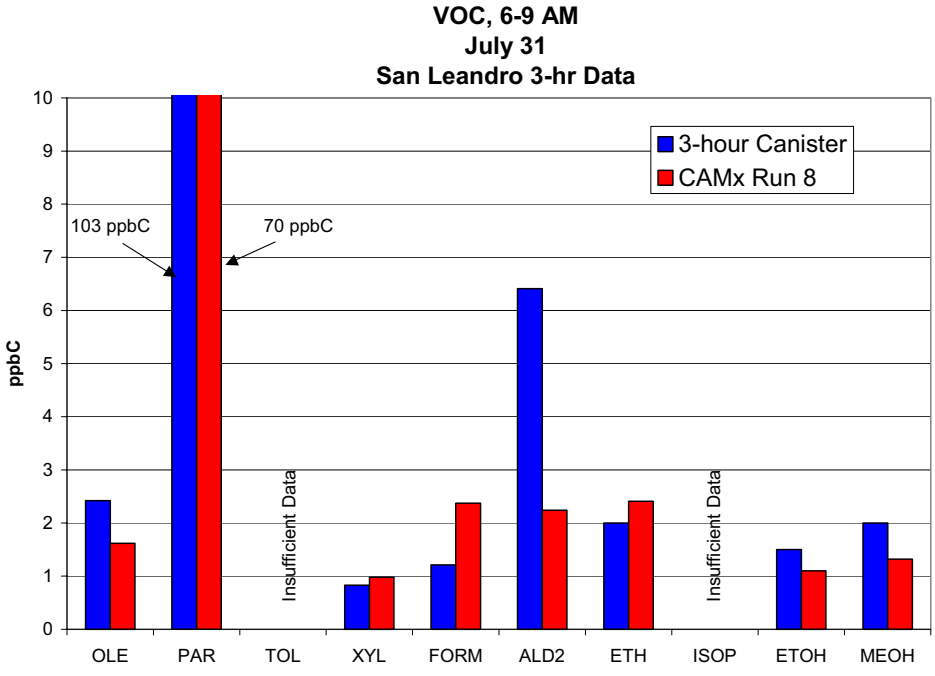

Figure 7-8. CB-IV speciated measurements and predictions at the San Leandro 3-hour canister site on July 31.

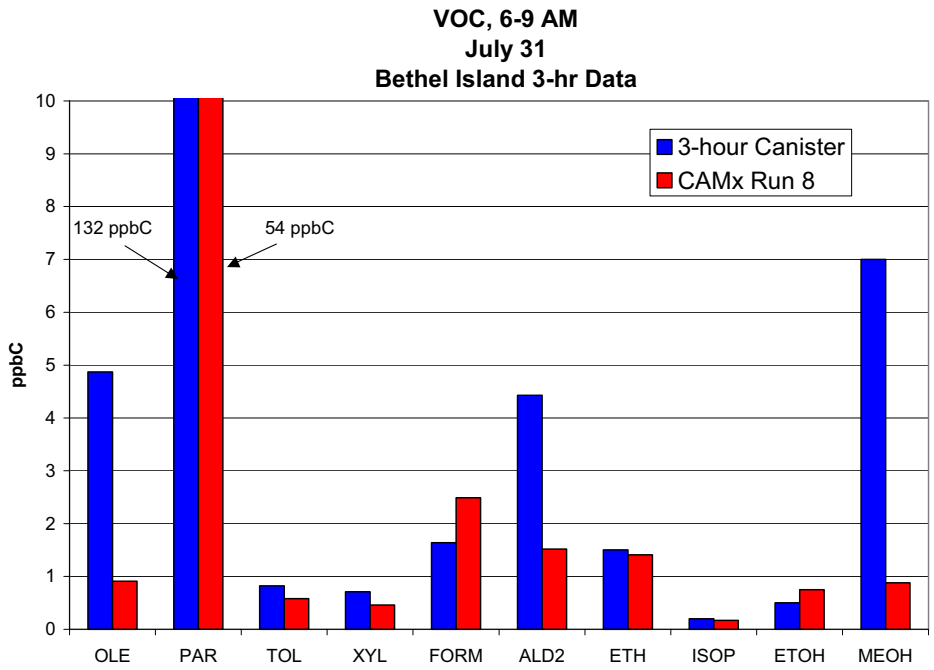

Figure 7-9. CB-IV speciated measurements and predictions at the Bethel Island 3-hour canister site on July 31.

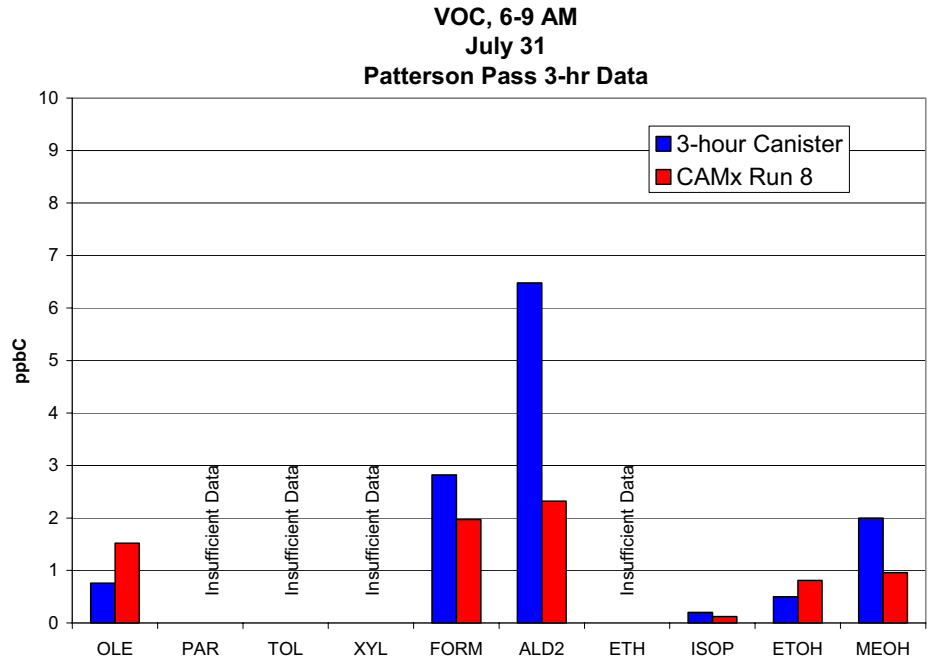

Figure 7-10. CB-IV speciated measurements and predictions at the Patterson Pass 3-hour canister site on July 31.

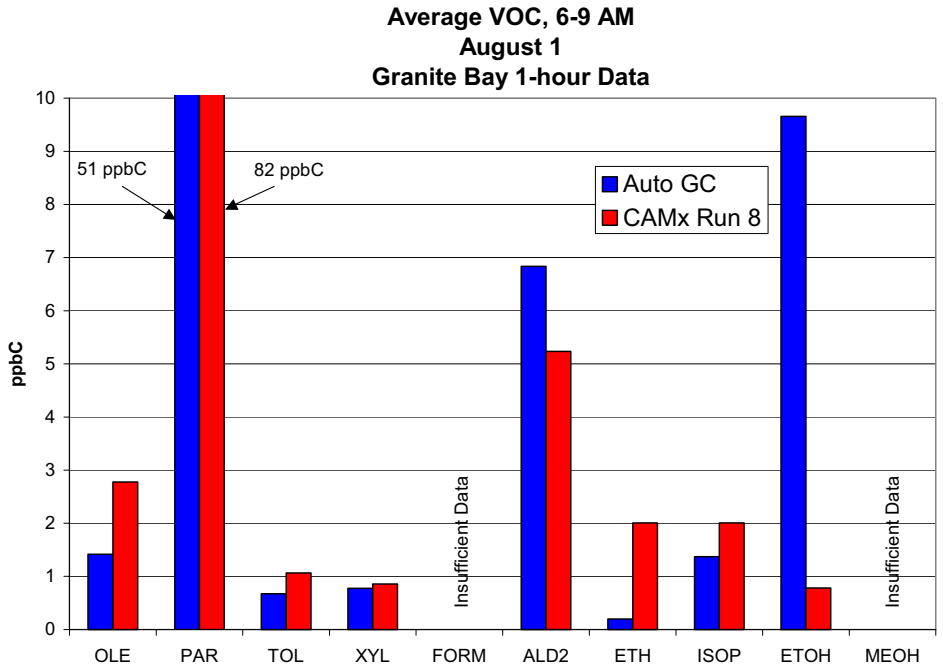

Figure 7-11. CB-IV speciated measurements and predictions at the Granite Bay 1-hour GC-MS site on August 1.

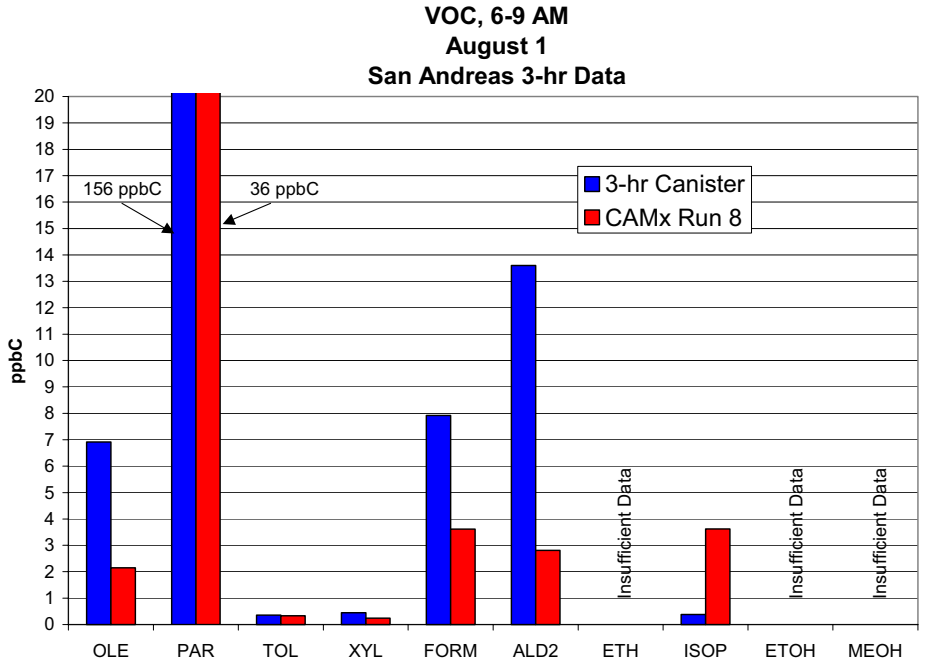

Figure 7-12. CB-IV speciated measurements and predictions at the San Andreas 3-hour canister site on August 1.

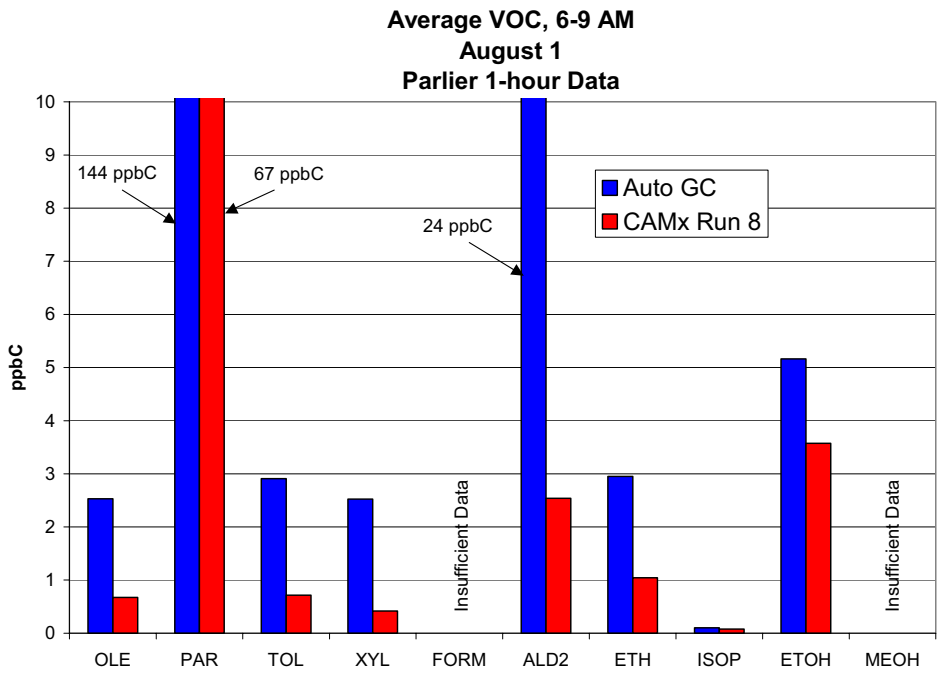

Figure 7-13. CB-IV speciated measurements and predictions at the Parlier 1-hour GC-MS site on August 1.

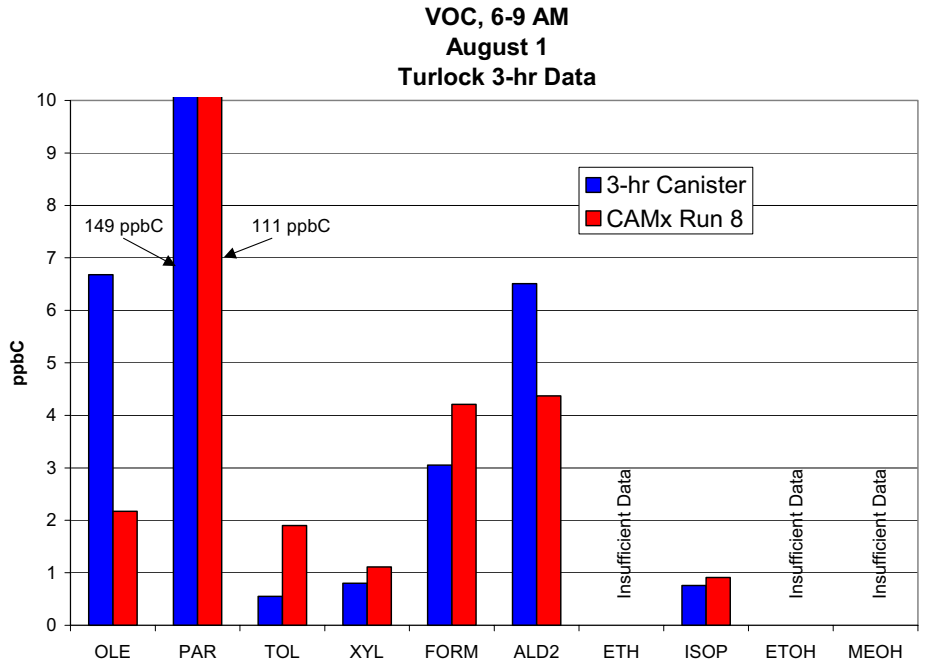

Figure 7-14. CB-IV speciated measurements and predictions at the Turlock 3-hour canister site on August 1.

Analysis of VOC:NOx Ratios

An analysis of VOC:NOx ratios was undertaken for those sites reporting both reliable VOC canister and GC-MS measurements and NOx data. Similarly to the analysis of VOCs reported above, the ratios were calculated for the 6-9 AM period for each day in which sufficient data were available. Results are shown in Table 7-2.

In the SFBA, 1- and 3-hourly observed and predicted VOC:NOx ratios were compared at Sunol, whereas 3-hourly ratios were compared at Bethel Island. Measurements from both sites show NOx-rich conditions and the predictions agree rather well with this. While VOC predictions agree with observations at Sunol, NOx is consistently under predicted. This is likely due to the close proximity of this site to freeway emissions that the grid model cannot resolve. The model varies between over and under predictions of both NOx and VOC at Bethel Island. The general agreement between observed and predicted VOC:NOx ratios in spite of generally poor performance for each component concentration in the SFBA suggests that emission are in basically correct proportion but that meteorological influences are playing a role in overall model performance (at least in the east bay).

In the Sacramento area, 1- and 3-hourly ratios were compared at Granite Bay (the only site with co-located instruments in the CCOS dataset). The data and model also both indicate NOx-rich conditions east of Sacramento, with model over predictions of both NOx and VOC on August 1. This may be due to an incorrect placement of the urban precursor plume on this day (a meteorological factor), but it does not suggest a significant problem with the proportion of emissions.

In the SJV, 1- and 3-hour ratios were calculated for Parlier and 3-hour ratios were determined for Turlock. At Parlier, the large under predictions of VOC (as described above) is causing a NOx-rich regime in the model while the measurement data inversely indicate a strong NOx-limited situation. NOx concentrations are also under predicted at Parlier, but not nearly to the extent of the VOC under predictions. At Turlock, the model is also far too NOx-rich, while the observed VOC:NOx ratio suggests conditions early in the episode that are much closer to optimum ozone formation potential. In this case, however, high VOC concentrations are replicated rather well on most days, and it is the over prediction of NOx that is driving the modeled VOC:NOx ratios downward. The simulated conditions in the SJV appear to be driven more by disproportionate emission estimates rather than meteorology.

Conclusions

Our conclusions from this analysis are as follows:

- The 3-hour canister data from most CCOS sites exhibited very few hydrocarbon species samples relative to the 1-hour GC-MS sites. Because of this, the 3-hour dataset did not provide sufficient information over CB-IV species and/or time period to allow inclusion into our analysis. We therefore believe the 1-hour data to be more robust.

Table 7-2. Compilation of observed and predicted 6-9 AM VOC and NOx concentrations at sites with co-located monitors in the CCOS air quality database. Data from both 1- and 3-hour instruments are shown for days in which data were available. Differences between observations and predictions greater than 30% are depicted in red.

Site / VOC sample duration / date		VOC (ppbC)	NOx (ppb)	VOC:NOx
Sunol 1-hr July 30	Obs	78	25	3.2
	Pred	65	16	4.1
Sunol 1-hr July 31	Obs	51	37	1.4
	Pred	55	23	2.4
Sunol 3-hr July 31	Obs	86	37	2.3
	Pred	59	23	2.6
Sunol 1-hr Aug 1	Obs	71	77	0.9
	Pred	62	27	2.3
Bethel Island 3-hr July 30	Obs	58	14	4.1
	Pred	109	20	5.6
Bethel Island 3-hr July 31	Obs	153	22	6.9
	Pred	64	17	3.7
Bethel Island 3-hr Aug 1	Obs	148	31	4.8
	Pred	63	13	4.9
Granite Bay 3-hr July 31	Obs	101	28	3.6
	Pred	106	27	4.0
Granite Bay 1-hr Aug 1	Obs	72	13	5.5
	Pred	97	28	3.4
Parlier 1-hr July 31	Obs	354	24	15.0
	Pred	83	15	5.7
Parlier 3-hr July 31	Obs	169	24	7.2
	Pred	92	15	6.3
Parlier 1-hr Aug 1	Obs	184	12	15.3
	Pred	76	13	5.8
Turlock 3-hr July 30	Obs	159	23	7.0
	Pred	139	44	3.1
Turlock 3-hr July 31	Obs	152	23	6.6
	Pred	132	54	2.4
Turlock 3-hr Aug 1	Obs	167	35	4.8
	Pred	126	43	2.9
Turlock 3-hr Aug 2	Obs	208	56	3.7
	Pred	140	57	2.5

- In spite of the assertion above, there still exists large uncertainty concerning overall data quality in the CCOS VOC dataset, both for canister and GC-MS samples. While certain findings from the analysis reported here are significant, they may be overly influenced by the inclusion of poor quality samples that appear to be reasonable from casual inspection without further supporting evidence to suggest otherwise.

- We wish to stress that the performance results reported here should not be taken as an implication of the emissions inventory only. If we are to believe the measurement data, then certainly some aspects of the results (e.g., significant differences for certain species, disagreement among observed/predicted VOC:NOx ratios) are likely associated with deficiencies in emissions, either in total mass, speciation profiles, temporal profiles, spatial allocation, etc. However, there exists a large range of plausible explanations that involve meteorological performance (inaccurate mixing heights, wind field errors that cause the modeled urban plumes to miss the monitors, etc.), and at this point none of these should be ruled out.

- Generally, there are consistent model performance issues that we have identified in the three basins and among most sites with useable measurements. First, there is a general under prediction of total VOC and this is mainly attributable to insufficient PAR (since this contributes the bulk of VOC mass). Second, the model lacks sufficient levels of higher aldehydes (ALD2), usually by large factors of 2 or more. This is a surprising result and possible explanations are made difficult by the fact that model-to-sample comparisons are largely an "apples-oranges" dilemma. Most ALD2 in the model is secondarily formed with some contributions from emissions (e.g., biogenics). ALD2 in the measurements is primarily from direct emissions, pieces of which are allocated to the CB-IV ALD2 bin for reactivity purposes (i.e., they are not necessarily carbonyl type compounds).

- VOC performance in the SFBA showed consistent under predictions of total VOC. A large discrepancy between 1-hour and 3-hour samples at Sunol (mainly PAR) remains unexplained. The Sunol site indicates under predictions for reactive species (OLE, TOL, XYL) in both 1-hour and 3-hour samples. There is evidence from Bodega Bay that background levels of PAR are too low, although this could be caused by old smoke plumes originating well to the north of the CCOS domain. Generally, performance for individual CB-IV species other than PAR was acceptable (with a few exceptions). Limited VOC:NOx ratio data and predictions indicate that the east bay is NOx-rich.

- VOC performance in the Sacramento region indicates mixed performance for total VOC on August 1. Granite Bay indicates just a slight over prediction of 1-hour data, with generally good performance across CB-IV species, while San Andreas shows significant under predictions of 3-hour PAR, OLE, and carbonyls. There were insufficient data to compare 1-hour and 3-hour data at Granite Bay. Observations and predictions of VOC:NOx ratios at Granite Bay agree that conditions east of Sacramento are NOx-rich.

- VOC performance in the SJV region showed consistent under predictions of total VOC, with especially poor performance at the Parlier GC-MS site. CB-IV species were under predicted across the board at that site. Results in Turlock were better, with a slight under prediction of total VOC from low PAR, OLE, and ALD2. There were insufficient data to

compare 1-hour and 3-hour data at Parlier. VOC:NOx analyses also suggest a problem with disproportionate VOC and NOx emissions in the SJV.

USE OF THE PROCESS ANALYSIS TOOL

"Process analysis" refers to techniques to quantitatively track individual physical and chemical process that contribute to changing pollutant concentrations for a grid cell or collection of grid cells within photochemical grid models. Process analysis provides dynamic information such as horizontal and vertical pollutant fluxes crossing cell boundaries, chemical production and consumption rates, emission rates, deposition rates, and initial and final concentrations. The latest version of the Process Analysis Tool (PAT) was designed to gain a better understanding of atmospheric reaction networks and to improve our ability to characterize the chemistry that leads to poor air quality.

Vizuete et al. (2004) detail the application of PAT in CAMx to study modeling phenomena in the San Francisco Bay Area during the Central California Ozone Study (CCOS) episode of July 30 – August 2, 2000. This evaluation employed CAMx v4.03, with process analysis code modifications applied by the University of Texas (UT). ENVIRON configured that version of the model to run a process analysis domain over the San Francisco Bay Area and ran the model for the episode. Evaluation of the Integrated Process Rate (IPR) and Integrated Reaction Rate (IRR) output generated for the Bay Area PA domain was then performed by UT. The focus of the analysis was on the key episode day of interest, July 31, 2000. The following summarizes the methodology and results; more details are provided by Vizuete et al. (2004).

Methodology

The process analysis tool aggregates CAMx grid cells horizontally and model layers vertically resulting in a single large cell that effective mimics a box model. This large cell, or process analysis box (PAB), represents the total system that the PAT analyzes. Pollutant fluxes are calculated crossing the boundary of this box and source and sink rates are represented within the box. The goal is to define a PAB that captures the modeling phenomena under investigation without diluting the characteristics of the performance in question with a large box. In contrast, a box of inadequate dimension will result in the dominance of transport processes erasing the chemical features of the modeling event. The location of the box is also a consideration. Large emission sources relatively close to the boundaries of the PAB may have to be incorporated. Sizeable concentration gradients will cause transport processes to dominate over all other rates. Vertically, the height of the sub-domain should match the evolution of the planetary boundary layer or mixing height throughout the simulation day.

For this analysis, two areas in the eastern San Francisco Bay Area were chosen. A northern domain was chosen to evaluate the region where the model predicts high ozone concentrations in the east bay. The southern domain was chosen to evaluate the region where the model under predicts the highest ozone recorded in the Bay Area. The horizontal domain chosen for the northern source region is represented in Figure 7-15. The 640 km^2 sub-domain encompasses a heavily industrial and suburban area along the Sacramento River. The southern region of this sub-domain consists largely of natural terrain, including Mt. Diablo State Park with a mountain peak 1,170 meters above sea level. This domain was chosen to include the source region near

A

B

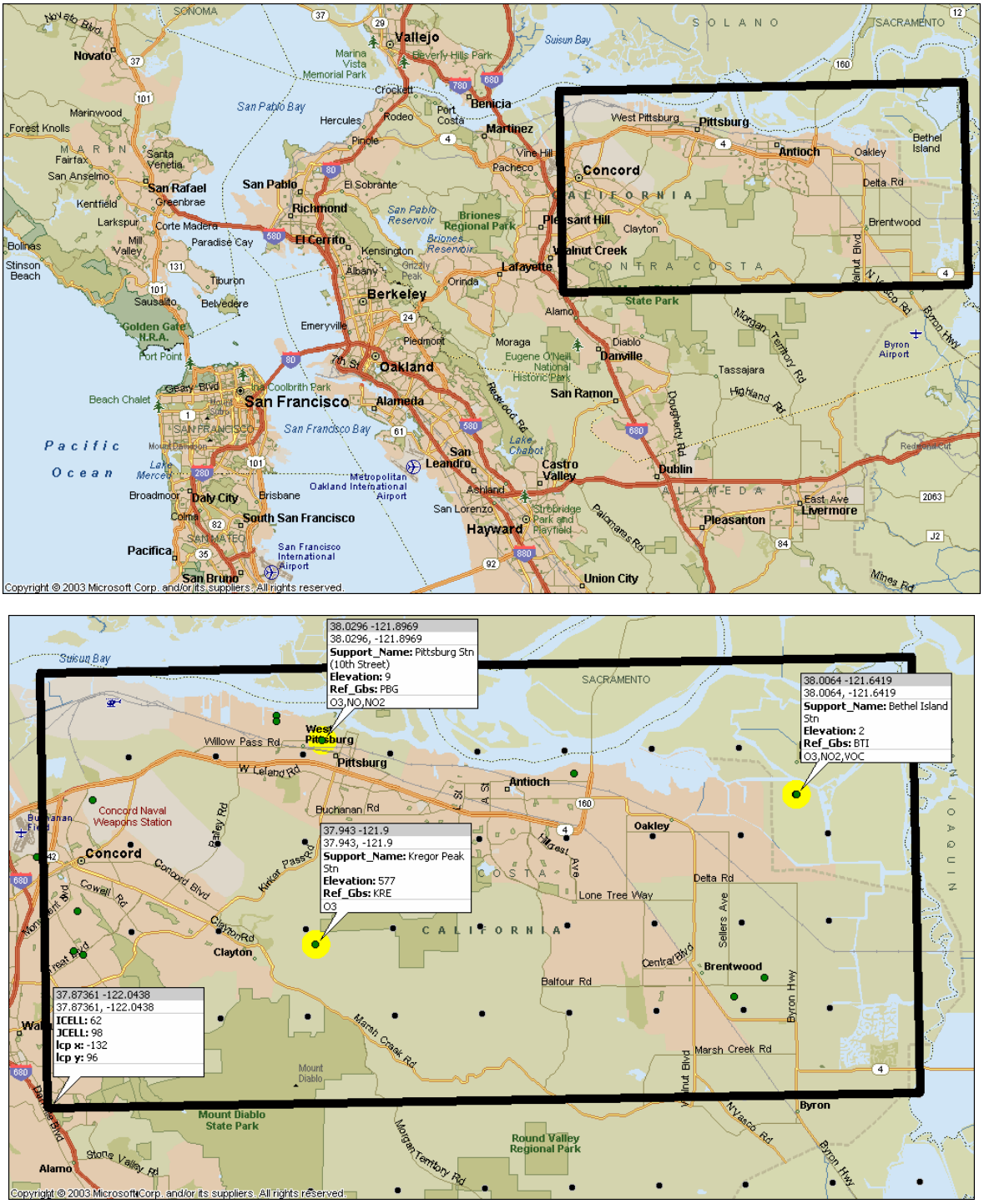

Figure 7-15. (A) The location of the 640 km^2 sub-domain, outlined in black, used by the process analysis tool for the northern source region. (B) A close up view of the sub-domain. The black dots represent the lower left corner of the 4 km CAMx grid cells. Observed data was used from the monitor stations that are highlighted on the map.

the river in addition to the region of high modeled ozone concentrations over the park area. This domain also contains three ground monitor stations where observed concentrations of NO, NO_2, ozone, and certain volatile organic carbons (VOC) were recorded. The location of these stations and the data collected at the stations are shown on the map.

The horizontal domain chosen for the southern ozone region is represented in Figure 7-16. The 640 km^2 sub-domain includes several interstate highways with heavy traffic activity and suburban areas. The northern and eastern region of this sub-domain consists largely of natural, hilly terrain. This domain contains four ground monitor stations where observed concentrations of NO, NO_2, ozone, and certain volatile organic carbons (VOC) were recorded. The location of these stations and the data collected at the station are shown on the map.

The PAT allows the process analysis box to follow changes in mixing height throughout the simulation day. In the CAMx model vertical mixing is a function of the layer interface diffusivity or "Kv" value. These values can vary spatially and temporally due to the heterogeneity of terrain and meteorological conditions. An incorrect input of mixing heights into the PAT will result in large vertical transport of pollutants across the top boundary. This is an undesired result as it will mask the important chemical processes that are occurring throughout the planetary boundary layer (i.e., ventilating the box model).

Mixing heights were determined by qualitatively analyzing the evolution of the Kv values for each grid cell in the PAB. Figure 7-17 shows the evolution of the mixing height within the process analysis box for the northern and southern PABs. The black horizontal grid lines represent the CAMx grid layers and the red line is the mixing height. The light blue and yellow boxes show the layers that were entrained and detrained respectively each hour. Once the vertical and horizontal dimensions of the process analysis box were determined they were then entered into the process analysis tool. The PAT generated two excel files representing the model's physical and chemical processes occurring within the box. These results will now be discussed.

Process Analysis Results

In both regions (northern and southern) vertical advection played an important role in the transport of pollutants across the boundaries of the process analysis boxes (Figures 7-18 and 7-19, respectively). This can be attributed to the heterogeneity of the terrain under analysis. These differences in terrain account for a wide range of mixing and vertical advection.

Similar chemical characteristics were evident in the atmospheres of both regions. The process analysis tool determined that the modeled atmosphere is NOx-rich and VOC-limited. The composition of the VOC that was available in the atmosphere was predominantly low-reactive paraffins. Since both areas incorporated natural terrain a significant amount of isoprene was emitted during the day into both process analysis boxes. Nevertheless, there were still inadequate amounts of reactive VOC available to generate large amounts of ozone chemically. This is evident in all the cycle diagrams that are output by the process analysis tool (Figure 7-20). The chemical NOx cycles, radical cycles, chemical production of ozone, and percentage of OH reacting with VOC were all at insufficient levels. The southern region was slightly more reactive and had higher radical cycles due to the inclusion of more olefins (Figure 7-21). This still fell far below the levels needed to reach observed ozone peaks in the Livermore area. In the

A

B

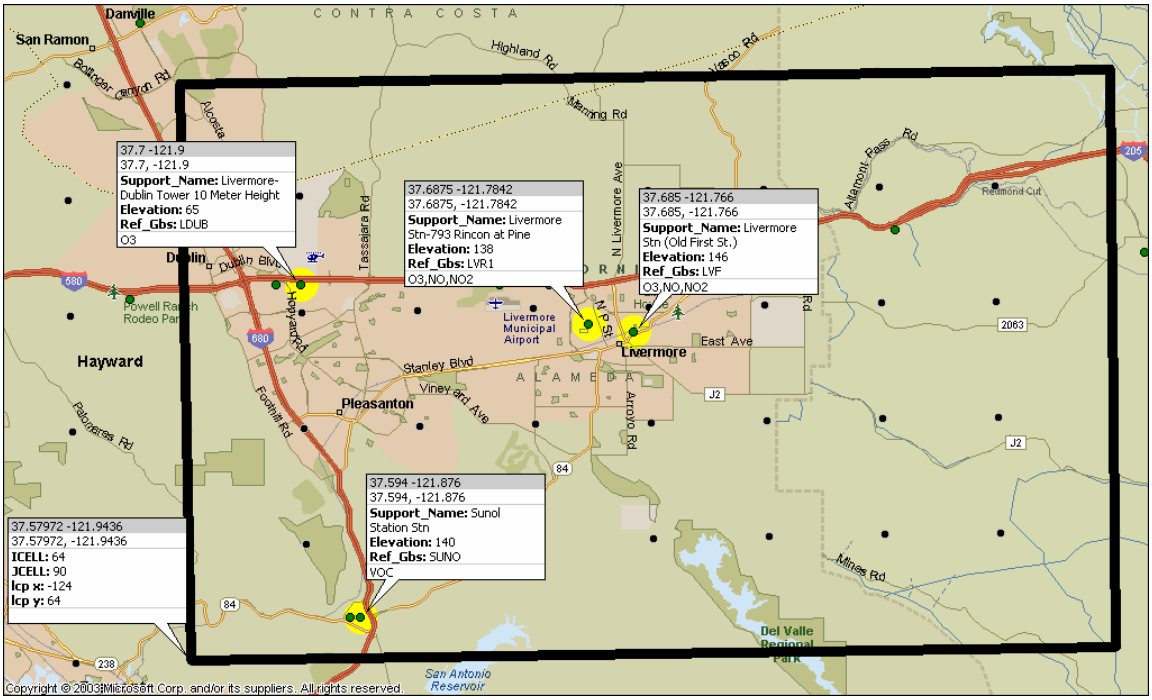

Figure 7-16. (A) The location of the 640 km^2 sub-domain, outlined in black, used by the process analysis tool for the southern ozone region. (B) A close up view of the sub-domain. The black dots represent the lower left corner of the 4 km CAMx grid cells. Observed data was used from the monitor stations that are highlighted on the map.

A

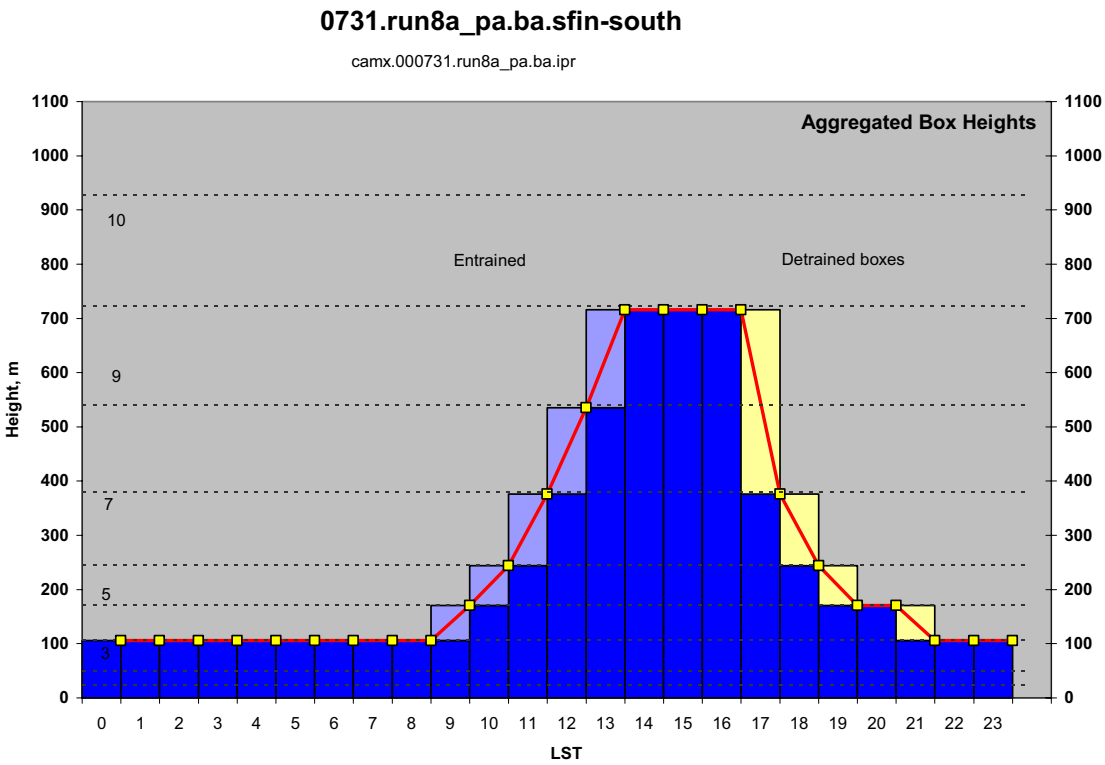

B

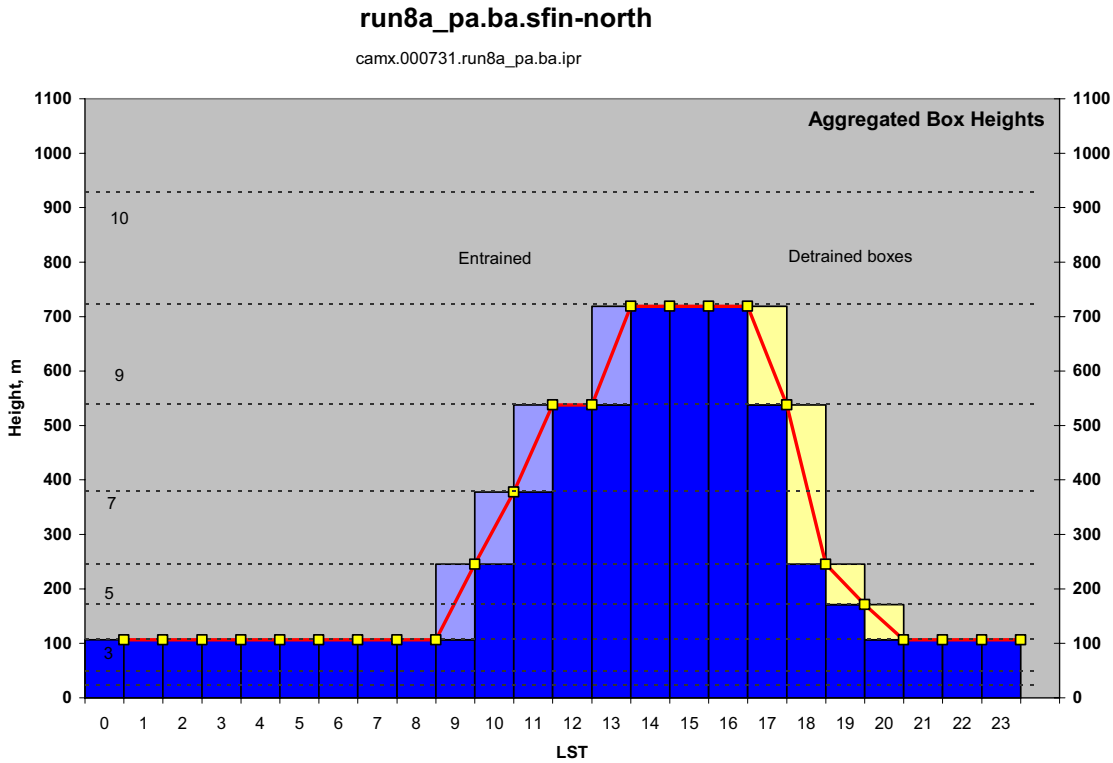

Figure 7-17. The evolution of the mixing height within the process analysis sub-domain for the (A) northern and (B) southern region. The x-axis represents the hours of the simulation day and the modeling height is shown vertically. The black horizontal grid lines represent the CAMx grid layers and the red line is the mixing height. The light blue and yellow boxes show the layers that were entrained and detrained, respectively.

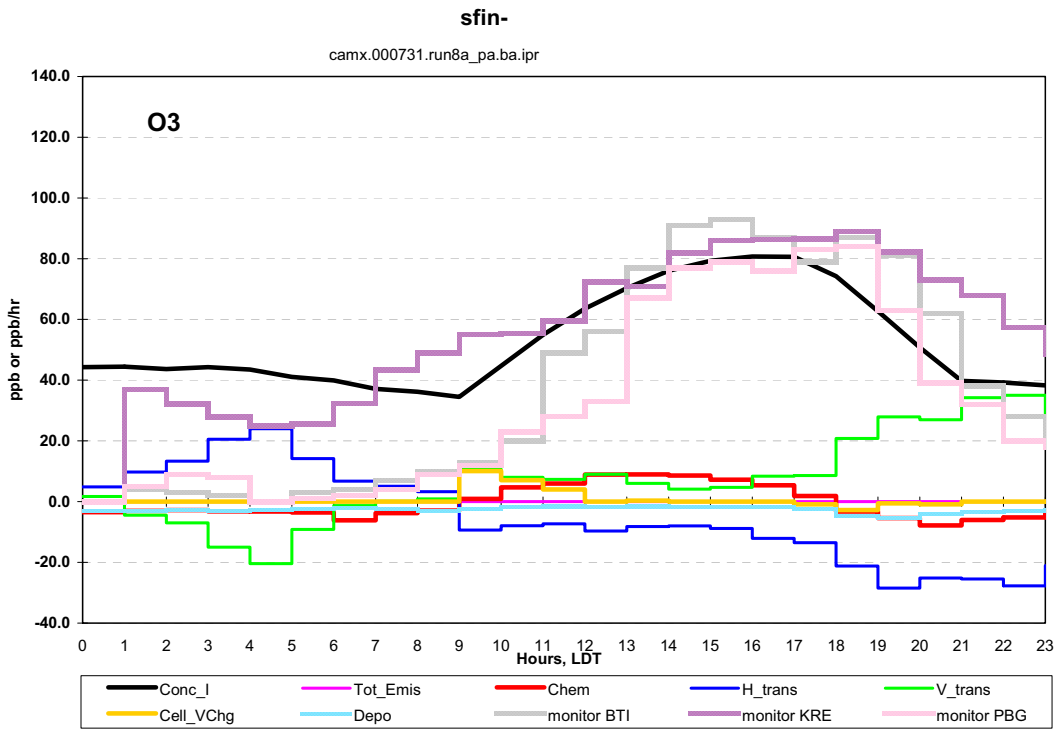

Figure 7-18. Ozone model concentrations and the processes that contribute to the final concentration for the northern ozone region. Observed data are shown from three monitor stations (BTI, KRE, PBG) as one hour averages.

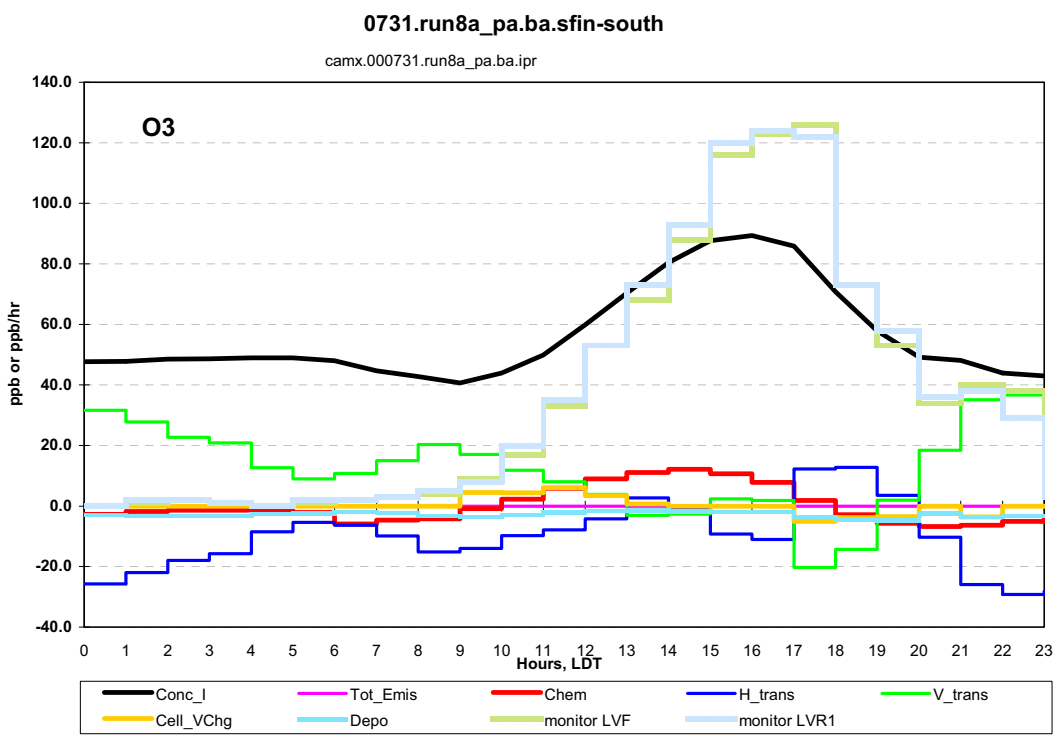

Figure 7-19. Ozone model concentrations and the processes that contribute to the final concentration for the southern ozone region. Observed data is shown from two Livermore monitor stations (LVF,LVR1) as one hour averages.

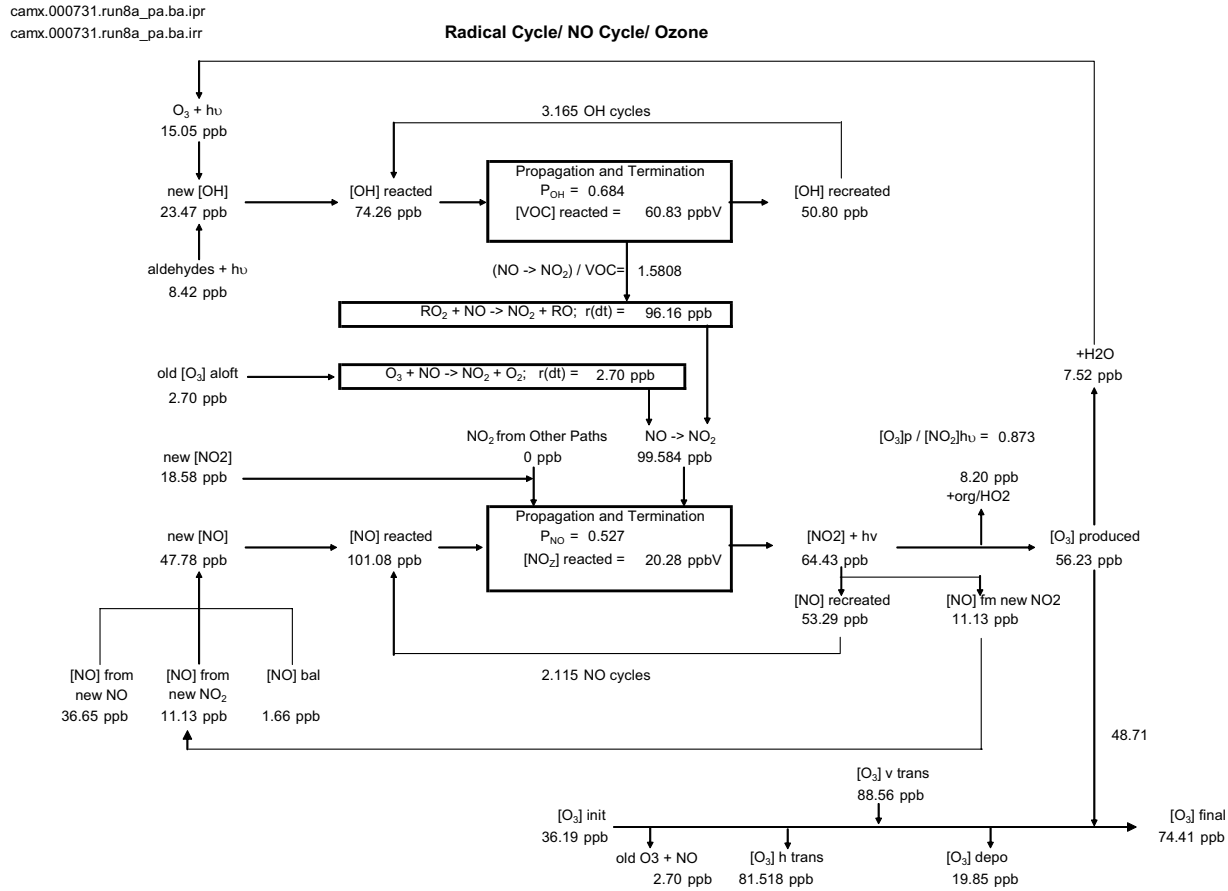

Figure 7-20. Ozone production diagram including radical and NOx cycles in the northern source region for hours 8-18.

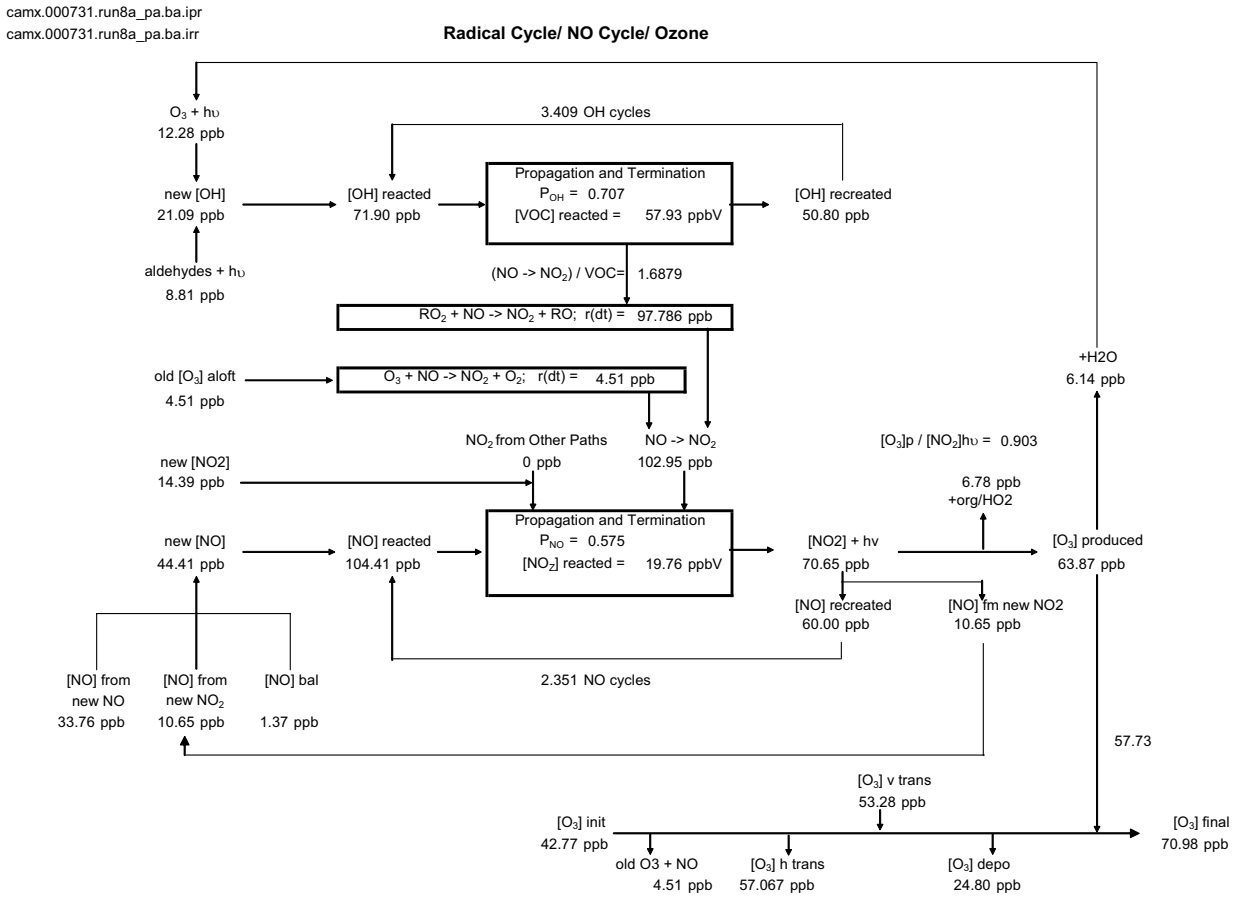

Figure 7-21. Ozone production diagram including radical and NOx cycles in the southern ozone region for hours 8-18.

full gridded CAMx model the areas of high ozone concentration occurred over natural areas where sufficient isoprene emissions mixed with pollutants from the urban plume.

The low concentrations of reactive VOCs in the atmosphere were not consistent with observed VOCs. The Bethel Island (BTI) station in the northern source region provided ground VOC data, but only at three hour averages and for a limited number of VOCs. In this region the model under predicts the amount of olefins and aldehydes in the atmosphere by a factor of 5. In the southern ozone region the Sunol (SUNO) ground station provided speciated VOC data at one hour averages for a limited number of VOCs. Similarly to the northern region, the model under predicts the amount of olefins, toluene, xylene, and aldehydes in the atmosphere by as much as a factor of 5. The model's inability to generate the observed concentrations of aldehydes could be evidence that the model is not fully capturing all the atmospheric VOC chemistry. However, some reactive olefins are also classified as ALD2 which points to an underrepresented emission inventory. Observed ethylene concentrations were consistent with model values. This suggests that the meteorology of the model has been properly simulated and is not the cause of the OLE/ALD2 discrepancies. Further investigation is needed to explore the discrepancies found in the OLE emission inventory. The strongest possibility for the low reactivity could be the lack of total VOC and/or the improper speciation of the general anthropogenic emission inventory.

USE OF THE DECOUPLED DIRECT METHOD FOR JULY 1999

The CARB has undertaken their own CAMx modeling of the July 1999 episode, using meteorological fields developed from their own in-house MM5 applications. They have reported very good air quality model performance for the Bay Area, Sacramento, and SJV areas for July 11 and 12. In contrast, the BAAQMD applications using a combination of RAMS and MM5 meteorology were not performing as well. It was noted that the CARB continued their use of a relatively shallow domain depth of 5 km and relatively high ozone top boundary conditions of 70 ppb (taken directly from their July/August 2000 applications). The basis for CARB's use of high top and lateral boundary conditions for the July/August 2000 case (established from SARMAP profiles) was the measured concentrations aloft attributed to the widespread fire activity. Given the lack of fires for the July 1999 episode, the lack of any aloft measurements, and the shallow domain depth, the question was posed as to whether their replication of high ozone throughout the state was serendipitously associated with high contributions from the boundaries.

To answer this question, the BAAQMD obtained the July 1999 CAMx configuration and input files from CARB and successfully replicated their results. ENVIRON invoked the Decoupled Direct Method (DDM) probing tool in CAMx v4.03 to investigate the sensitivity of ozone to boundary conditions of ozone, VOC, and CO[2]. Further, since this configuration led to acceptable ozone performance throughout the state, the DDM was used to assess ozone sensitivity to emission categories and source regions as a first glimpse into potential transport impacts. A brief summary of DDM is provided below, followed by the methodology and results of the analysis performed for the July 1999 episode.

[2] Note that for some unknown reason the CARB provided zero boundary conditions for NOx.

Description of DDM

The model sensitivity of one model parameter (e.g., ozone) to another parameter (e.g., NOx) is expressed as a differential d[O3]/d[NOx] that can be expanded into a Taylor series, where each term represents a successively higher-order contribution to the total sensitivity. The DDM treatment determines the first-order term of this differential; the output parameter is termed a "sensitivity coefficient." DDM can track and report the sensitivity of any species to any other species, whether the latter is generated from chemistry, initial/boundary conditions, or emissions.

The DDM thus provides some information on how the primary species concentration would change given a change in the secondary species. Since this approach determines only the first-order effect, DDM cannot explain the entire spectrum of impact that would actually result if CAMx were to be rerun with a specific change in the target species/source. As a rule of thumb, DDM can explain approximately 2/3 of the expected signal, with the higher order terms taking up the remaining 1/3. This means that DDM is accurate in explaining sensitivity from relatively modest changes in emissions, boundary conditions, or chemical production on the order of 20-30%. Larger relative changes lead to a stronger contributions from higher-order terms and thus reduce the representativeness of the DDM sensitivity coefficients. A more complete description of the CAMx DDM approach is provided in the model's User's Guide (ENVIRON, 2003).

Evaluation of Ozone Sensitivity to Boundary Conditions

An initial DDM run was conducted to test the influences of initial/boundary/top conditions provided to CAMx in the CARB configuration. DDM sensitivity coefficients were defined to separately track ozone, VOC, and CO on the north, east, west, south, and top boundaries, along with the initial conditions specified over the entire modeling grid at the start of the simulation. Plots of the resulting sensitivity coefficient fields for each species and source were plotted at 3 PM local time on July 11.

The baseline surface ozone distribution simulated by CAMx at 3 PM on July 11 is shown in Figure 7-22. High ozone near and above 120 ppb is seen ringing the Bay Area, and north of Sacramento. Elevated ozone can be seen from Modesto, Stockton, Fresno, and Bakersfield as well. Plots of the largest sensitivities are shown in Figures 7-23 through 7-25. Northern boundary ozone (Figure 7-23) shows contributions in the northwestern portion of the state and all along the California coastline (nearly identical transport patterns were seen for July/August 2000). The sea-breeze circulation into the Bay Area provides 10-15 ppb sensitivity in the east bay. One way to look at this result is that a scaling of the northern ozone boundary conditions by 10% would reduce the ozone signal in the east bay by 10%*(15 ppb), or a reduction of ~1.5 ppb. A 100% reduction would likely lead to a somewhat larger impact than 15 ppb because of DDM's lack of influence from the higher order terms.

Northern boundary VOC leads to a surprisingly large sensitivity in the east bay, approaching 15 ppb (Figure 7-24). This is due to transport along the coast (where very little chemistry is active to convert low-reactive VOC such as PAR) and the inland penetration with the sea breeze that mixes with local NOx emissions and generates a sudden ozone contribution. A similar pattern is seen for northern boundary CO, with a peak sensitivity of 6 ppb in the east bay (Figure 7-25). No significant contributions from any other species, from any other boundary (top included)

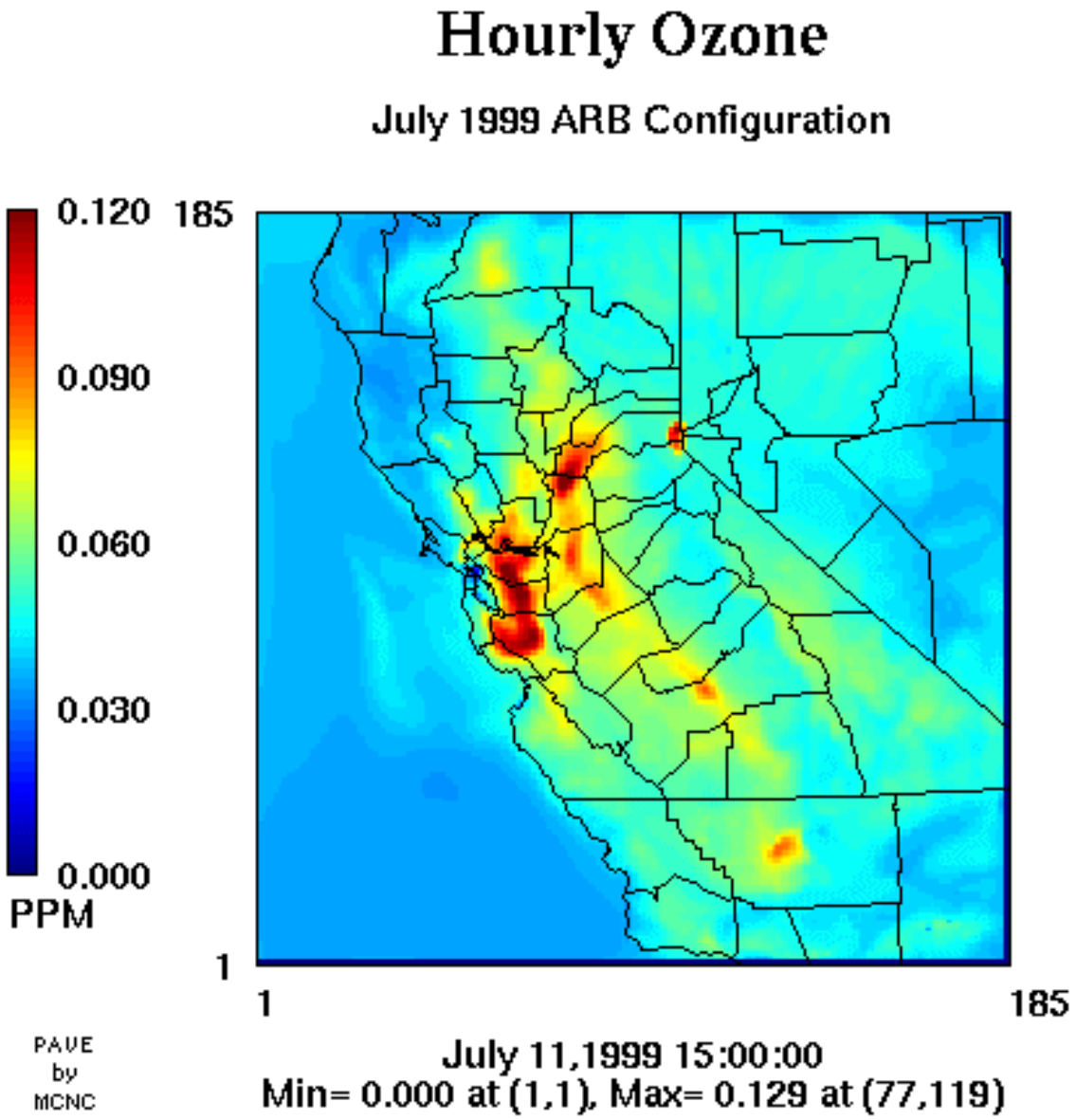

Figure 7-22. Simulated ozone (ppm) in the CCOS modeling domain at 3 PM local time on July 11, 1999 using the CARB CAMx configuration.

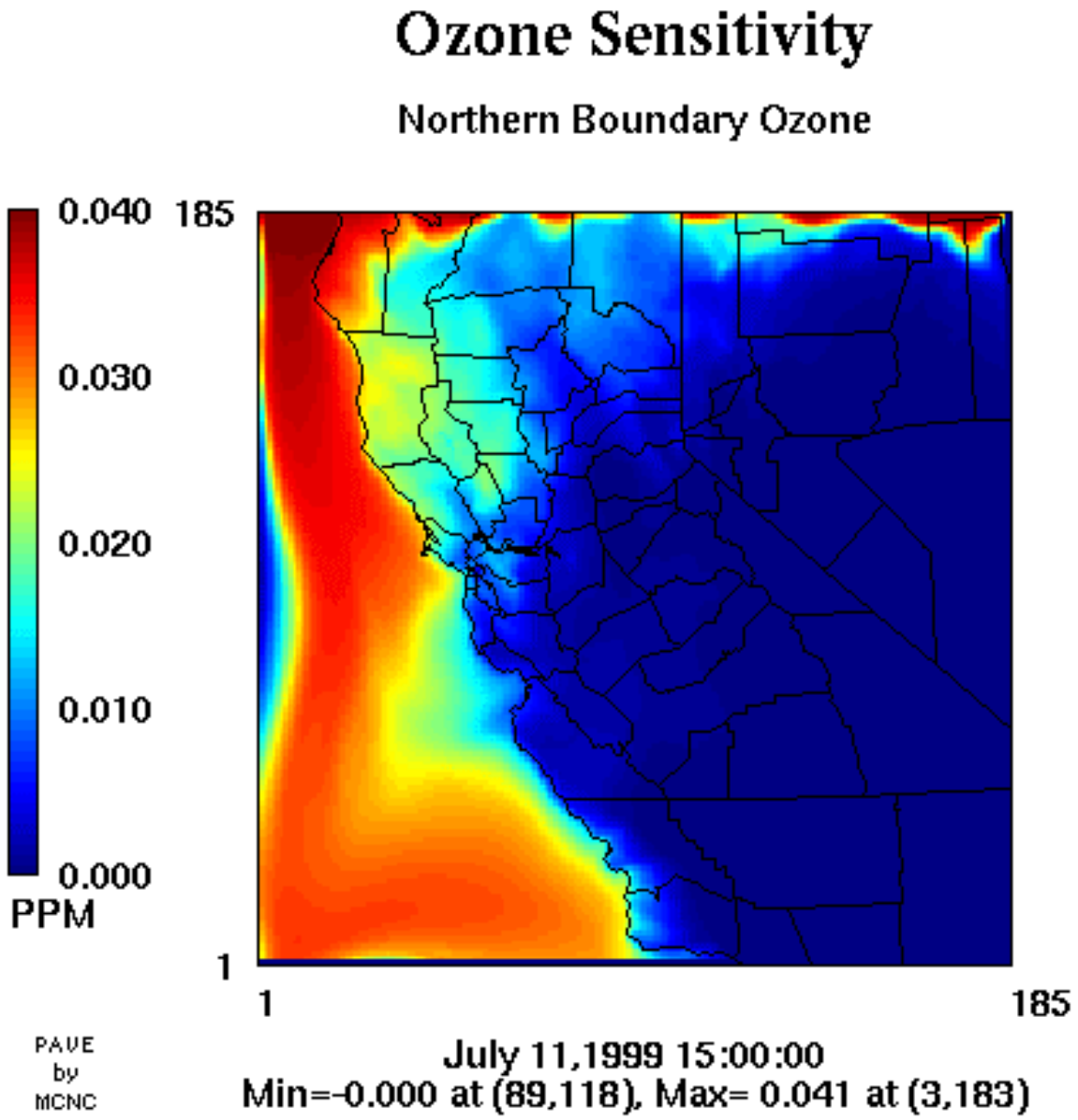

Figure 7-23. DDM ozone sensitivity coefficient field for northern boundary ozone at 3 PM local time on July 11, 1999.

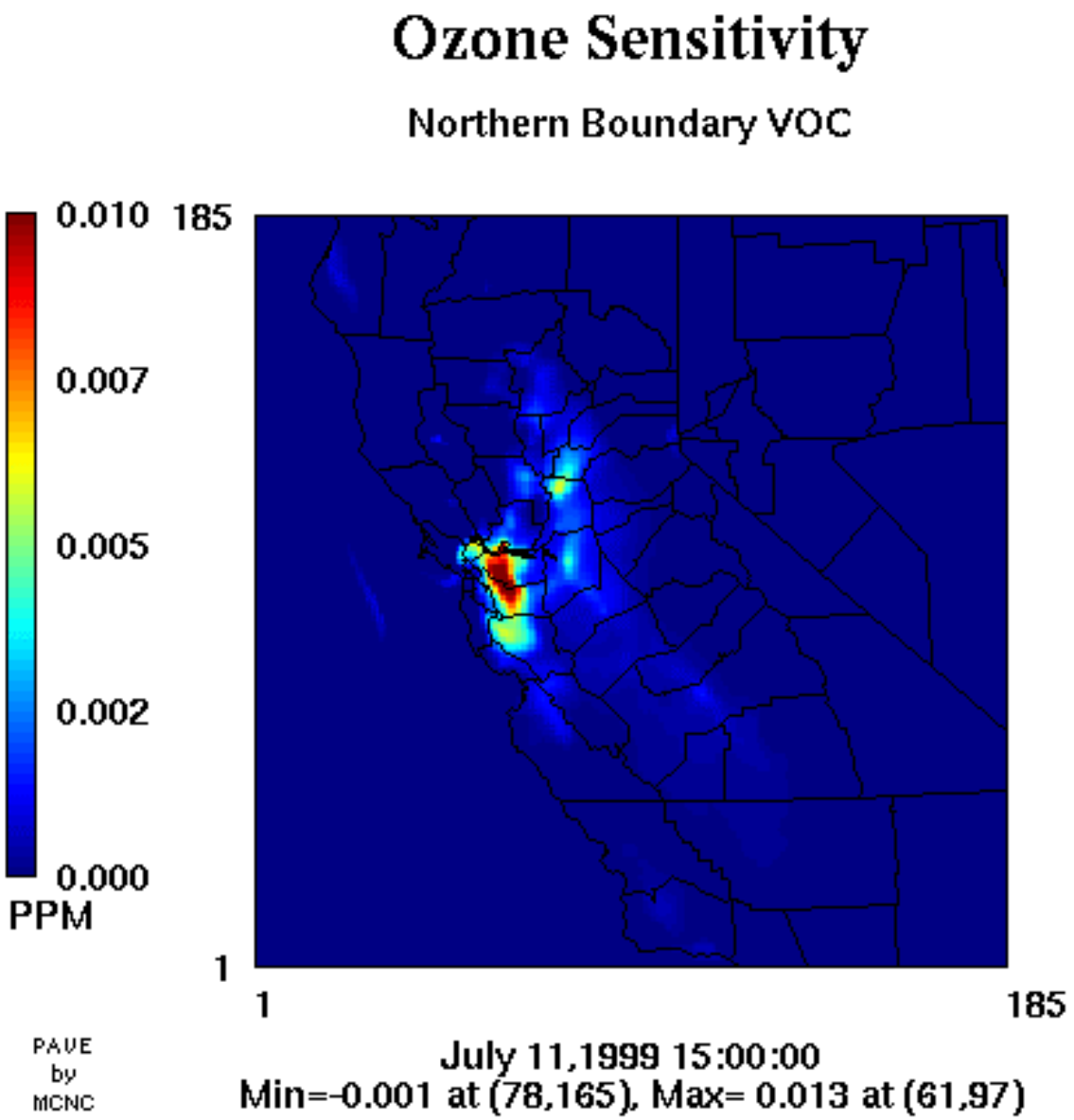

Figure 7-24. DDM ozone sensitivity coefficient field for northern boundary VOC at 3 PM local time on July 11, 1999.

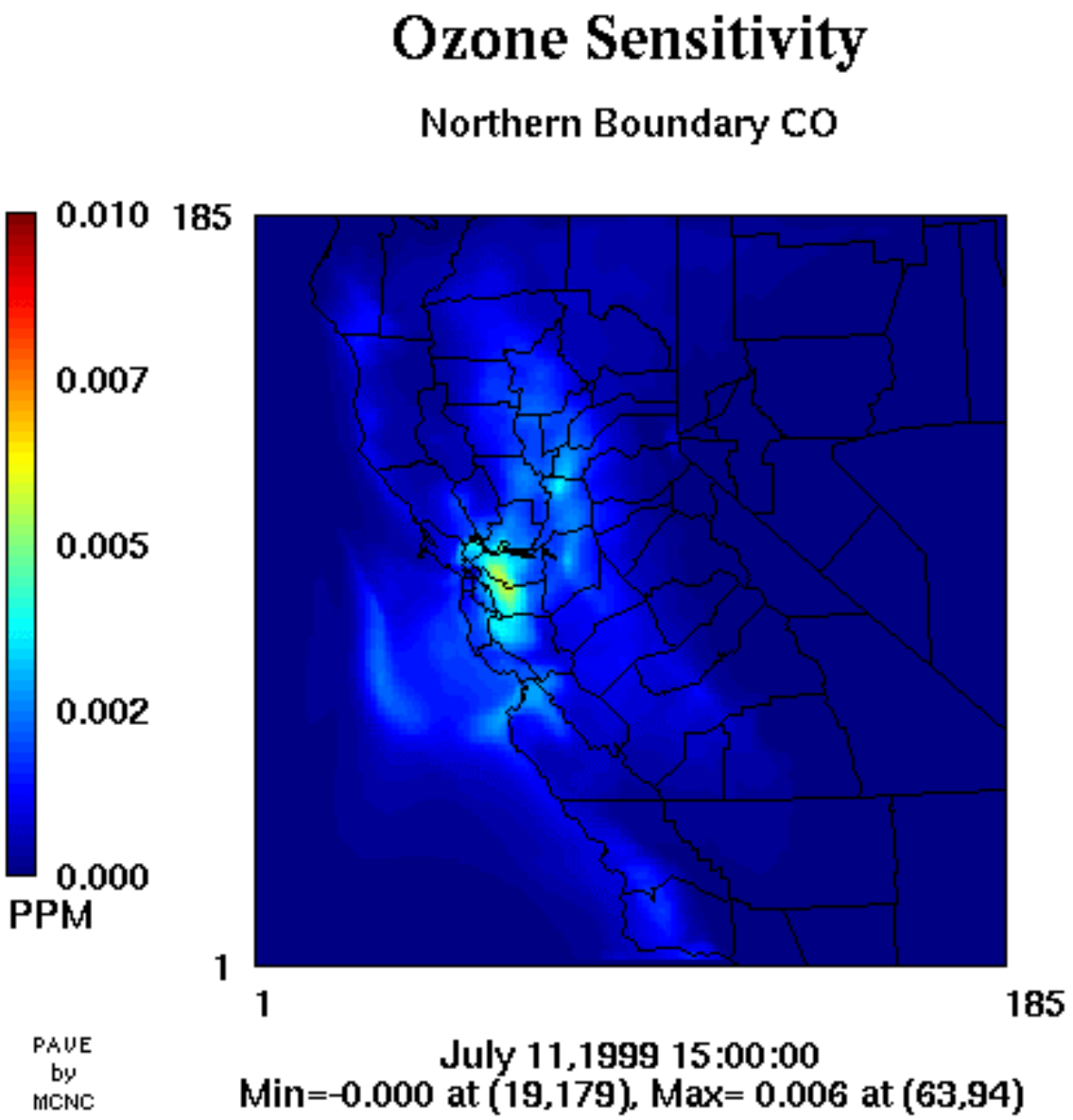

Figure 7-25. DDM ozone sensitivity coefficient field for northern boundary CO at 3 PM local time on July 11, 1999.

were seen in the Bay Area. The top boundary conditions resulted in the largest surface ozone sensitivity over the Sierras.

Total sensitivity from all species from the northern and top boundaries are plotted in Figure 7-26. A local peak sensitivity is seen in the east bay, due to the contribution from northern boundary ozone, VOC, and CO, while the high sensitivity over the Sierras is evident from the top boundary. In order to gauge the relative importance of these sensitivity levels, the plot in Figure 7-26 was normalized by the total ozone field in Figure 7-22 and is shown in Figure 7-27. Note that over the central valley in particular, there is no significant relative sensitivity to top or northern boundary conditions, with values of 20% or less.

In summary, the maximum sensitivity in the Bay Area relative to total peak ozone in the east bay is ~35% in these tests (mainly from north boundary ozone and VOC). However, the key result of this analysis is that the low model top and fairly large top boundary conditions specified in the CARB model configuration are not significantly impacting model performance in areas of central California where high ozone is simulated.

Evaluation of Ozone Sensitivity to Emissions

Two additional DDM runs were conducted to track ozone sensitivity to emissions of NOx, VOC, CO:

- Anthropogenic vs. biogenic emissions over the entire domain
- Total emission (anthropogenic + biogenic) from 5 source regions (see Figure 7-28).

The sensitivity coefficient fields for anthropogenic and biogenic NOx at 3 PM local time on July 11, 1999 are shown in Figure 7-29. The NOx-rich conditions that suppress ozone formation is quite obvious in the Bay Area, and near-zero sensitivity is seen for the central valley cities (as depicted by green "holes" in the plots). However, the rural central valley, and particularly rural Sacramento Valley and Sierra foothills are rather sensitive to anthropogenic NOx. Biogenic NOx is insufficient to generate more than a few ppb ozone anywhere in the domain. Figure 7-30 shows a similar plot for anthropogenic and biogenic VOC. Both emission sources show very similar results, and as expected the largest sensitivity is seen in the NOx-rich Bay Area (~60 and ~40 ppb, respectively). Smaller areas of sensitivity are seen in the central valley cities, with much lower sensitivity in rural areas of the central valley.

The sensitivity to NOx by source region is shown for the same date and time in Figure 7-31. For NOx originating in the Bay Area (Figure 7-31a), the largest positive and negative sensitivity exists within the Bay Area (although it is mostly negative). There is some minor sensitivity to Bay Area NOx in the southern Sacramento Valley and the northern SJV. For NOx originating in the central valley, there is only modest local positive NOx sensitivity, but it is practically zero in the urban areas.

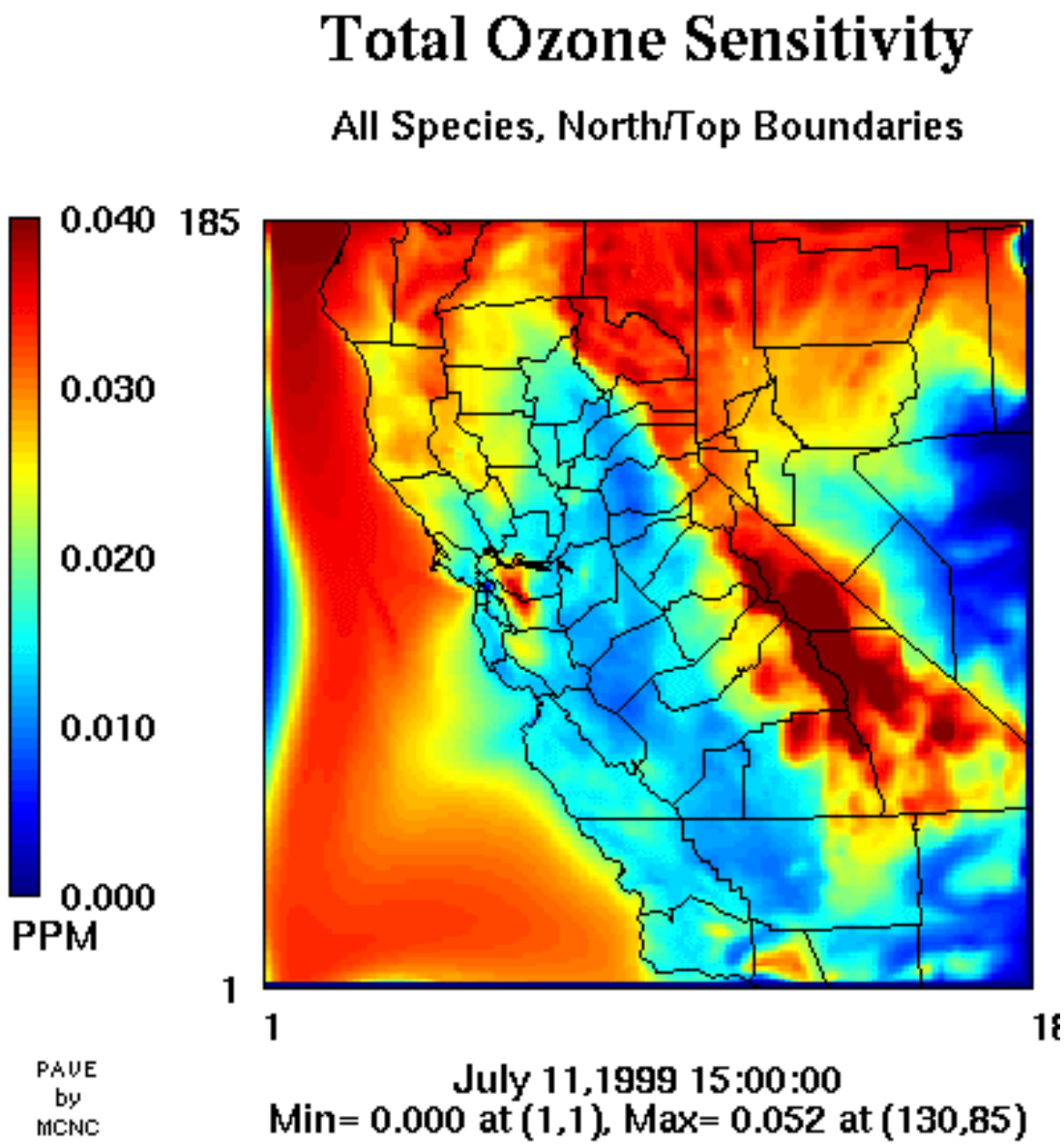

Figure 7-26. Total DDM ozone sensitivity coefficient field for northern and top boundary conditions (all species) at 3 PM local time on July 11, 1999.

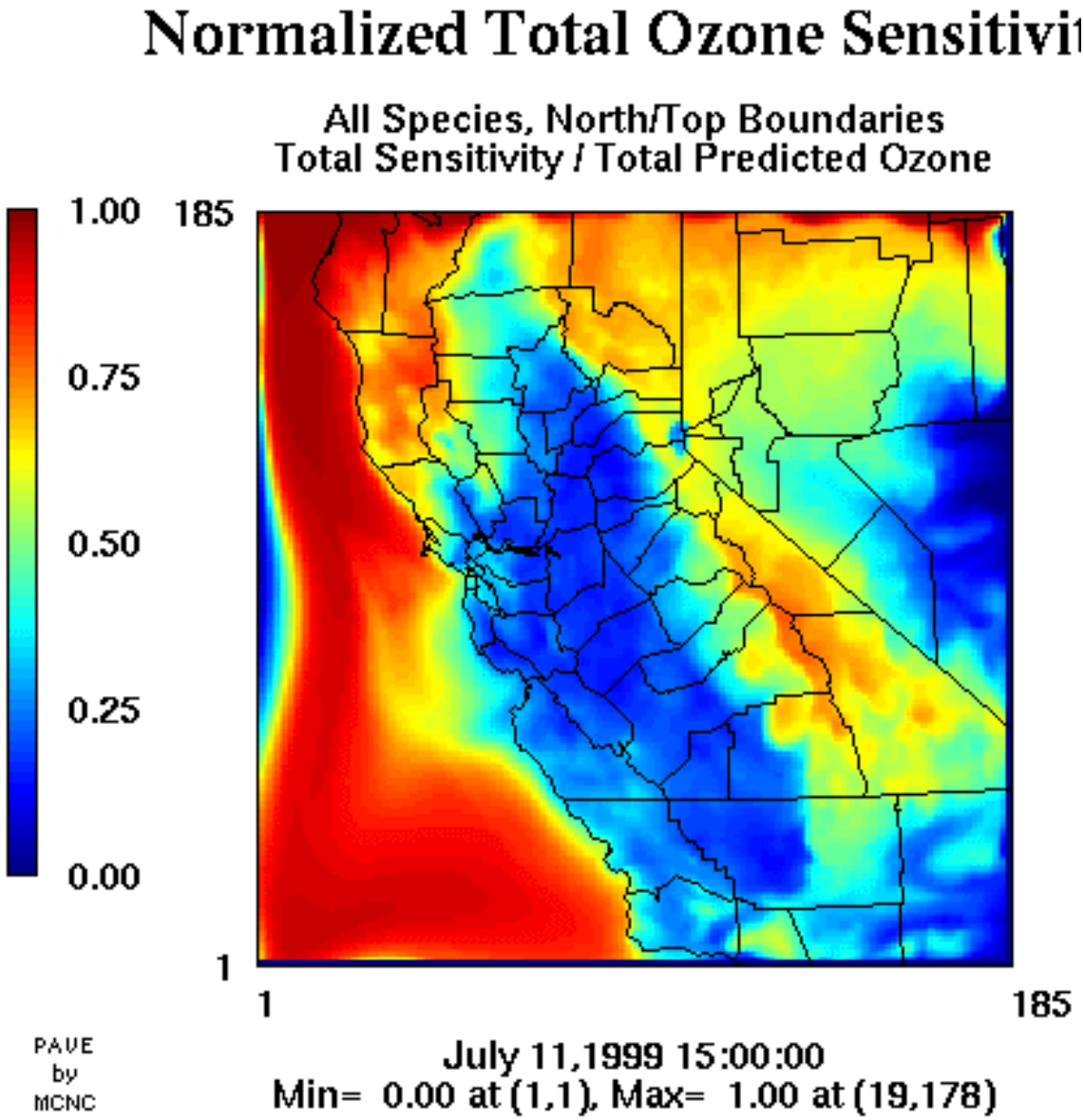

Figure 7-27. Total DDM ozone sensitivity coefficient field for northern and top boundary conditions (all species) normalized by the total ozone field at 3 PM local time on July 11, 1999.

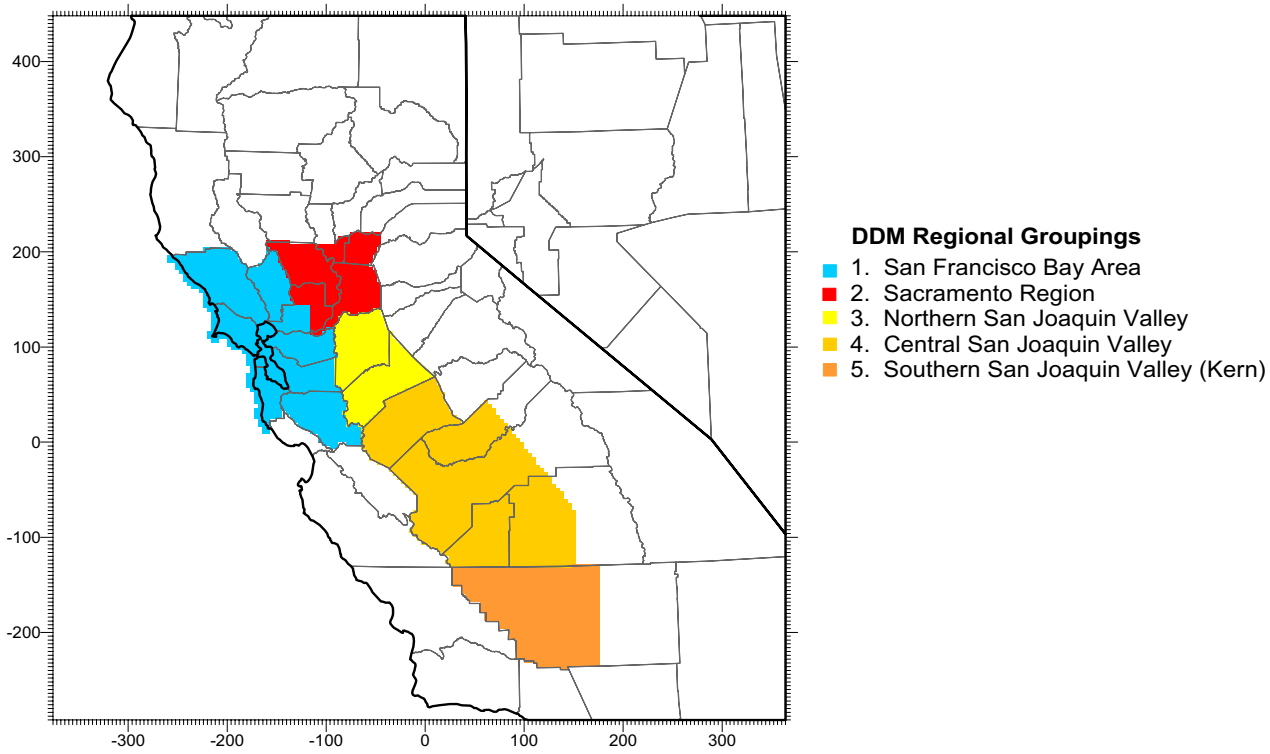

Figure 7-28. Definition of source regions for the CAMx DDM application.

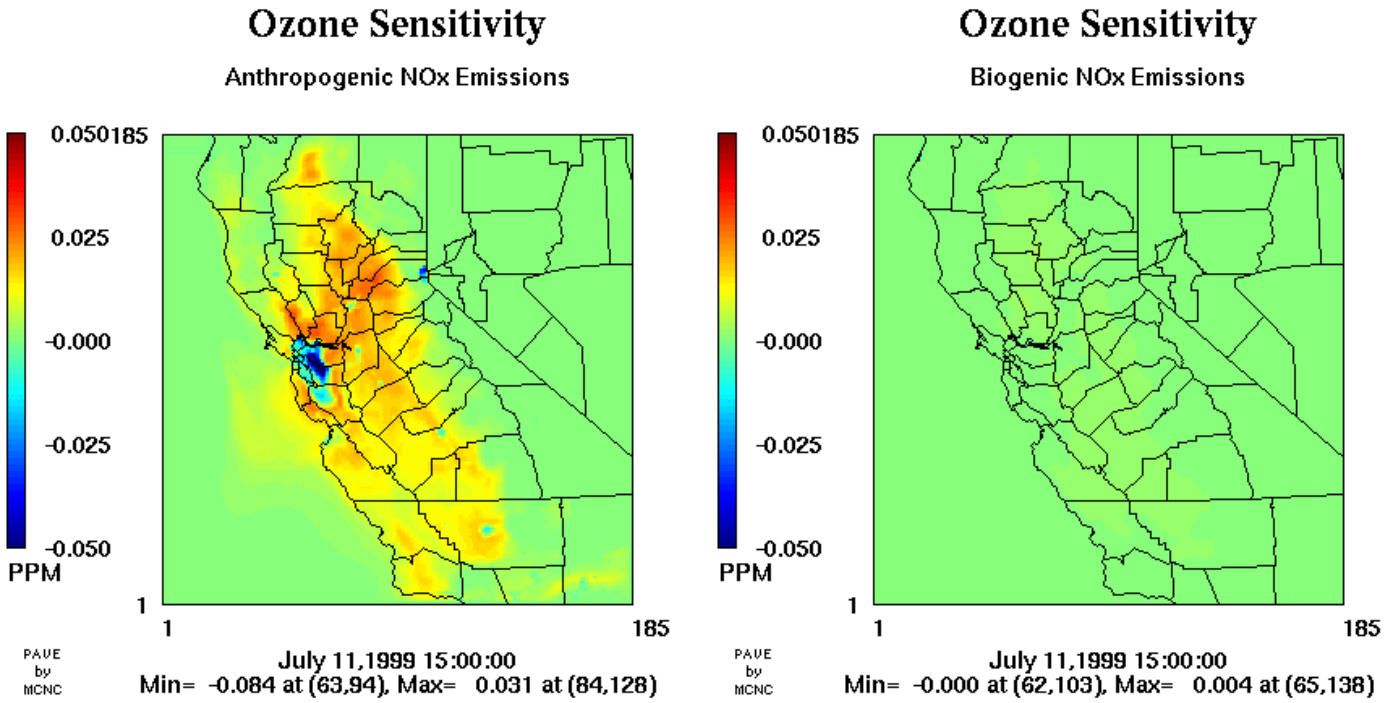

Figure 7-29. DDM ozone sensitivity coefficient field for anthropogenic and biogenic NOx emissions at 3 PM local time on July 11, 1999.

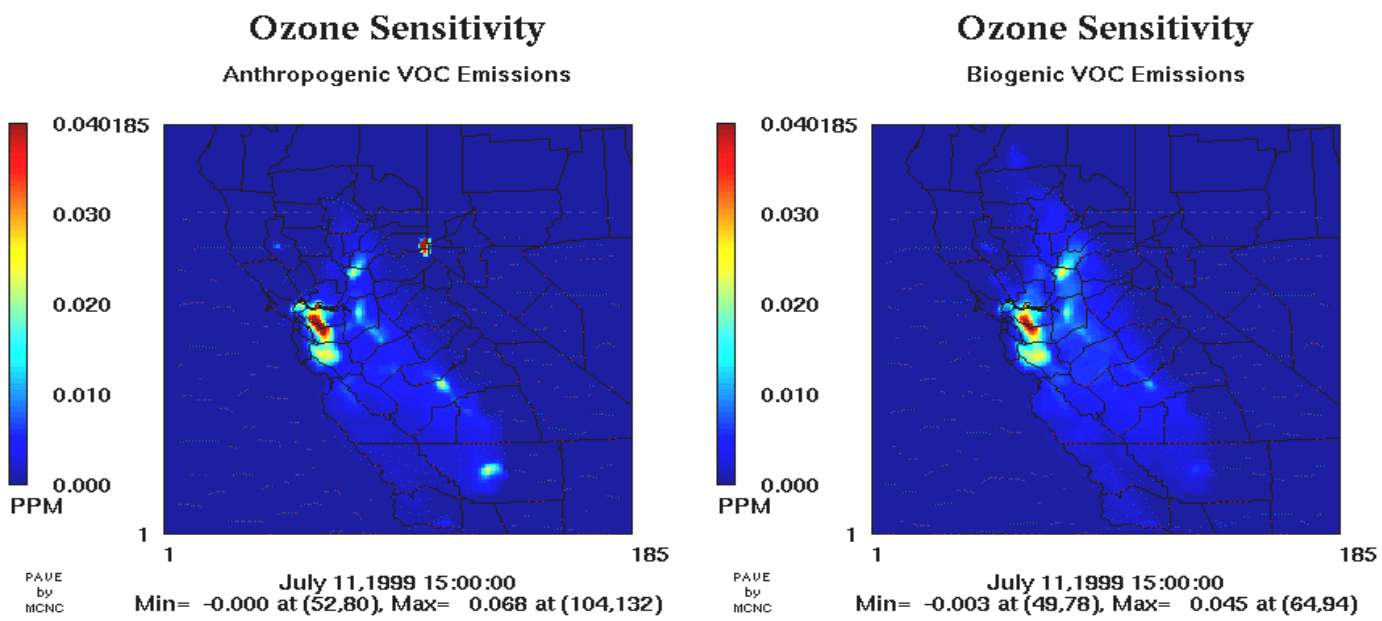

Figure 7-30. DDM ozone sensitivity coefficient field for anthropogenic and biogenic VOC emissions at 3 PM local time on July 11, 1999.

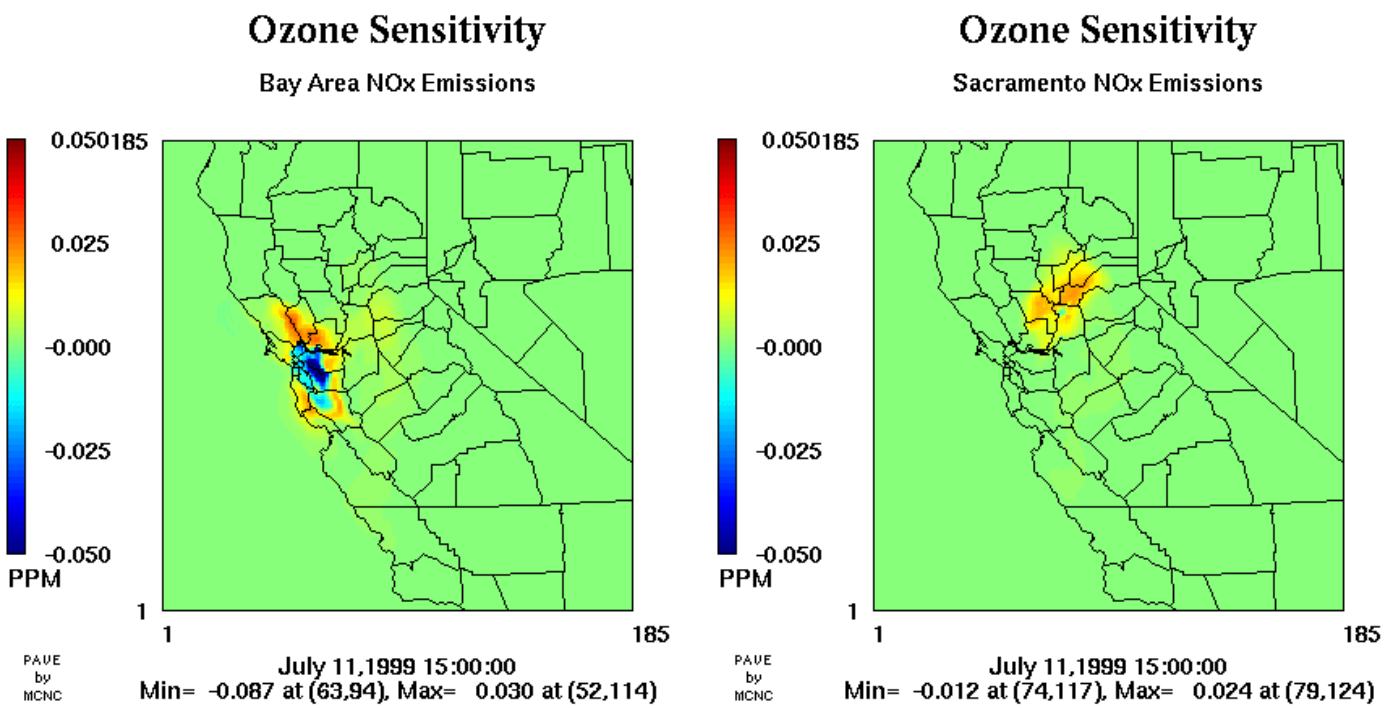

Figure 7-31. DDM ozone sensitivity coefficient field for (a) total NOx emissions from the Bay Area and (b) total NOx emissions from Sacramento at 3 PM local time on July 11, 1999.

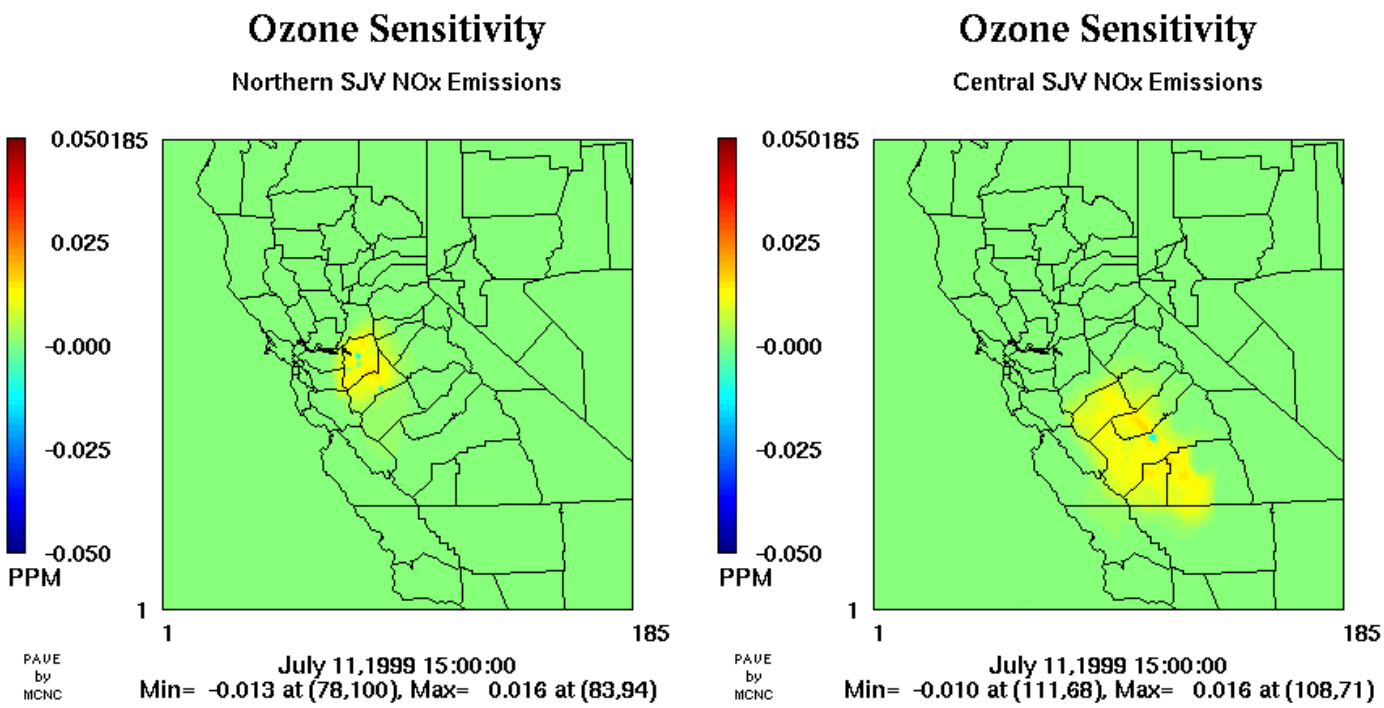

Figure 7-31 (continued). DDM ozone sensitivity coefficient field for (c) total NOx emissions from the northern SJV and (d) total NOx emissions from the central SJV at 3 PM local time on July 11, 1999.

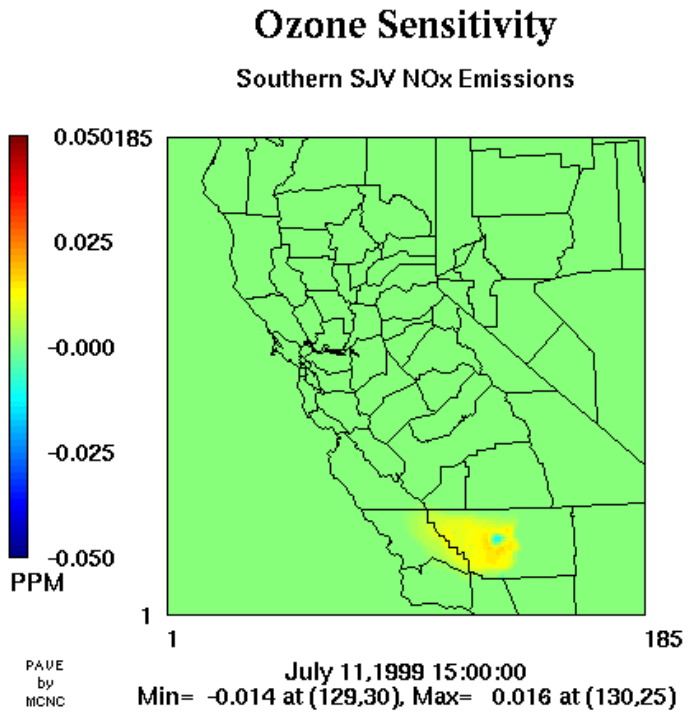

Figure 7-31 (concluded). DDM ozone sensitivity coefficient field for (e) total NOx emissions from the southern SJV at 3 PM local time on July 11, 1999.

The sensitivity to VOC by source region is shown in Figure 7-32. Again, the Bay Area shows the highest VOC sensitivity; the maximum exists in the east bay and is nearly co-located with the maximum negative NOx sensitivity. In the central valley, the urban areas are most sensitive to VOC. Ozone in rural southern Sacramento and northern SJV are about equally sensitive to local and Bay Area-generated VOC. The CO pattern by source region (not shown) is very similar to the VOC pattern, but at much lower levels.

In summary, ozone sensitivity to emissions is much larger than to boundary conditions. Ozone is nearly as sensitive to biogenic VOC than anthropogenic VOC in all regions. The Bay Area shows the most sensitivity to NOx, VOC, and CO emissions. More anthropogenic and/or biogenic VOC will increase ozone in the east bay, while less anthropogenic NOx will also increase ozone. A weaker or delayed sea breeze can delay the onset of negative NOx sensitivity from moving into the Concord and Livermore areas.

Ozone in the southern Sacramento and northern SJV regions is modestly sensitive to Bay Area NOx and VOC emissions (sensitivity coefficients are ~10 ppb). In the central valley, ozone in the major urban areas is insensitive to NOx, but very sensitive to VOC; rural areas are equally or more sensitive to NOx than VOC.

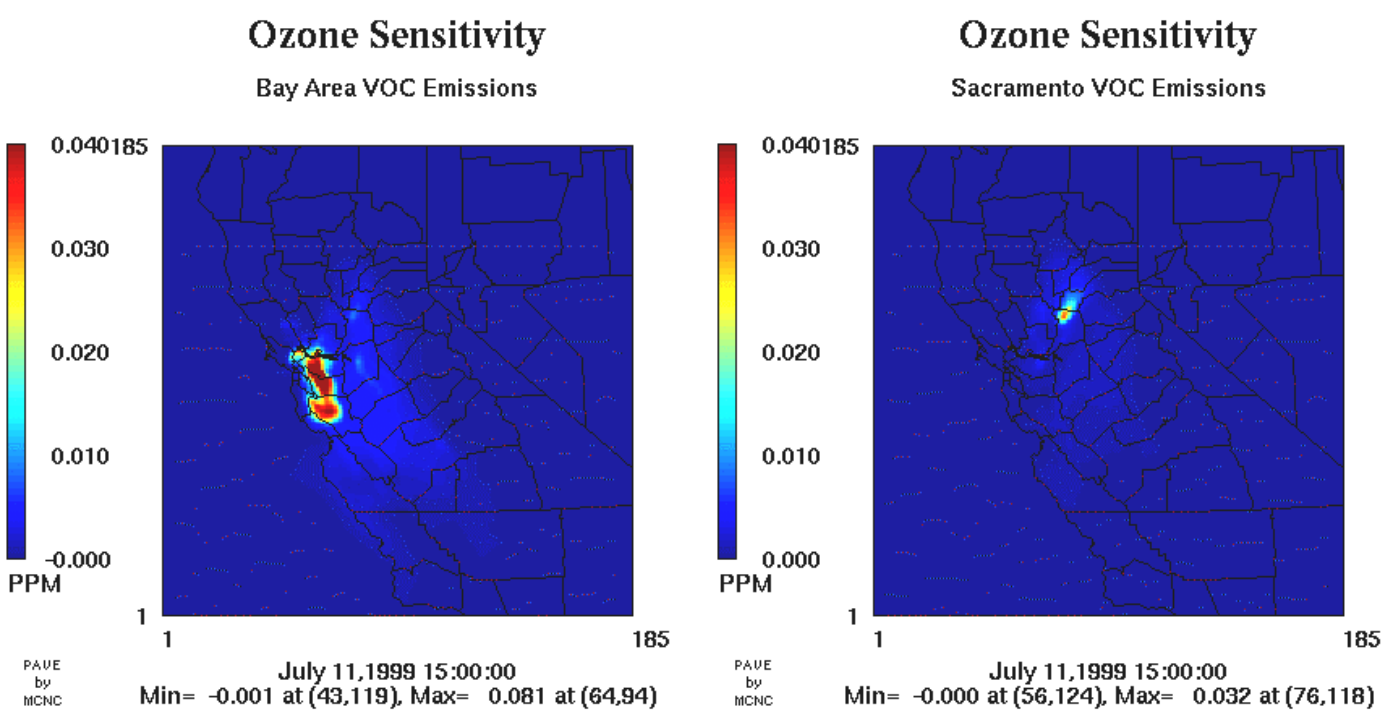

Figure 7-32. DDM ozone sensitivity coefficient field for (a) total VOC emissions from the Bay Area and (b) total VOC emissions from Sacramento at 3 PM local time on July 11, 1999.

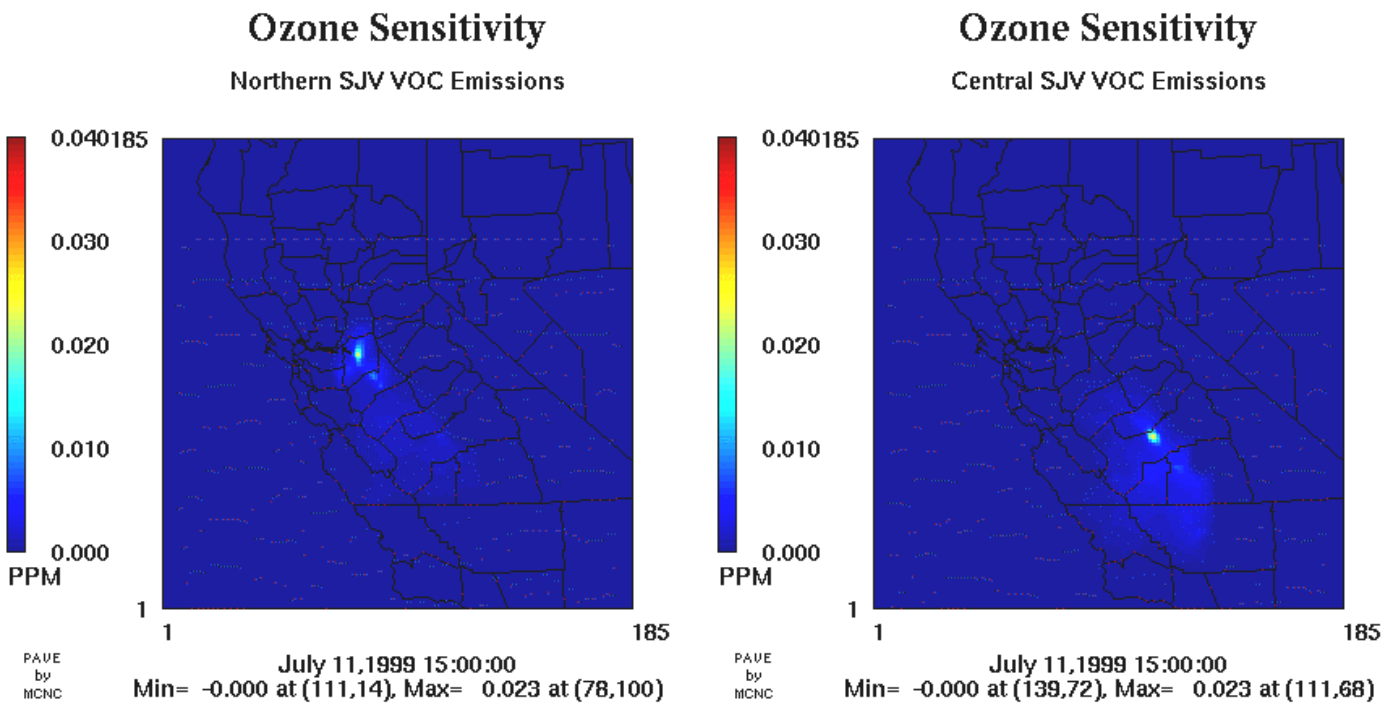

Figure 7-32 (continued). DDM ozone sensitivity coefficient field for (c) total VOC emissions from the northern SJV and (d) total VOC emissions from the central SJV at 3 PM local time on July 11, 1999.

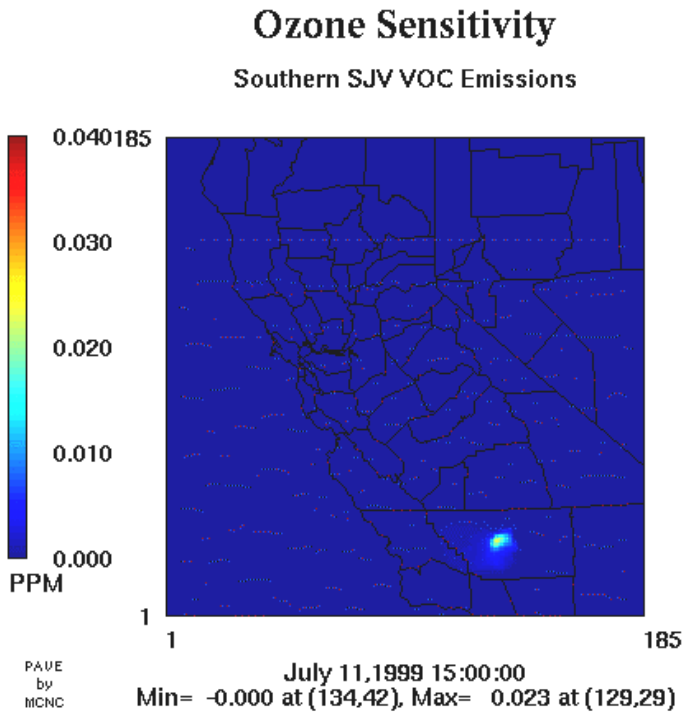

Figure 7-32 (concluded). DDM ozone sensitivity coefficient field for (e) total VOC emissions from the southern SJV at 3 PM local time on July 11, 1999.

BAAQMD CAMx APPLICATIONS FOR CCOS 2000

Previous photochemical modeling studies conducted for central California have shown mixed results in terms of the benefit of applying FDDA in generating meteorological fields for the purpose of improving simulations of ozone. Tanrikulu et al. (2000) applied FDDA in the MM5 meteorological model and produced improved statistical performance for wind and temperature fields, which in turn improved ozone modeling. Umeda and Martien (2002) applied FDDA in the RAMS meteorological model and also improved statistical performance of meteorological fields. However, they showed that the photochemical model performance did not improve when they used the meteorological fields generated with FDDA. In this section, we build on these earlier studies, by applying the CAMx version 4.03 using the BAAQMD MM5 simulations described at the end of Section 4:

- Run 1 used the Noah Land-Surface Model (LSM; Chen and Dudhia, 2001) without FDDA;
- Run 2 used the Noah LSM with analysis nudging on the 36-km domain and observational nudging on the 4-km domain;
- Run 3 used the 5-layer soil model (Dudhia, 1996) without FDDA.

The two objectives are, first, to present the ozone performance in central California for this modeling system with Run 3 meteorological fields, and second, to determine whether the meteorological fields with the best statistical performance necessarily generate the best ozone performance. To carry out the second objective, we investigate the importance of relatively subtle flow features, such as the location of a mesoscale convergence zone, to the photochemical modeling. Such features cover a small geographic area and may therefore be given little weight in a statistical evaluation of the meteorological model performance, but they could have a significant influence on the location and timing of peak ozone values, which are important in regulatory modeling applications.

Model Description and Inputs

CAMx was run for a 5-day period for each of the three MM5 meteorological inputs described above. For easy reference, the CAMx runs are referred to as Run 1, Run 2 and Run 3, corresponding to the names of the three MM5 runs described at the end of Section 4. All simulations started on 0400 PST on July 29, 2000, and continued to 0000 PST on August 3, 2000. All simulations described here applied the SAPRC-99 chemical mechanism (Carter, 2000). Day-specific emissions for point, area, biogenic, and on-road mobile sources for this modeling period were prepared by the CARB. Initial and boundary conditions were adapted from those used in the SARMAP air quality modeling (DaMassa et al., 1996). As described in Section 6, these boundary conditions were modified slightly based on an average of four CCOS aircraft flights collected over the Pacific Ocean at about 250 km offshore.

Results

Figure 7-33 shows the peak simulated ozone distribution in Run 3 over the entire CCOS domain at 1600 PST, July 31, 2000, the date and time of the peak simulated ozone in the SFBA. There is a clear relationship between the areas of predicted high ozone and the distribution of the region's

metropolitan areas and a large forest fire that occurred during this period. Figure 7-33 shows five areas of high ozone mixing ratios in the Central Valley. Starting from the north, there is an area of high ozone just east of Sacramento, followed to the south by regions of high ozone close to the two Central Valley cities of Stockton and Modesto. Continuing further southward, there is an ozone high just south of Fresno and another near Bakersfield. The high ozone northeast of Bakersfield in the southern Sierra Nevada is due to the Manter forest fire, which had burned more than 60,000 acres by July 31, 2000.

A scatter plot of simulated versus observed surface-level ozone (Figure 7-34) shows a reasonable degree of correlation for each of the three days. The correlation coefficient of the linear regression for the three days combined is 0.78. The slope of the regression equation is 0.92 and the intercept is 0.2 ppb. However, there are some disagreements between predicted and observed peak values. There is an over prediction of the daily maximum ozone in the Sacramento Valley on July 31 (crosses in Figure 7-34). The simulated maximum ozone for July 31 in the Sacramento area was 145 ppb, whereas the observed maximum was 103 ppb. In the San Joaquin Valley, the simulated maximum ozone for July 31 was 132 ppb (outside the area obviously influenced by the Manter forest fire) versus the observed 115 ppb. However, this over prediction problem is not systematic. The model under predicted the daily maximum ozone in the Sacramento area by 9 ppb on August 1 (circles) and in the San Joaquin Valley by 38 ppb on August 2 (triangles), respectively – the days when each area exceeded the federal 1-hour ozone standard.

Table 7-3 shows the three key EPA 1-hour ozone performance statistics for three regions: the SFBA, the Sacramento area and the San Joaquin Valley. In computing the unpaired peak prediction accuracy, the predicted peak is taken within a 25 km radius of the location of the observed peak for a given region. In computing the normalized bias and error, the predicted ozone is paired (in time and space) to the observed value. Prediction-observation pairings in which the observation was below 40 ppb were not included in the statistics. Table 7-3 shows that most of the statistics are within the EPA's suggested performance criteria, according to their 1-hour ozone modeling guidance (EPA, 1991). The features of the predicted ozone described here for Run 3 also appear in Run 1 and Run 2. There are slight differences in the locations and the values of the maximum ozone among these runs. Yet, these slight differences can have important implications for regulatory applications. A detailed discussion of the differences among the runs for the SFBA on July 31 will be presented in the next subsection.

Table 7-3. Model performance statistics for Run 3.

Day	**7/31/2000**			**8/1/2000**			**8/2/2000**		
Statistic	UPP (%)	NB (%)	NE (%)	UPP (%)	NB (%)	NE (%)	UPP (%)	NB (%)	NE (%)
SFBA	-2	15	22	-16	-16	26	10	-12	27
Sacramento Area	11	9	20	-6	-21	25	12	-2	26
San Joaquin Valley	12	3	19	9	-3	22	-23	-10	26

EPA guidance suggests that the unpaired peak prediction accuracy (UPP) should be within ± 20%; the normalized bias should be within ± 15%; and the normalized error should be < 35%.

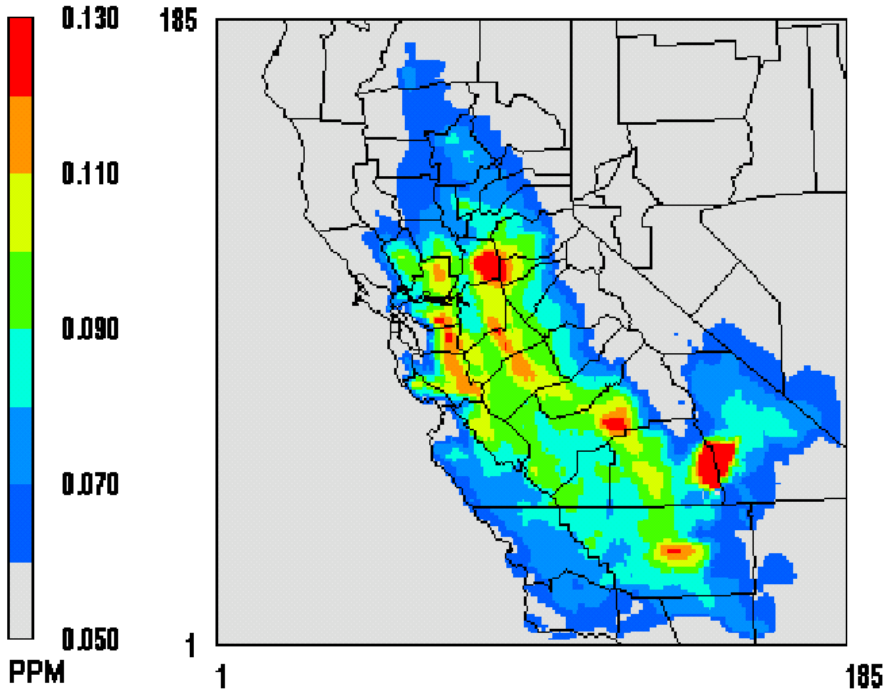

Figure 7-33. Simulated ozone distribution in Run 3 over the CCOS domain at 1600 PST, July 31, 2000.

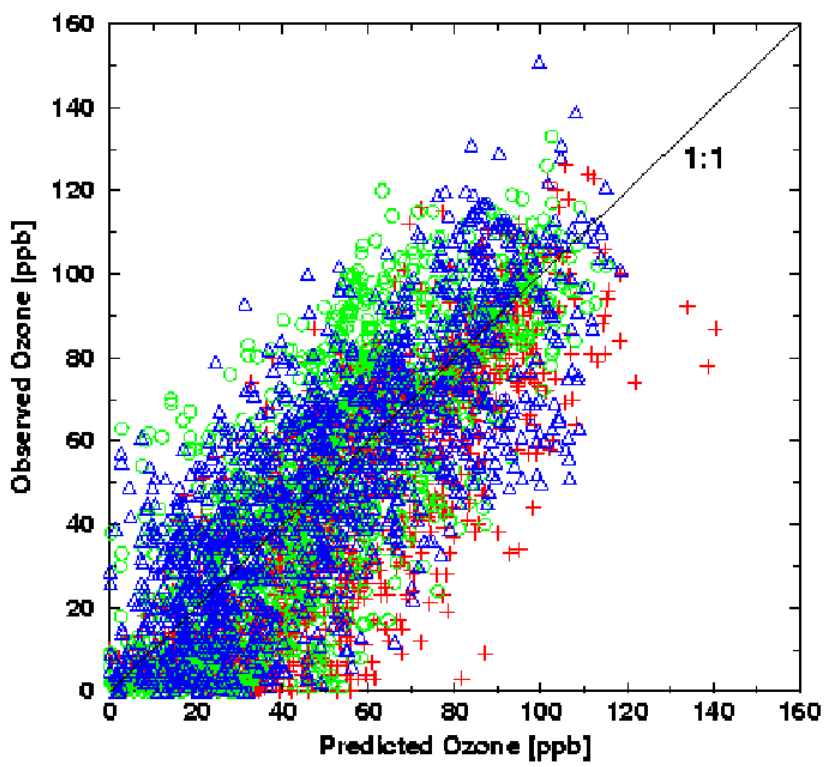

Figure 7-34. Scatter plot of observed and simulated ozone with Run 3 meteorological inputs for July 31 (crosses), August 1 (circles), and August 2 (triangles).

Simulated Ozone Distribution in the SFBA on July 31, 2000

As mentioned in Section 2, the ozone exceedances at Livermore account for nearly half of the total ozone exceedance in the SFBA. Livermore is situated in the south end of the Tri-Valley, an L shaped valley area that roughly connects Concord to Livermore. A major highway (I-680) runs north-south in the western part of the valley and another highway (I-580) runs east-west in the southern part of the valley. The traffic is often congested on both highways and the mountains around the valley channel the local winds and reduce their speed.

Figure 7-35 shows the wind pattern at 1400 PST, July 31, 2 hours before the observed ozone maximum at Livermore. The wind coming from the Pacific Ocean splits into two branches after entering the San Francisco Bay: one tends southward toward the Santa Clara Valley, and the other tends northward through the Carquinez Strait. The northwesterly wind at the north end of the Tri-Valley is correlated with high ozone in Livermore. Several large refineries and power plants are located along the Carquinez Strait. We suspect that this northwesterly wind transports additional emissions to Livermore. It may be the combination of the abundant emission sources and the enclosed valley that make the Livermore area particularly conducive to the formation of high ozone.

The simulated ozone distribution in the SFBA for Run 3 at 1600 PST, July 31, 2000 is shown in Figure 7-36. The ozone mixing ratios are less than 60 ppb by the coast and in the central urban region rimming the San Francisco Bay. The predicted high ozone in the northeastern corner of Figure 7-36 is located downwind of Sacramento. In the SFBA, there is an arc-shaped line of high ozone surrounding Livermore. The maximum simulated ozone in the SFBA was 123 ppb 16 km north of Livermore. The maximum observed ozone at Livermore was 126 ppb.

Figure 7-37 shows the MM5-generated surface-level wind vectors superimposed on the ozone distribution. One of the most prominent features of this wind field is the strong sea breeze, which transports the relatively clean offshore air to the onshore coastal areas. Over the land, this simulation captured most of the main wind features presented in Figure 7-35: the northward and southward branching of the wind over the San Francisco Bay, the northwesterly flow at the north part of Tri-Valley, and the wind convergence near Livermore. Just east of Livermore, the direction of the wind is from north, matching the observed wind direction. Figure 7-37 also indicates that, in this particular case, the wind and emissions did not pass over the Altamont Pass (between Livermore and Tracy) to the Central Valley. There is a close association between the location of maximum wind convergence and the location of the peak ozone. This association between convergence zones and peak ozone also exists in Run 1 and Run 2 simulations.

The overall simulated ozone distribution and wind pattern at 1600 PST, July 31, 2000 for Run 1 (Figure 7-38) and Run 2 (Figure 7-39) are quite similar to those for Run 3. There are some subtle differences in the Tri-Valley area. The wind in Run 1 has a more westerly component south of the Carquinez Strait. This may prevent the stationary-source emissions along the Strait from entering the Tri-Valley. Near Livermore, the westerly wind is also stronger. These stronger westerly winds can be attributed to the stronger temperature contrast between the ocean and the Central Valley in the runs with the Noah LSM. The effect of this stronger westerly is to move the southern part of the high ozone area further to the east, from near Livermore to Tracy, a station 20 km east of Livermore. The northern part of the high ozone area also moved eastward slightly. The simulated maximum ozone is located 23 km northeast of Livermore with a magnitude of 120 ppb.

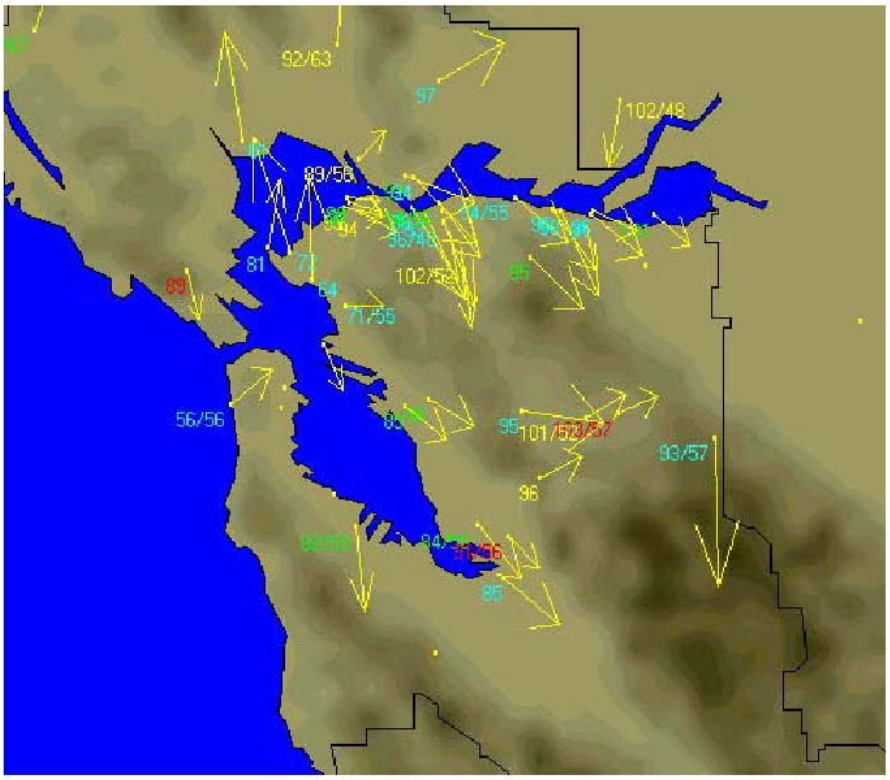

Figure 7-35. The wind distribution in the SFBA at 1400 PST, July 31, 2000.

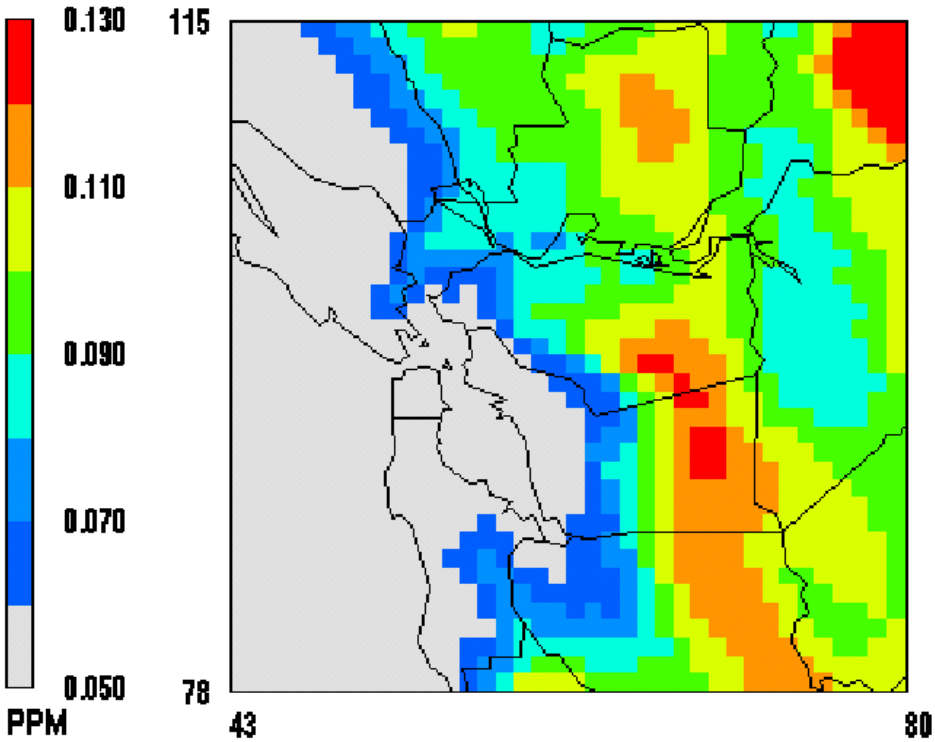

Figure 7-36. The simulated ozone distribution over the SFBA for Run 3 at 1600 PST, July 31, 2000.

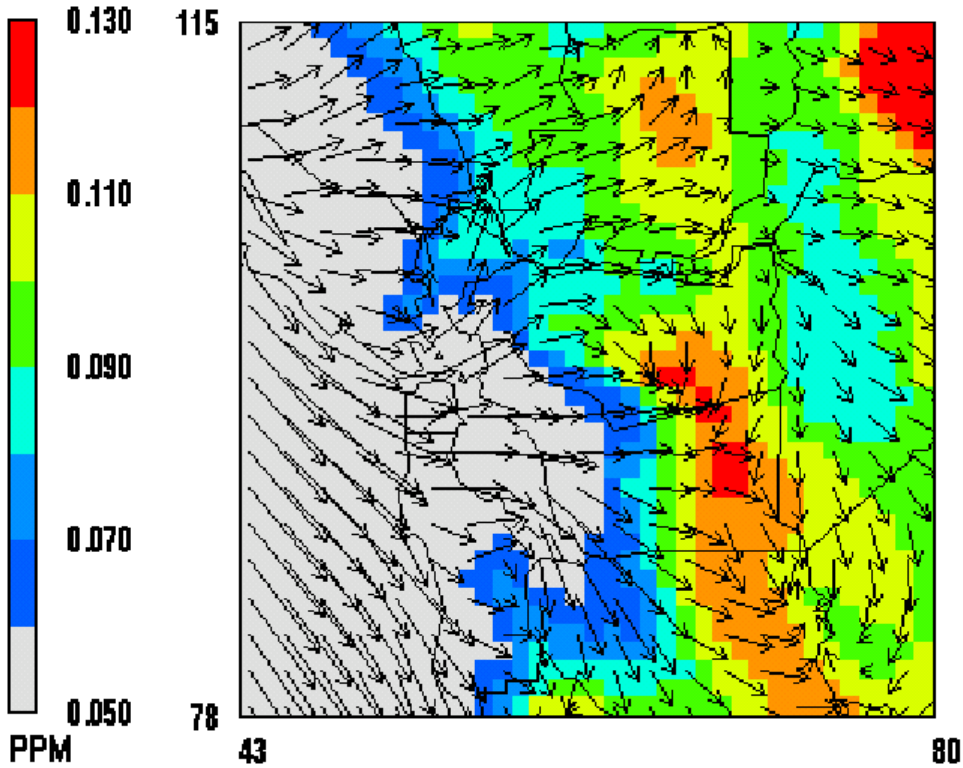

Figure 7-37. The simulated ozone distribution over the SFBA for Run 3 at 1600 PST, July 31, 2000, with wind vectors overlaid.

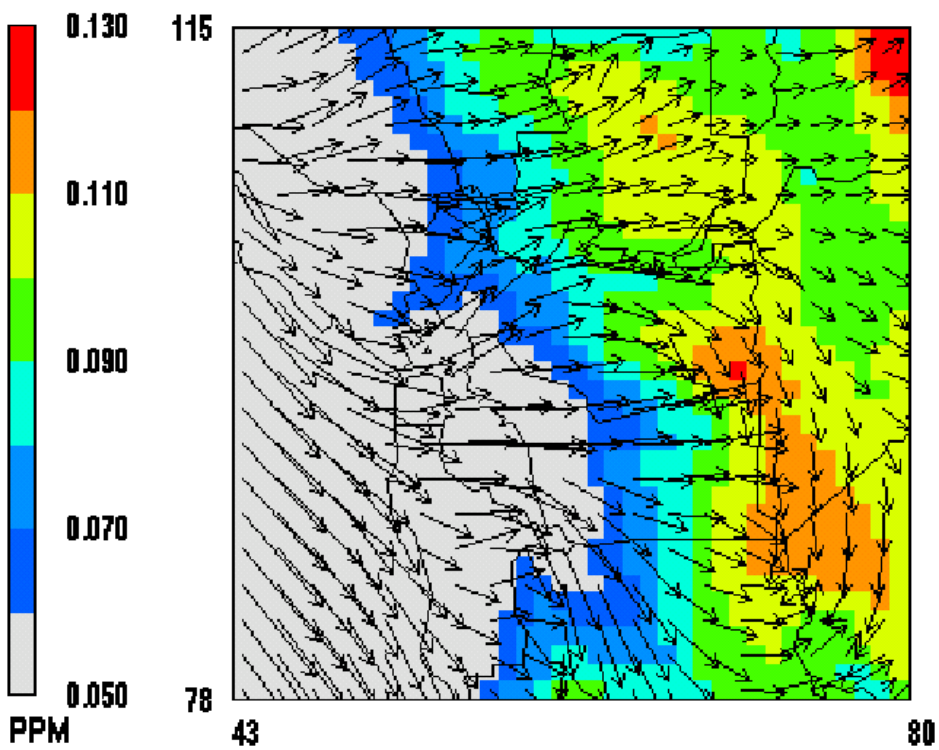

Figure 7-38. As in Figure 7-37, but for Run 1.

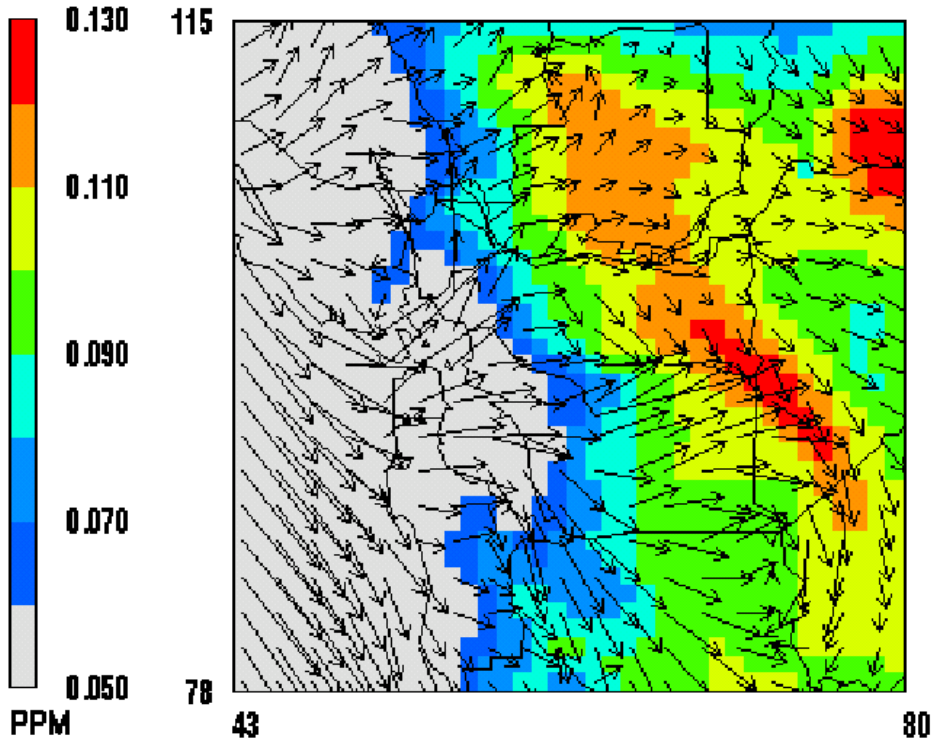

Figure 7-39. As in Figure 7-37, but for Run 2.

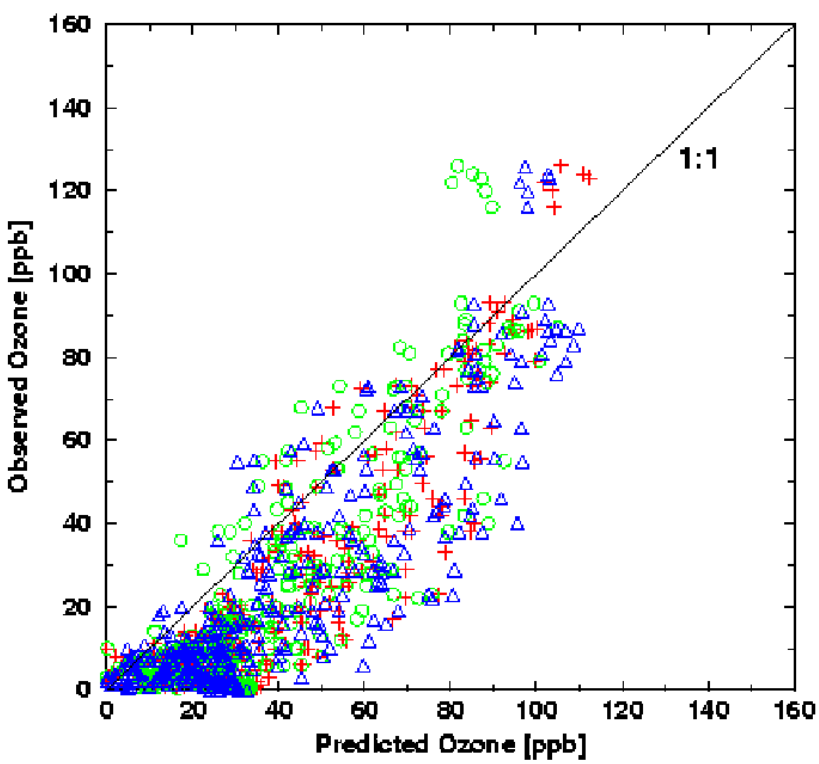

Figure 7-40. Scatter plots of the observed and the simulated ozone in the SFBA for Run 1 (circles), Run 2 (triangles), and Run 3 (crosses).

The application of FDDA in Run 2 improved the wind near the Carquinez Strait, but it further increased the westerly wind speed near Livermore and moved the southern part of the convergence line further toward the east. As a result, the southern part of the high ozone line moved past Tracy into the Central Valley (the maximum observed ozone at Tracy was 91 ppb on this day, significantly less than that at Livermore). The northern part of the high ozone line also moved further eastward but it stayed in the boundary of the SFBA. The location of maximum ozone did not change from that in Run 1. The magnitude of the simulated peak was 126 ppb, which is identical to the observed maximum ozone at Livermore.

Statistical Ozone Performance

The errors of the simulations can also be defined and compared via statistical methods. A scatter plot of the simulated versus observed ozone for the three runs for all hours of July 31, 2000, in the SFBA is shown in Figure 7-40. This is a paired comparison wherein all simulated values were interpolated to the location of the observation stations. The plotted pairs in Figure 7-40 can be classified into 3 distinct regimes: (1) a few observations with ozone around 120 ppb; (2) a large cluster of ozone observations below 20 ppb; and (3) the rest of the observations with ozone between 20 and 100 ppb. There is a general over prediction of ozone in regimes 2 and 3. This over prediction may be caused in part by the lateral boundary conditions, where the ozone is set to a constant 40 ppb. Most of the plotted pairs in regime 2 are nighttime values, when the observed ozone mixing ratios were very small, but when the simulated ozone tends to be in the range of 10-30 ppb.

Figure 7-40 suggests that Run 3 is performing best for the observed high ozone in regime 1. Run 2 appears to be the second best simulation, followed by Run 1. Since the difference between the simulated and the observed values in regime 1 is a combination of errors in the prediction of the maximum ozone and the prediction of the location of the maximum ozone, the better performance of Run 3 is actually a reflection of the fact that Run 3 gives the most accurate prediction of the location of the peak ozone. As mentioned previously, the maximum ozone simulated in Run 2 exactly matches the observed maximum value; however, that value is not located at an observation station and therefore does not appear in Figure 7-40.

Figure 7-41 shows the normalized bias and error and the unpaired peak prediction accuracy for the 3 runs. The normalized bias and errors are derived from the paired values shown in Figure 7-40. Using the unpaired peak prediction accuracy as the measure, Run 2 performed the best with no error and Run 1 performed the worst with an under prediction of 5%. However, the normalized bias for Run 1 is the smallest, less than 10%. This smaller bias occurred because while Run 1 under predicted the high ozone values in regime 1, it has less of a tendency to over predict the lower values in regimes 2 and 3. The normalized errors in Run 3 and Run 1 are comparable while the normalized error in Run 2 is the largest. The cause for this larger normalized error in Run 2 is the larger over prediction of ozone in regime 3, the mid-range ozone values.

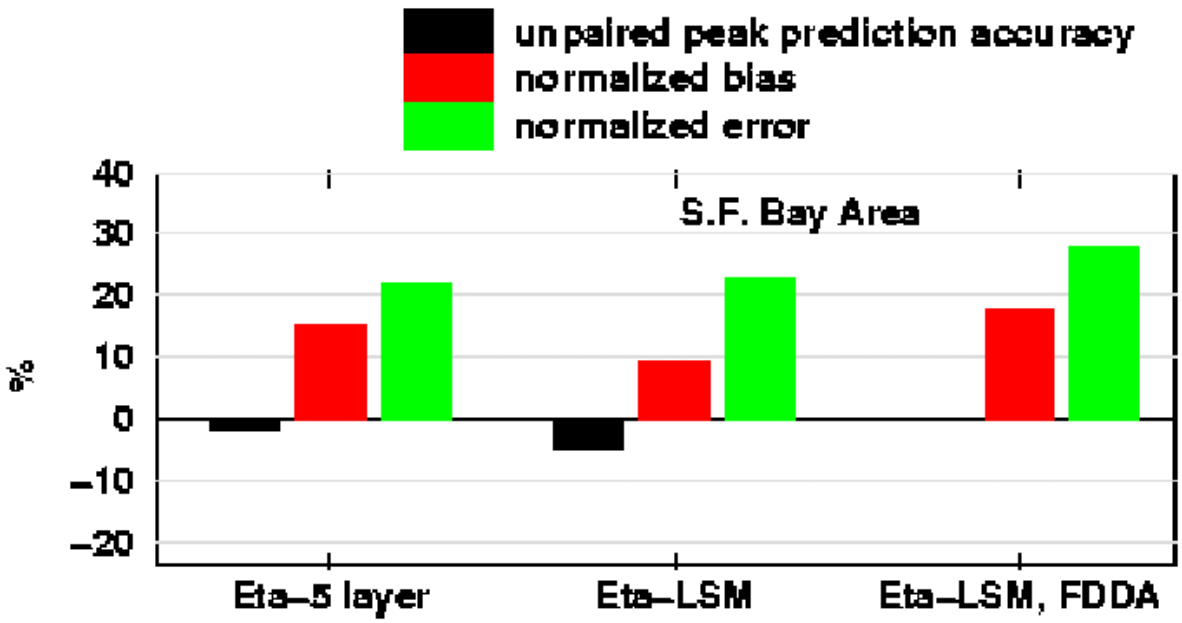

Figure 7-41. The normalized bias, error and the unpaired peak prediction accuracy of ozone on July 31, 2000 for Run 3 (Eta-5layer), Run 1 (Eta-LSM) and Run 2 (Eta-LSM, FDDA).

Figure 7-42 through 7-44 shown additional CAMx performance statistics for the SFBA, Sacramento, and the entire SJV for MM5/CAMx Run 3 using both the CB-IV and SAPRC99 chemical mechanisms. Note that results for the CB-IV case are only available for July 30 and 31, while the SAPRC results are shown for the entire modeling period July 30 – August 2. On the key day of interest for SFBA ozone (July 31), the use of SAPRC99 has increased the peak ozone substantially (by nearly 20 ppb in some areas of eastern Contra Costa County), and this shows as a near zero unpaired peak accuracy and a general shift to over predictions in the average paired (in space) peak accuracy over all sites in the SFBA measuring above 40 ppb. The overall normalized bias has also shifted upwards to over predictions while the gross error remains well within the EPA guidance range of 35%. The over prediction tendency on July 30 and 31 are mostly associated with low- to mid-range ozone levels.

In Sacramento (Figure 7-43), the key day of interest is August 1; on this day the unpaired peak accuracy shows less than a 10% under prediction, and gross error is quite acceptable during the entire modeling period. However, the normalized bias shows quite a large degree of under prediction and this is also reflected in the average paired peak accuracy over all sites in the region measuring more than 40 ppb. While the unpaired peak is acceptable (meaning that peak ozone is simulated downwind of Sacramento at levels near the peak observation), overall the model performance in Sacramento is not yet at levels useable for regulatory modeling.

Over the entire SJV (Figure 7-44), the model performs rather well for all days, although the unpaired peak accuracy is just outside the guidance value and shows a strong under prediction on August 2, the key day of interest for this region. While it is known that CAMx dramatically under predicts ozone in the southern SJV, these statistics mask those problems and show that overall the model performs adequately on average over the entire region.

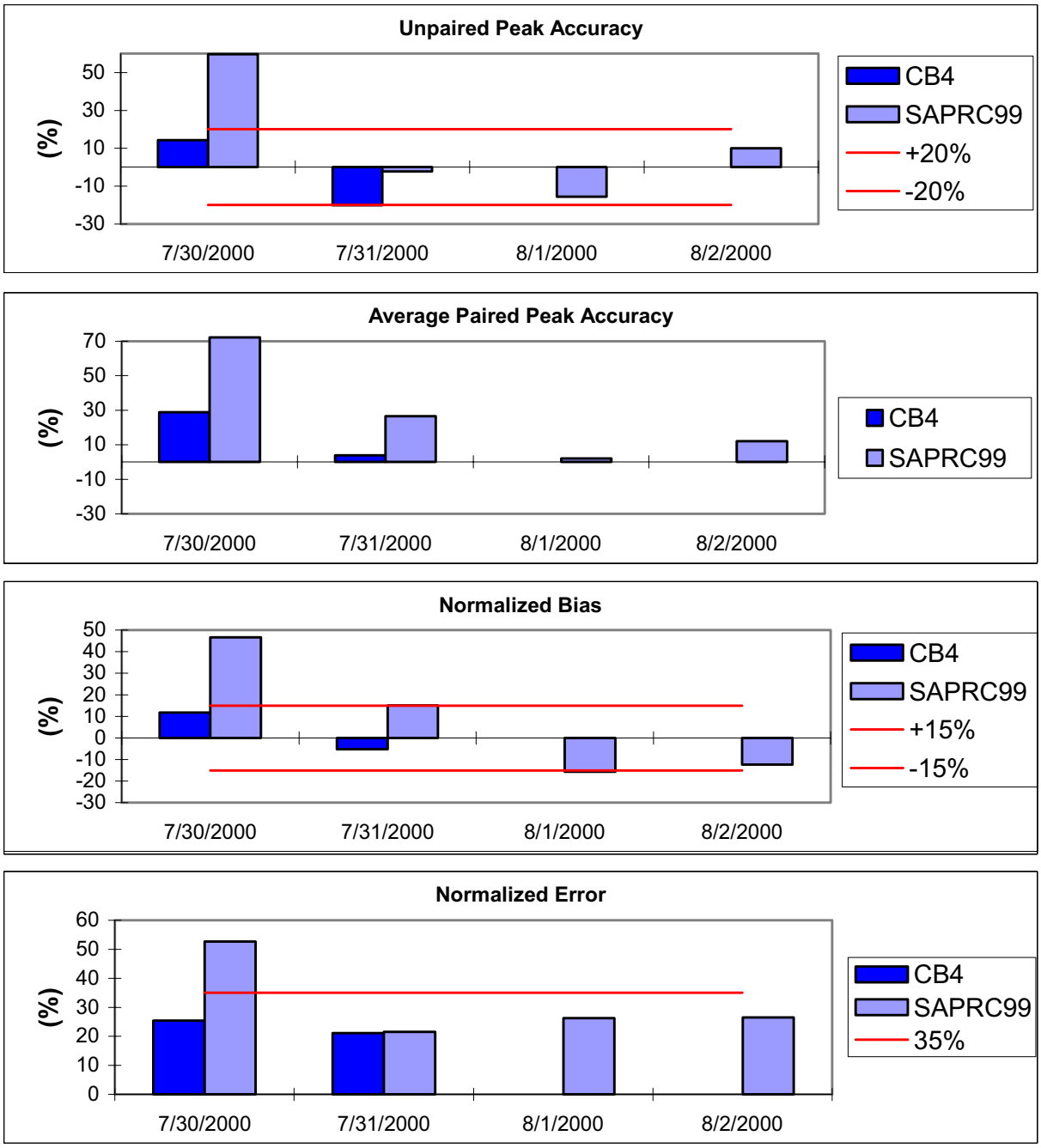

Figure 7-42. Daily photochemical model performance statistics for the BAAQMD Run 3 using both CB-IV and SAPRC99 chemical mechanisms. Statistics for the SFBA region.

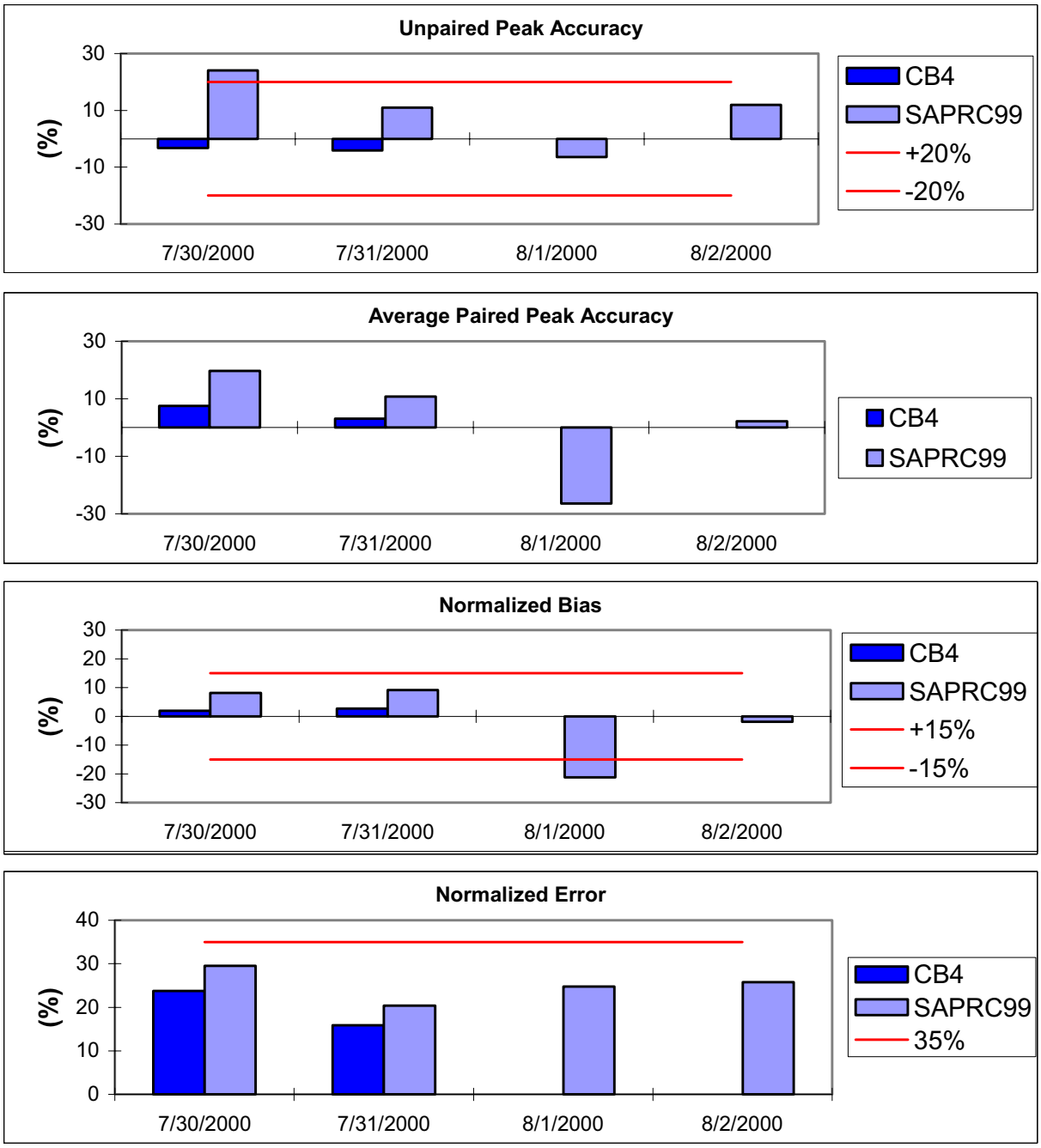

Figure 7-43. Daily photochemical model performance statistics for the BAAQMD Run 3 using both CB-IV and SAPRC99 chemical mechanisms. Statistics for the Sacramento region.

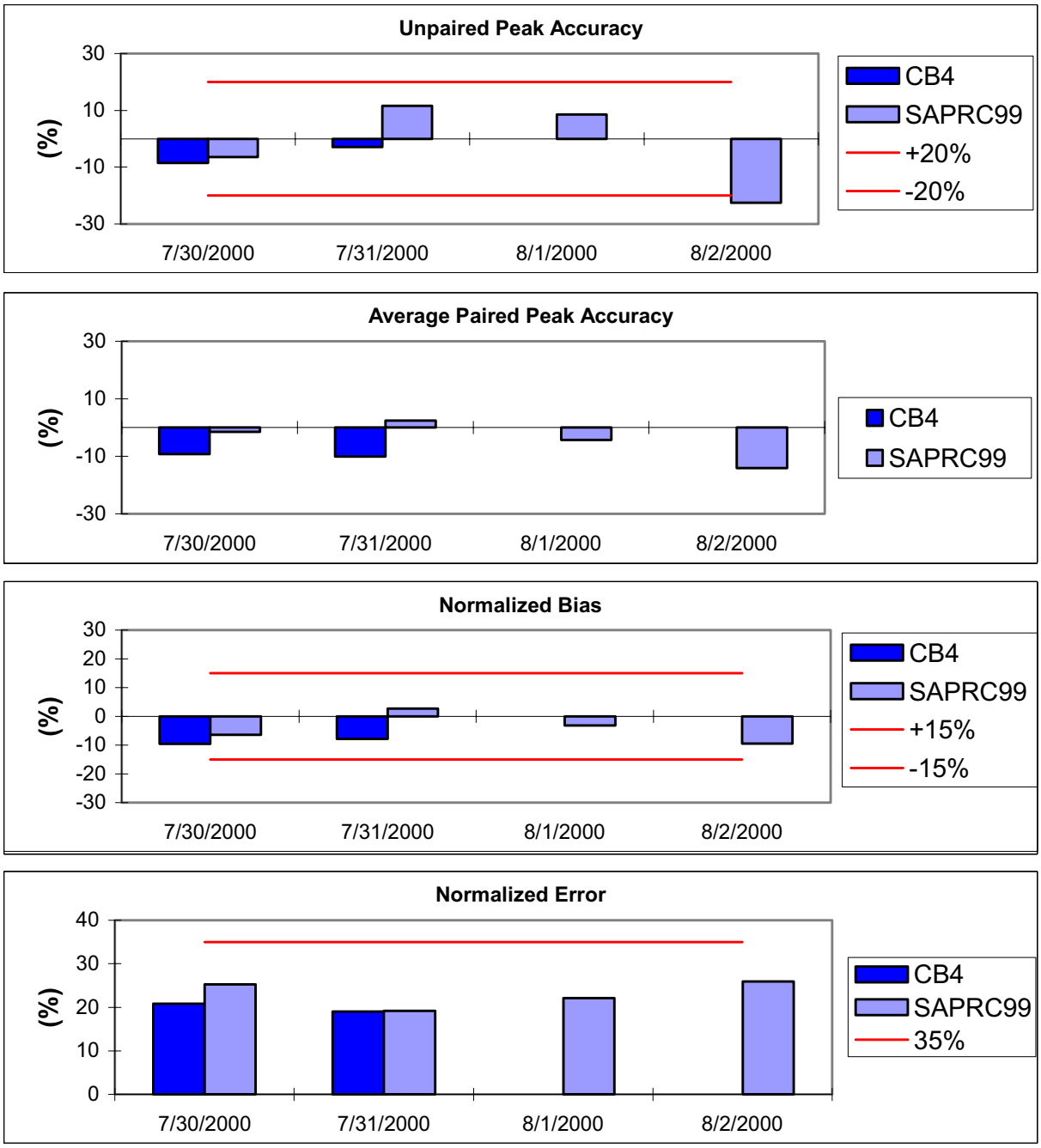

Figure 7-44. Daily photochemical model performance statistics for the BAAQMD Run 3 using both CB-IV and SAPRC99 chemical mechanisms. Statistics for the entire SJV region.

Summary of CAMx Simulations for CCOS 2000

We have shown that the MM5-CAMx couple using the SAPRC99 chemical mechanism produced reasonable predictions of ozone in central California during the July 31-August 2, 2000, period. It also produced reasonable predictions of the locations and timing of peak ozone in the SFBA on July 31, 2000. The prediction skill varied from region to region and from time to time. Under predictions continue to be a problem for the modeling in Sacramento and the southern SJV on their specific days of interest (August 1 and 2, respectively).

Locations of the wind convergence zone and the locations of simulated high ozone were found to be closely related. The overall surface-wind patterns in the SFBA are similar in the 3 MM5 runs, but there are subtle differences in the wind patterns among the runs in and near the Livermore Valley. The runs with the 5-layer soil model, as reported in Section 4, under predicted Central Valley temperatures and therefore produced a weaker sea breeze. This weaker sea breeze created a convergence line close to Livermore and produced an ozone pattern that, among the three simulations, compared best with observations. The MM5 runs using the Noah LSM, while producing a reasonable Central Valley temperature, created a much stronger sea breeze. This stronger sea breeze moved the convergence zone about 20 km east of Livermore.

This trade-off between accurate inland temperature and accurate sea-breeze predictions may indicate a deficiency in the current MM5 model. There are several possible explanations for this problem. The first is that the second-order advection scheme used in MM5 requires such large diffusion values that the mountain-blocking effect is reduced and the sea breeze front is propagated too far inland. Another possible explanation is the lack of a mountain drag parameterization that would tend to reduce the speed of the sea breeze in the Tri-Valley and more accurately channel the flow. A third possible explanation is the lack of vertical resolution in the original data input to MM5 to define the inversion layer during this high ozone period. A comparison between the MM5 output and the observed vertical profiles of temperature did show that the strength of the inversion is under predicted.

An important conclusion, then, is that some relatively subtle flow features, which may not be fully appreciated in meteorological model performance evaluations, can have a significant influence on the performance of a photochemical model.

BAAQMD CAMx APPLICATIONS FOR JULY 1999

The BAAQMD undertook photochemical modeling of the July 9-12, 1999 period using meteorological input fields from the CARB's MM5 simulation (MRF PBL scheme with the 5-layer soil model). Recall from Section 4 that of the single CARB and several BAAQMD MM5 runs for this period, the CARB's was one of the overall best performing simulations. An additional MM5 simulation carried out by the BAAQMD that replaced the MRF PBL scheme with the Eta scheme was also used in CAMx for a comparative assessment (a later MM5 simulation that replaced the 5-layer soil model with the NOAH LSM was not available in time to use in CAMx and be documented in this report). As with the CCOS 2000 simulations, the BAAQMD performed CAMx using both the CB-IV and SAPRC99 chemical mechanisms. An important point to note is that the vertical domain extent was taken from the configuration defined by the CARB, in which the model top was set at ~5 km. Also recall from Section 6 that the CB-IV initial and boundary conditions were also taken from the CARB setup, and these were

simply copied from the July/August 2000 boundary conditions, which included high ozone top boundary conditions to reflect the observed high ozone aloft from forest fires in the southern Sierra Nevada mountains.

Spatial Ozone Patterns

This section displays results for the BAAQMD's CAMx run using CARB MM5 meteorology and the SAPRC99 chemical mechanism. The simulated surface-layer ozone field over the entire modeling domain on July 11 at 1400 PST is shown in Figure 7-45a. High ozone is seen covering a large portion of the south and east SFBA, the Sacramento metropolitan area, and stretching south along U.S. Route 99 to Fresno. Some higher ozone concentrations are also seen over Bakersfield. In the SFBA specifically (Figure 7-45b), peak ozone is nearing 150 ppb along the I-680 corridor. Ozone is high over much of the urbanized south and east bay areas, as suggested by observations on this day.

On July 12 at 1400 PST, the domain-wide ozone distribution (Figure 7-46a) is similar to the previous day, but even wider areas of elevated ozone concentrations are evident. This is particularly true over the southern Sacramento and northern San Joaquin Valleys. Higher ozone levels reaching near 70 ppb are pushed along the coastline and even offshore, suggesting the influence of off-shore directed winds. In the SFBA (Figure 7-46b), peak ozone is again reaching near 150 ppb over eastern Contra Costa County, while ozone reaching near 100 ppb is spread throughout the east bay from Solano County south to southern Santa Clara County.

Given that the input emissions for this episode are not dramatically different from the July/August 2000 episode, the higher and more widespread ozone patterns generated by CAMx in this simulation suggests a more extreme meteorological condition conducive to poor ozone air quality was successfully modeled with MM5 and translated to CAMx.

Statistical Performance Evaluation

The influence of the meteorological inputs from two different MM5 simulations (CARB's MRF vs. BAAQMD's Eta) on ozone model performance was evaluated quantitatively by comparing scatter diagrams and associated linear regressions for the SFBA, Sacramento, and SJV regions. These are shown in Figures 7-47 through 7-49. Again, these simulations were run with the SAPRC99 mechanism.

In the SFBA, the MRF meteorology generally leads to less of an under prediction of the highest observed ozone levels. The linear regression is nearly equivalent, with a similar slope and correlation coefficient. These results suggest that very little difference (statistically) results from the two meteorological realizations. In Sacramento, differences are more obvious among the two simulations; MRF meteorology leads to much wider scatter and a worse regression slope. However, the wider scatter is more balanced than in the Eta meteorology case (where low observations are over predicted and high observations are under predicted), which leads to a better correlation for the MRF case. Therefore, there is no clear winner in this region either. In the SJV, both simulations are very similar and show the consistent under predictions of high ozone and over predictions of low ozone. Model performance shows very little skill in this region.

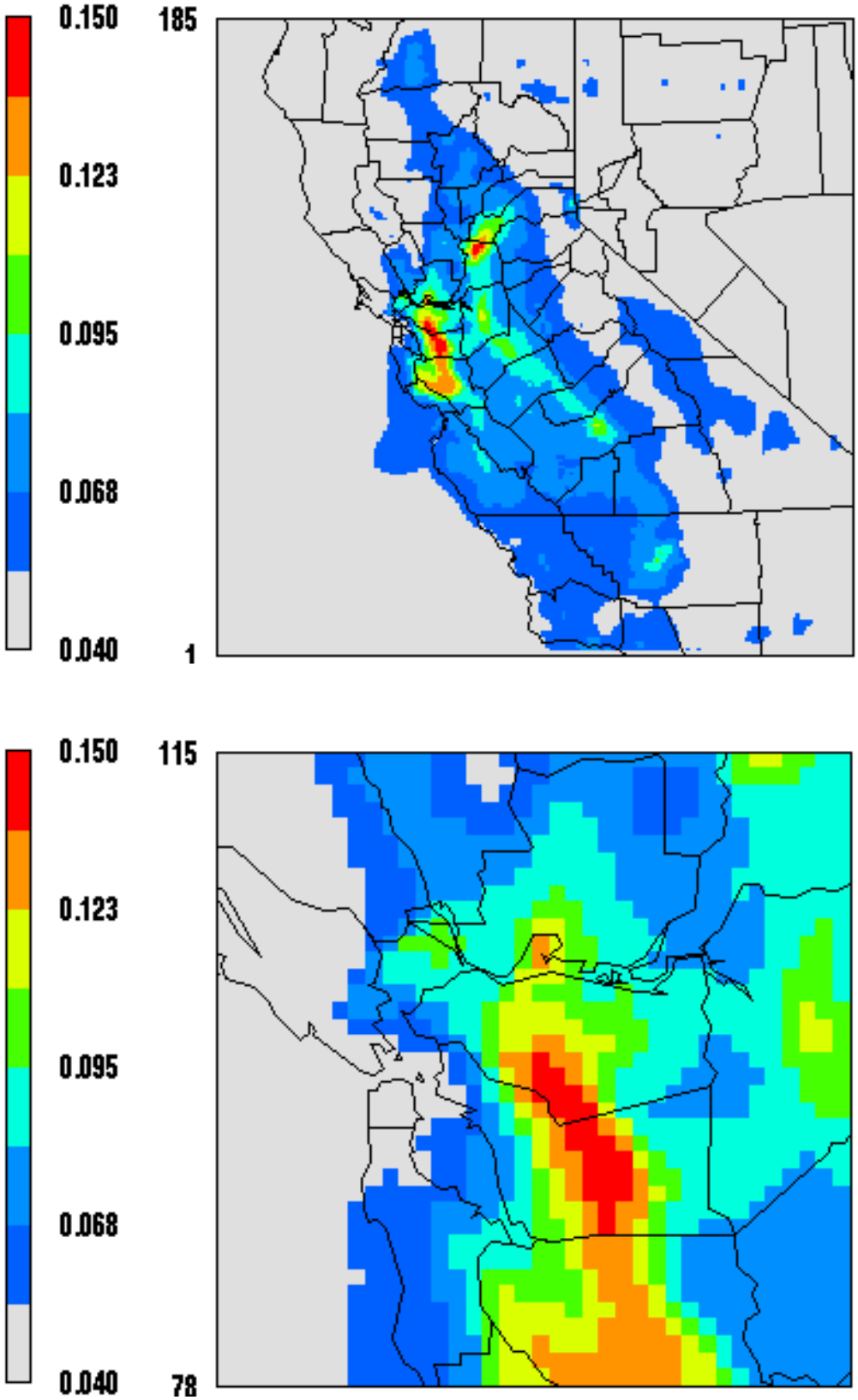

Figure 7-45. CAMx/SAPRC99 simulated ozone on July 11, 1999 at 1400 PST (a) over the entire domain and (b) over the SFBA region.

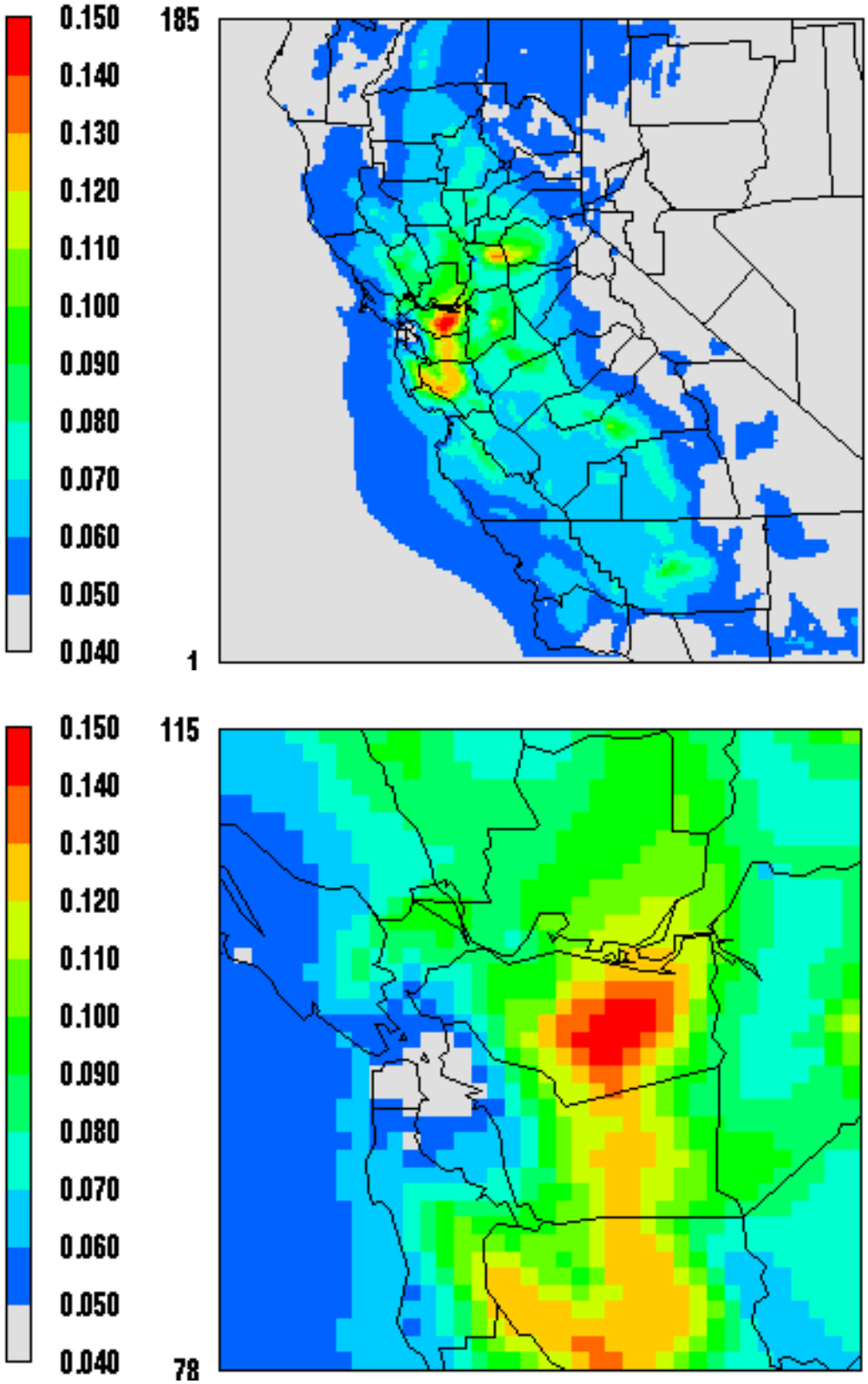

Figure 7-46. CAMx/SAPRC99 simulated ozone on July 12, 1999 at 1400 PST (a) over the entire domain and (b) over the SFBA region.

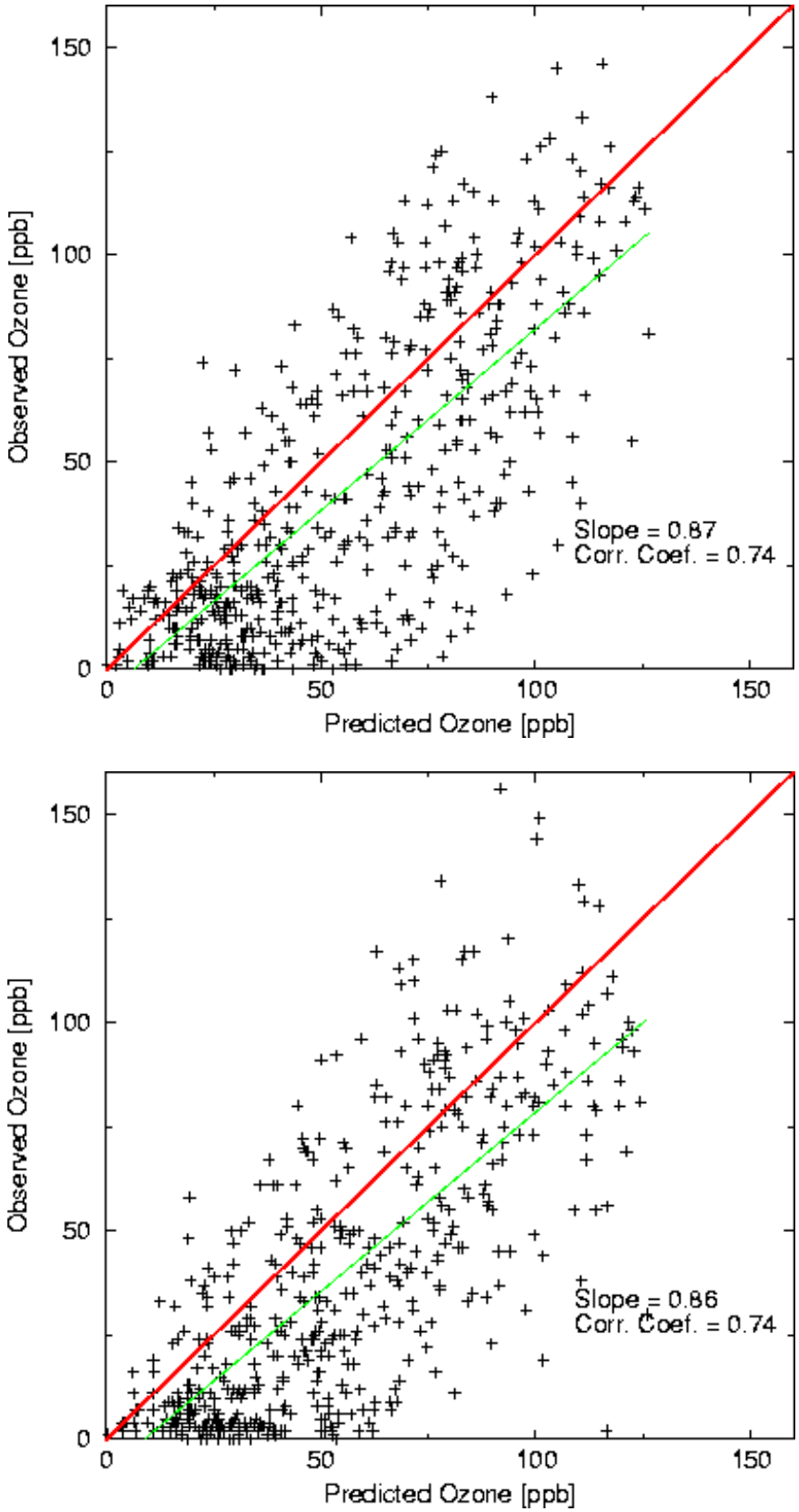

Figure 7-47. Scatter diagrams of observed ozone vs. predicted ozone in the SFBA region on July 11 and 12, 1999 using (a) the CARB's MM5/MRF meteorology, and (b) the BAAQMD's MM5/Eta meteorology.

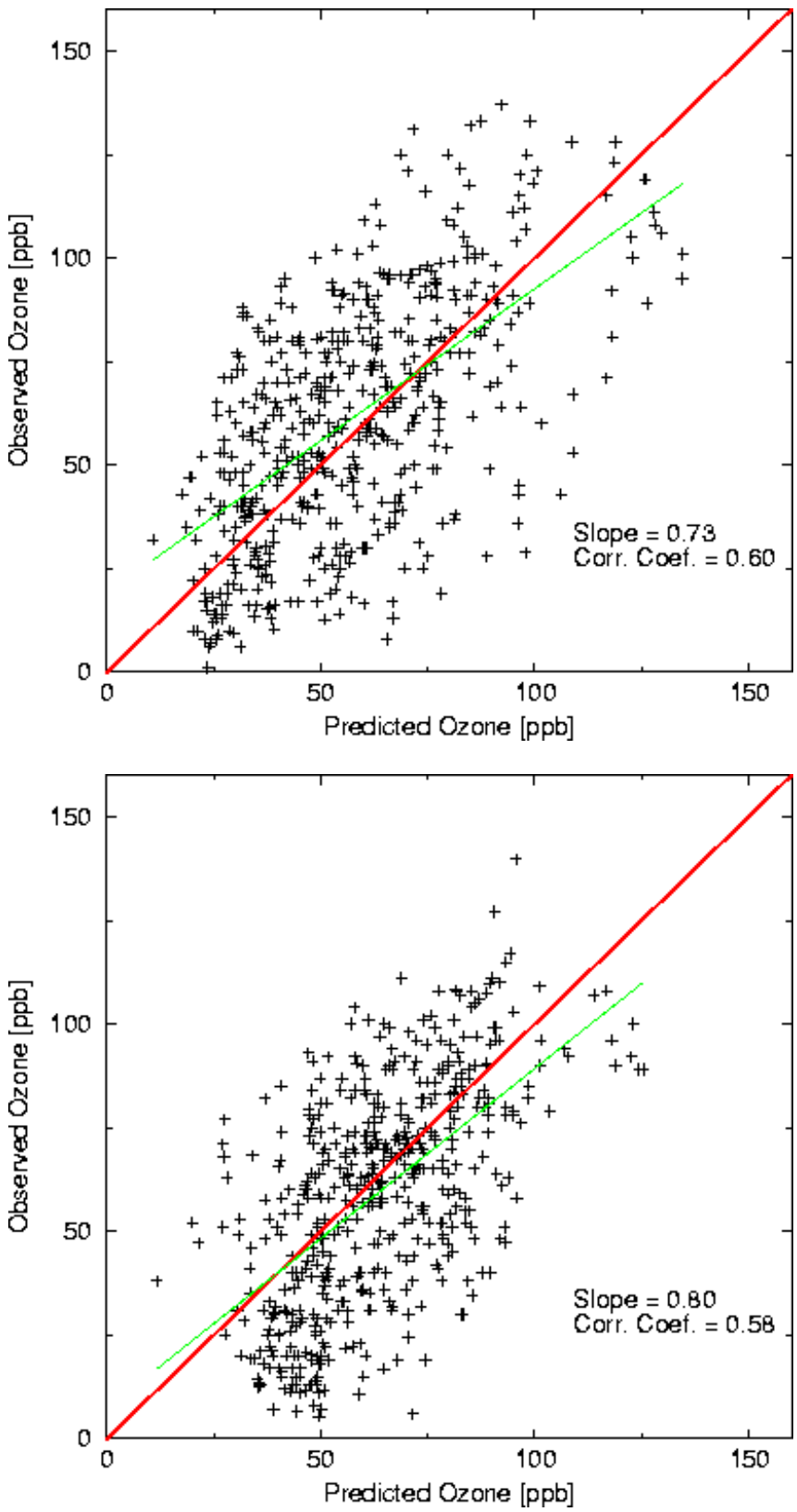

Figure 7-48. Scatter diagrams of observed ozone vs. predicted ozone in the Sacramento region on July 11 and 12, 1999 using (a) the CARB's MM5/MRF meteorology, and (b) the BAAQMD's MM5/Eta meteorology.

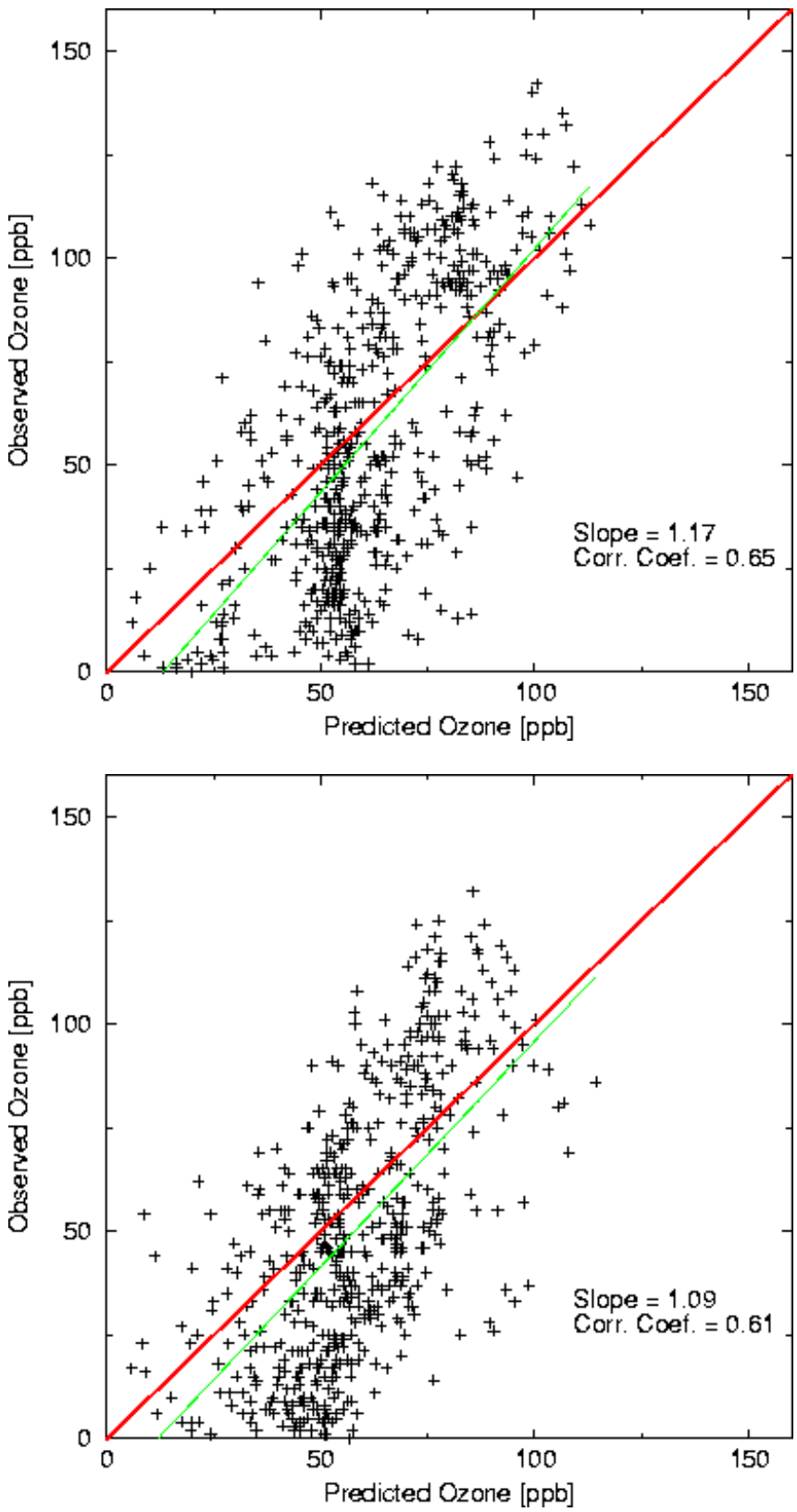

Figure 7-49. Scatter diagrams of observed ozone vs. predicted ozone in the SJV region on July 11 and 12, 1999 using (a) the CARB's MM5/MRF meteorology, and (b) the BAAQMD's MM5/Eta meteorology.

In Figure 7-50, the three ozone statistical measures from EPA guidance are shown for July 11 and 12, for both the CARB MRF and BAAQMD Eta run, and for all three analysis regions. Also shown in the plot is the performance in each region on July 31, 2000 using the NOAA/BAAQMD Eta MM5 simulation for comparison.

In the SFBA, the unpaired peak and bias metrics are quite good on both days and for both sets of meteorological inputs. However, the gross error is rather high in all cases (but still within EPA acceptance). There is no obvious best case for this area. In Sacramento, the unpaired peak accuracy shows extreme under predictions on July 12 for both sets of meteorology. Note that the bias is worse in the MM5 Eta case; gross error is not impacted by the different cases. In the SJV, peak ozone performance is not sensitive to meteorology, but bias and gross error are worse in the BAAQMD Eta run. From this analysis, we conclude that CAMx performance is slightly degraded in the central valley with the use of the BAAQMD Eta MM5 meteorology.

The BAAQMD further investigated the model performance impacts between the use of the CB-IV and SAPRC99 chemical mechanisms. These runs were made with the original CARB MM5/MRF meteorology. Figures 7-51 through 7-53 show daily performance statistics in the SFBA, Sacramento, and SJV regions over July 10-12, 1999 for both mechanisms.

Unlike the July/August 2000 episode results, the ozone performance differences between the two mechanisms are minor. In fact, these differences are much more in line with the expected ozone signal in moving from CB-IV to SAPRC99. Given the fact that the emission inventories provided to CAMx for the 2000 and 1999 episodes are very similar, the vastly differing SAPRC response among the episodes is an unexpected outcome. The differences in meteorology between the two episodes is clearly significant, with the 1999 episode being warmer, more stagnant, and more conducive to high ozone, but it is difficult to develop an explanation for how the meteorological differences play into the CB-IV/SAPRC chemistry differences.

In the SFBA (Figure 7-51), the unpaired peak, bias, and gross error are all within EPA acceptance criteria for the entire episode and for both chemical mechanisms. SAPRC does lead to consistently higher gross error than CB-IV, and this is somewhat reflected in the bias as well. This is a result of SAPRC's tendency to over predict the low to moderate observed ozone concentrations throughout the SFBA. In Sacramento (Figure 7-52), performance is degraded relative to SFBA for both simulations, with a large under prediction of the unpaired peak on July 12 and a strong overall under prediction bias on July 11. Note, however, that the averaged paired peaks, the overall bias, and the gross error on July 12 show the best performance of the episode on July 12. This means that CAMx is performing well over the entire range of concentrations, but that the single peak observation for that day is under predicted by a large margin. In the entire SJV (Figure 7-53), the model performance is quite promising for July 11 and 12, with the metrics at or well within the EPA acceptance criteria.

Summary of CAMx Simulations for July 1999

The BAAQMD undertook photochemical modeling of the July 9-12, 1999 period using two different sets of meteorological input fields (CARB's MM5/MRF run and BAAQMD's MM5/Eta run) and two different chemical mechanisms (CB-IV and SAPRC99). Besides meteorology, the only other significant difference in model configuration between the CCOS

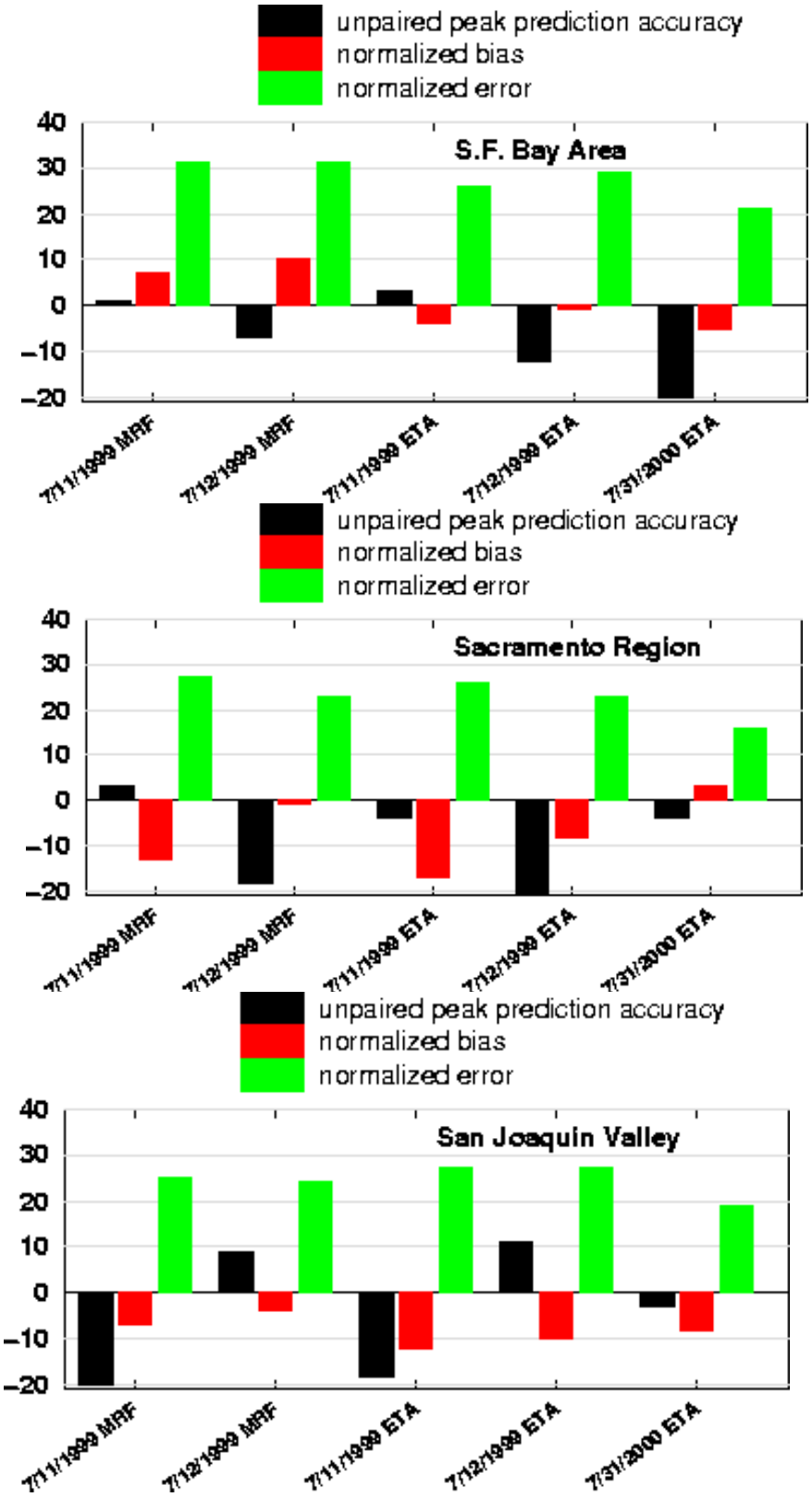

Figure 7-50. EPA guidance statistics for daily ozone performance on July 11 and 12, 1999 in SFBA (top), Sacramento (middle), and SJV (bottom), for two CAMx simulations using different meteorology. The BAAQMD's CAMx simulation using MM5/Eta meteorology from July 31, 2000 is shown for comparison.

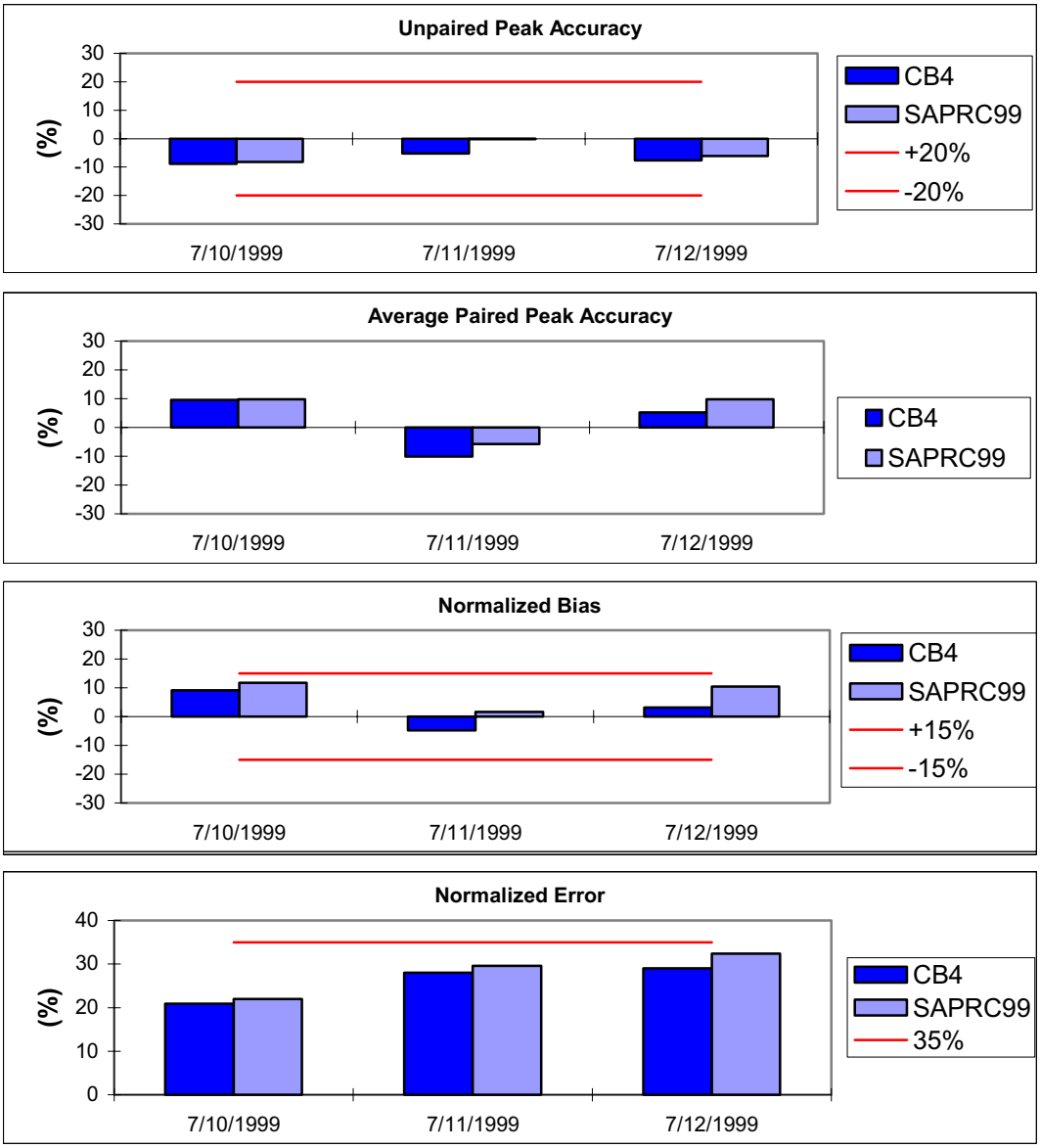

Figure 7-51. Daily photochemical model performance statistics for the July 10-12, 1999 episode using both CB-IV and SAPRC99 chemical mechanisms and the CARB MM5/MRF meteorology. Statistics for the SFBA region.

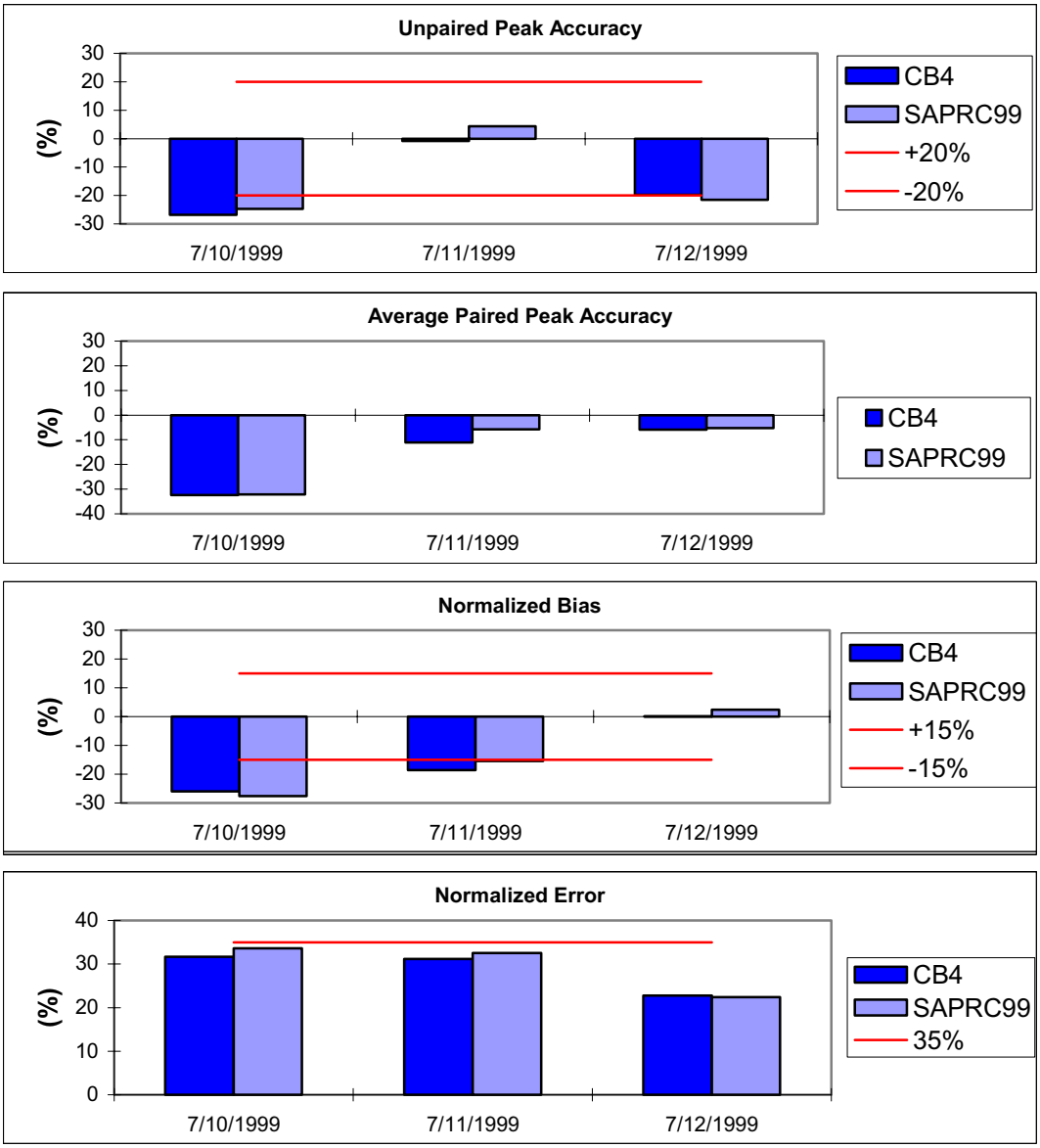

Figure 7-52. Daily photochemical model performance statistics for the July 10-12, 1999 episode using both CB-IV and SAPRC99 chemical mechanisms and the CARB MM5/MRF meteorology. Statistics for the Sacramento region.

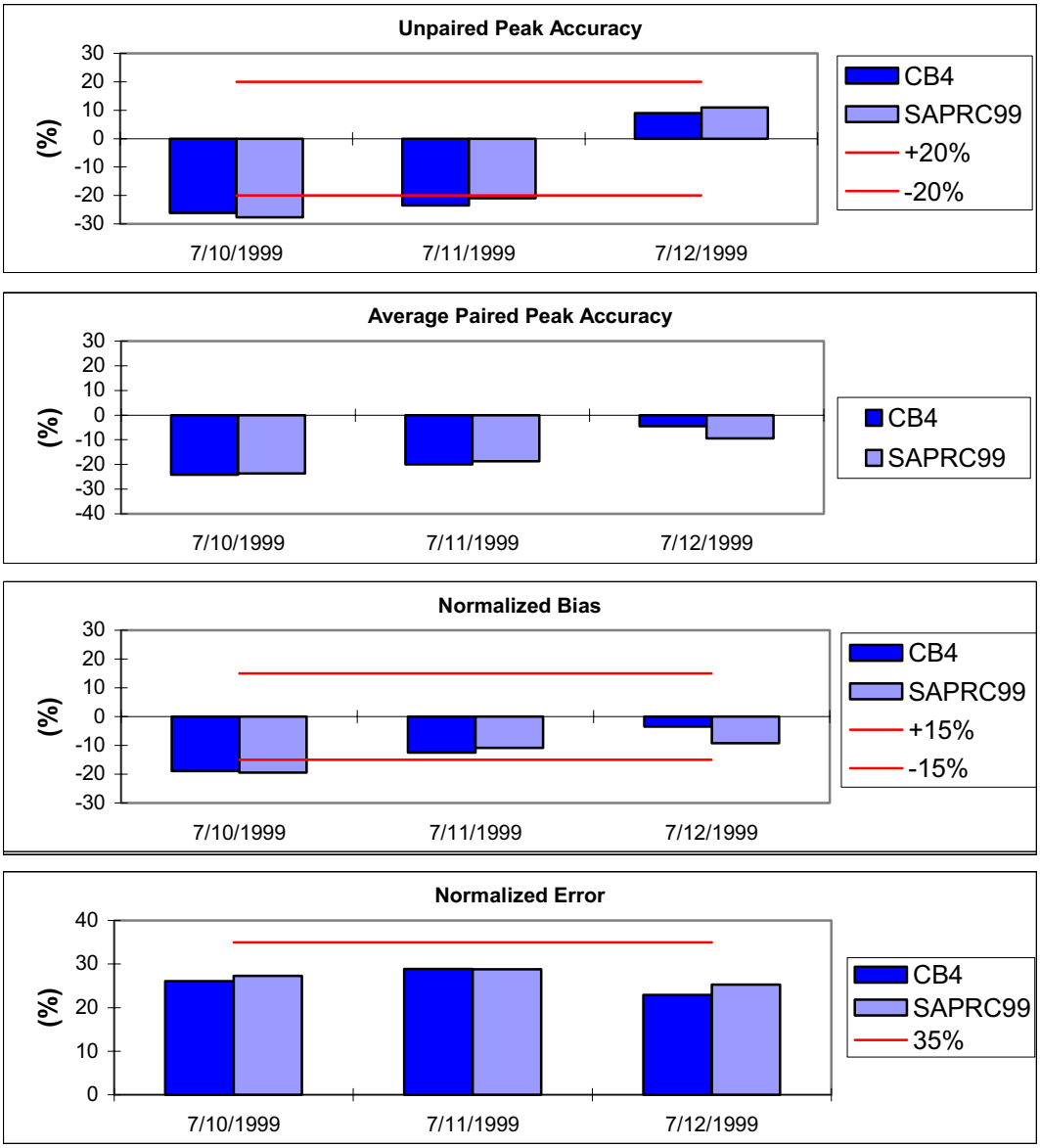

Figure 7-53. Daily photochemical model performance statistics for the July 10-12, 1999 episode using both CB-IV and SAPRC99 chemical mechanisms and the CARB MM5/MRF meteorology. Statistics for the entire SJV region.

2000 and July 1999 simulations was the lower model top (set at 5 km in the July 1999 applications).

CAMx tests conducted with different meteorological inputs used the SAPRC99 chemistry. Both sets of inputs resulted in much higher ozone concentrations over the entire urbanized portions of the modeling domain than achieved in the July/August 2000 episode, with simulated ozone reaching near 150 ppb in several areas each day. Given that the input emissions for this episode are not dramatically different from the July/August 2000 episode, the higher and more widespread ozone patterns generated by CAMx in this simulation suggests a more extreme meteorological condition conducive to poor ozone air quality was successfully modeled with MM5 and translated to CAMx. This is particularly evident from the fact that high ozone concentration patterns were pushed to the coast and even offshore along the central California coastline, suggesting proper replication of the offshore wind system that set up between July 11 and 12.

In the SFBA, the MRF meteorology generally leads to less of an under prediction of the highest observed ozone levels, but very little difference (statistically) resulted from the two meteorological realizations. The daily unpaired peak and bias metrics are quite good on both days and for both sets of meteorological inputs. However, the gross error is rather high in all cases (but still within EPA acceptance). There is no obvious best case for this area.

In Sacramento, differences are more obvious among the two simulations both visually and statistically; however, the mix of improvements and degradations result in no clear winner in this region as well. The unpaired peak accuracy shows extreme under predictions on July 12 for both sets of meteorology, but gross error is not impacted by the different cases.

In the SJV, both simulations are very similar and show the consistent under predictions of high ozone and over predictions of low ozone. Model performance shows very little skill in this region. Peak ozone performance is not sensitive to meteorology, but bias and gross error are worse in the BAAQMD MM5/Eta run. We conclude that CAMx performance is slightly degraded in the central valley with the use of the BAAQMD MM5/Eta meteorology.

CAMx tests conducted with different chemical mechanisms used the CARB MM5/MRF meteorological inputs. Ozone performance differences between the two mechanisms were minor on all days and for all three analysis regions; this result is much more in line with expectations as opposed to the surprisingly higher peak ozone achieved in the July/August 2000 episode using SAPRC99 over CB-IV. This difference in sensitivity among the episodes apparently is related to the different local meteorology (which differs substantially from the CCOS episode) than any differences in emissions (which are very similar among the episodes). However, it is difficult to explain how the meteorological differences play into the CB-IV/SAPRC chemistry differences. Tools such as Process Analysis are needed to further understand the source of the CB-IV/SAPRC signal among these two episode.

For the July 1999 episode, SAPRC99 has a tendency to over predict the low to moderate observed ozone concentrations throughout the SFBA. In Sacramento, CAMx performs well over the entire range of concentrations, but the single peak observation on July 12 is under predicted by a large margin. In the entire SJV, the model performance is quite promising for July 11 and 12, with the metrics at or well within the EPA acceptance criteria.